

T. R.  
VAN YUZUNCU YIL UNIVERSITY  
INSTITUTE OF NATURAL AND APPLIED SCIENCES  
DEPARTMENT OF MECHANICAL ENGINEERING

**EXPERIMENTAL ASSESSMENT OF THE PERFORMANCE FOR A WEDGE  
STORAGE SOLAR COLLECTOR**

M.Sc. THESIS

PREPARED BY: Marwan Rija JASSIM  
SUPERVISOR: Assist. Prof. Dr. Altuğ KARABEY  
CO-SUPERVISOR: Prof. Dr. Omar Khalil AHMED

VAN- 2021



T. R.  
VAN YUZUNCU YIL UNIVERSITY  
INSTITUTE OF NATURAL AND APPLIED SCIENCES  
DEPARTMENT OF MECHANICAL ENGINEERING

**EXPERIMENTAL ASSESSMENT OF THE PERFORMANCE FOR A WEDGE  
STORAGE SOLAR COLLECTOR**

M.Sc. THESIS

PREPARED BY: Marwan Rija JASSIM  
SUPERVISOR: Assist. Prof. Dr. Altuğ KARABEY  
CO-SUPERVISOR: Prof. Dr. Omar Khalil AHMED

This project was supported by Scientific Research Projects Coordination Unit of Van  
Yuzuncu Yil University with project no: 2020-8907

VAN-2021



## ACCEPTANCE and APPROVAL PAGE

This thesis entitled “**EXPERIMENTAL ASSESSMENT OF THE PERFORMANCE FOR A WEDGE STORAGE SOLAR COLLECTOR**” presented by Marwan Rija JASSIM under supervision of Assist. Prof. Dr. Altuğ KARABEY in the department of Mechanical Engineering has been accepted as a M.Sc. Thesis according to Legislations of Graduate Higher Education on ...../...../2020..... With unanimity / majority of votes members of jury.

Chair: Prof. Dr. Sedat YAYLA

Signature:

Member: Assist. Prof. Dr. Altuğ KARABEY

Signature:

Member: Assist. Prof. Dr. Kadir GELİŞ

Signature:

This thesis has been approved by the committee of The Institute of Natural and Applied Science on ...../...../..... with decision number .....

Signature

.....

Director of Institute



## **THESIS STATEMENT**

All information presented in the thesis obtained in the frame of ethical behavior and academic rules. In addition all kinds of information that does not belong to me have been cited appropriately in the thesis prepared by the thesis writing rules.

Signature

Marwan Rija JASSIM





## ABSTRACT

### EXPERIMENTAL ASSESSMENT OF THE PERFORMANCE FOR A WEDGE STORAGE SOLAR COLLECTOR

JASSIM, Marwan Rija  
M.Sc. Thesis Department of Mechanical Engineering  
Supervisor: Assist Prof. Dr. Altuğ KARABEY  
January 2021, 71 pages

This research includes an experimental investigation of a novel design of the domestic solar collector. This design is inspired by cutting the cylinder with two levels: the first level is a vertical plane, and the second level is inclined with  $45^\circ$ . The experiments were conducted in two locations, the first in the Iraqi Kirkuk city ( $35.47^\circ$  N,  $44.39^\circ$  E), and the other in the Turkish van city ( $38.5^\circ$  N,  $43.33^\circ$  E). Two similar experimental models were built for this purpose.

The results of the research confirmed the maximum water temperature of the model under Iraqi weather conditions is higher than the water temperature of the collector in Turkish weather conditions. when we put continuous load 0.2 liters/min, the water temperature outlet collector in Iraq  $34^\circ\text{C}$ ,  $42^\circ\text{C}$  and  $68^\circ\text{C}$  at 3 pm for the month of December, March and July respectively. But in Turkey at the same months,  $28^\circ\text{C}$ ,  $33^\circ\text{C}$  and  $55^\circ\text{C}$  at 1 pm respectively. when we put continuous load 0.4 liters/min, the water temperature outlet in Iraq  $31^\circ\text{C}$ ,  $38^\circ\text{C}$  and  $61^\circ\text{C}$  at 3 pm for the month of December, March and July respectively. The total efficiency without load was obtained 49% in Iraq, while in Turkey it was obtained 38%. But the total efficiency was for the wedge collector operating in Iraqi weather conditioning, where it recorded 61% and 65%. Either in Turkey efficiency in, reached 53% and 67% when the of the volume water flow rate 0.2liter/min and 0.4 liter/min respectively.

**Keywords:** Collector, Performance, Solar, Storage, Wedge



## ÖZET

### DAİRESEL DILIM KESİTE SAHİP GÜNEŞ DEPOLAMA KOLLEKTÖRÜNÜN PERFORMANS DEĞERLENDİRMESİ

JASSIM, Marwan Rija  
Yüksek Lisans Tezi, Makine Mühendisliği Anabilim Dalı  
Tez Danışmanı : Dr. Öğr. Ü. Altuğ KARABEY  
Ocak 2021, 71 sayfa

Bu çalışmada, bir güneş kolektörüne ait yeni bir tasarımın deneysel bir incelemesi amaçlanmıştır. Bu tasarım, silindirik tankın iki seviyede kesilmesiyle elde edilmiştir; öncelikle silindirik tank, enine ortadan ikiye kesilmiş, ardından 45° eğimli olacak şekilde tekrar kesilerek yeni bir geometri oluşturulmuştur. Deneylerin, ilki Kerkük-İrak (35.47 °K, 44.39 °D) diğeri ise Van-Türkiye ilinde (38.5 °K, 43.33°D) olmak üzere iki farklı ortamda gerçekleştirilmiştir. Bu amaçla iki benzer deneysel model oluşturulmuştur.

Yeni tasarıma ait araştırma sonuçları, genel olarak, modelin farklı iklimlerdeki ölçümleri göz önüne alındığında, Irak şartlarındaki ortalama su sıcaklığının, Türkiye şartlarındaki ortalama su sıcaklığından daha yüksek olduğu gözlemlenmiştir.. Çalışmanın ikinci aşamasında, farklı mevsimlerde çalışmanın ilk aşamasıyla eş zamanlı olacak şekilde, tasarımın 0.2 l/dk ve 0.4 l/dk'lık yük durumu altındaki davranışı incelenmiştir. Tasarımın ölçüm sonuçlarına göre, 0.2 l/dk yük durumu altında yeni kollektörden çıkan ortalama su sıcaklığı Kerkük'te Aralık, Mart ve Temmuz aylarında saat 15:00'de sırasıyla 34°C, 42°C, 68 °C olarak ölçülmüştür. Tasarımın ölçüm sonuçlarına göre, 0.4 l/dk yük durumu altında yeni kollektörden çıkan ortalama su sıcaklığı Kerkük'te Aralık, Mart ve Temmuz aylarında saat 15:00'de sırasıyla 31°C, 38°C, 61 °C olarak ölçülmüştür. Türkiye'de ise ortalama su sıcaklığı saat 14:00'de sırasıyla 28°C, 33°C, 55°C olarak ölçülmüştür. Sonuçlar, kollektörden çıkan ortalama su sıcaklığının suyun debisine ve çevredeki iklim koşullarına bağlı olduğunu göstermiştir.

**Anahtar kelimeler:** Güneş, Depolama, Toplayıcı, Dairesel dilim kesiti



## ACKNOWLEDGMENT

To begin with I would like to thank "Allah" then Assist Prof Dr. Altuğ KARABEY, my dissertation research advisor, for his invaluable advice, guidance, and support that made this work possible. His encouraging words and positive way of thinking motivated me throughout my M.Sc. research. It has been enjoyable.

I would also like to thank the other members of my advisory committee. I am grateful to Prof. Dr. Omer Khalil AHMED for his help and support from the very first day of my graduate life both in experimental and academic activities. His enthusiasm and dedication towards the scientific research has been an inspiration to my research. Prof. Dr. Omer Khaill has been a tremendous asset. It is rare to find an instructor that has such a genuine concern for students as Dr. Omer.

I also thank teacher Serhat Bozan for helping me and standing with me throughout the time of my research, during my M.Sc. research. I thank everyone who helped me in Turkey.

I would like to thanks of Van Yuzuncu Yil University, Faculty of Mechanical Engineering Department.

Lastly but not least, I would like to thank my parents and brothers for their sacrifices and unselfish love and support.

2021

Marwan Rija JASSIM



## TABLE OF CONTENTS

	<b>Page</b>
ABSTRACT .....	i
ÖZET .....	iii
ACKNOWLEDGMENT .....	v
TABLE OF CONTENTS .....	vii
LIST OF TABLES .....	ix
LIST OF FIGURES .....	xi
SYMBOLS AND ABBREVIATIONS .....	xv
1. INTRODUCTION .....	1
2. LITERATURE REVIEW .....	9
2.1 A brief history of integrated collector storage solar water heaters .....	9
3. MATERIALS AND METHODS.....	25
3.1. Materials .....	25
3.1.1. Insulation.....	27
3.1.2. Glass.....	27
3.1.3. Iron material.....	27
3.1.4. Wood.....	27
3.1.5. Thermocouple .....	27
3.1.6. Solar radiation program .....	28
3.1.7. Pyranometer .....	30
3.2. Methods .....	31
3.2.1. Irradiance calculation.....	31
3.2.2. Measurement flow rate.....	31
3.2.3. Uncertainty.....	32
3.2.4 Performance Calculations .....	33
4. RESULTS AND DISCUSSION.....	35
4.1. Results of the Storage Collector .....	35
4.1.1. Under Iraqi Weather Conditions .....	35

	<b>Page</b>
4.1.2. Results of the Storage Collector under Turkish Weather Conditions.....	45
4.1.3. The Comparison Between Iraq and Turkey .....	53
4.2. Efficiency of the Proposed Storage Collector.....	58
5. CONCLUSIONS AND RECOMMENDATIONS .....	65
REFERENCES .....	67
GENİŞLETİLMİŞ TÜRKÇE ÖZET .....	71
(EXTENDED TURKISH SUMMARY) .....	71
CURRICULUM VITAE .....	75



## LIST OF TABLES

<b>Table</b>	<b>Page</b>
Table 1.1. Uncertainty of the experimental device .....	32
Tabel 4.1. Calculate the efficiency of the wedge collector without load.....	62
Tabel 4.2 Efficiency of the wedge collector (0.2 liters/min -Iraq and Turkey).....	63
Table 4.3. Efficiency of the wedge collector (0.4 liters/min Turkey and Iraq).....	65





## LIST OF FIGURES

<b>Figure</b>	<b>Page</b>
Figure 1.1. Thermosyphon system (Duffie and Beckman, 1980). .....	2
Figure 1.2. Forced circulation system (Duffie and Beckman, 1980). .....	3
Figure 1.3. Rectangular storage collector (Joudi et al, 2004).....	3
Figure 1.4. Triangular storage collector (Ahmed, 2018).....	4
Figure 1.5. Numerical study of wedge collector (Ahmed, 2018).....	5
Figure 1.6. PV/storage collector (Abdullah, 2019). .....	6
Figure 1.7. Distribution of the total installed capacity in operation by collector type (Mauthner F, 2014). .....	7
Figure 2.1. Photo and Schematic diagram of the integrated solar water heater (Alawi, 2004).....	10
Figure 2.2. The experimental set up showing the central receiver cum storage tank along with the reflecting mirrors (Zakariya, 2014).....	11
Figure 2.3. Assembling cylinder of solar water heater (Al-shamkhi, 2016). .....	12
Figure 2.4. Cylindrical storage collector (O.K.Ahmed, 2017).....	13
Figure 2.5. Photo of two units of built in storage type solar water heater suitable for urban use (Garg, 1974).....	14
Figure 2.6. (A) Diagram of the positioning of the temperature sensors within the cavities; (b) photo of the device (Fraisseaet al, 2014).....	14
Figure 2.7. Three types of storage solar collector. ....	15
Figure 2.8. Exploded view of new ICS-SWH design (Garnieret al, 2018).....	16
Figure 2.9. Schematic diagram of triangular built-in-storage solar water heater with baffle plate (Kaushik, 1994). .....	17
Figure 2.10. Front view of the integrated collector storage solar water heater. ....	18
Figure 2.11. Schematic diagram of the integrated solar collector-storage tank (Mohamad, 1997). .....	19

<b>Figure</b>	<b>Page</b>
Figure 2.12. Modified cuboid solar integrated-collector-storage system.....	19
Figure 2.13. System with Baffle plate (Garge and Rani, 1982). .....	20
Figure 2.14. General arrangement of the Hybrid Photovoltaic/Solar Thermal (HyPV/T)module. ....	21
Figure 3.1. The experimental model implemented in the city of Kirkuk - Iraq. ....	26
Figure 3.2. The experimental model implemented in the city of Van – Turkey. ....	26
Figure 3.4. Digital Thermometer.....	28
Figure 3.5. Solar radiation program. ....	30
Figure 4.1. Variation of solar radiation for Kirkuk city. ....	36
Figure 4.2. Variation of storage average temperature of the collector without load under Iraqi weather conditions. ....	37
Figure 4.3. Variation of maximum water temperature of the collector without load under Iraq weather conditions. ....	37
Figure 4.4. Effect of load (0.2 liters/min) on the system temperature under Iraqi weather conditioning. ....	38
Figure 4.5. Effect of load (0.4 liters/min) on the system temperature under Iraqi weather conditioning. ....	39
Figure 4.6. Effect of load (0.2 liters/min) on the system temperature under Iraqi weather conditioning. ....	40
Figure 4.7. Effect of load at (0.4 liters/min) on the system temperature under Iraq weather conditioning. ....	40
Figure 4.8. Effect of load at (0.2 liter/min) on the system temperature under Iraq weather conditioning. ....	41
Figure 4.9. Effect of load at (0.4 liter/min) on the system temperature under Iraq weather conditioning. ....	42
Figure 4.10. Variation of outlet temperature of the wedge collector on typical winter, spring and summer days with load 0.2 liter/min. ....	43

<b>Figure</b>	<b>Page</b>
Figure 4.11. Variation of outlet temperature of the wedge collector on typical winter, spring and summer days with load 0.4 liter/min. ....	43
Figure 4.12. Variation of solar radiation for Van city. ....	44
Figure 4.13. Variation of mean water temperature without load under Turkish weather conditions. ....	45
Figure 4.14. Maximum water temperature changes without load within Turkey weather conditions. ....	45
Figure 4.15. Effect of load (0.2 liters/min) on the system temperature within Turkey weather conditions ....	46
Figure 4.16. Effect of load (0.4 liters/min) on the system temperature under within Turkey weather conditions. ....	47
Figure 4.17. Effect of load at (0.2 liters/min) on the system temperature within Turkey.....	48
Figure 4.18. Effect of load (0.4 liters/min) on the system temperature within Turkey weather conditions. ....	48
Figure 4.19. Effect of load (0.2 liters/min) on the system temperature within Turkey weather conditions. ....	49
Figure 4. 20. Effect of load (0.4 liters/min) on the system temperature within Turkey weather conditions. ....	50
Figure 4.21. Variation of outlet temperature of the wedge collector on typical winter spring and summer days with load 0.2 liter/min. ....	51
Figure 4.22. Variation of outlet temperature of the wedge collector on typical winter, spring and summer days with load 0.4 liter/min. ....	52
Figure 4.23. A comparison of the mean temperature for the winter between the Turkey and Iraq conditions without load.....	53
Figure 4.24. A comparison of the mean temperature for the spring between the Turkey and Iraq conditions without load.....	54
Figure 4.25. A comparison of the mean summer temperature between Turkey and Iraq conditions without load. ....	54

<b>Figure</b>	<b>Page</b>
Figure 4.26. Variation of maximum storage temperature of wedge collector on winter days Iraq and Turkey conditions without load. ....	55
Figure 4.27 Variation of maximum storage temperature of wedge collector on spring days Iraq and Turkey conditions without load. ....	55
Figure 4.28. Variation of maximum storage temperature of wedge collector on summer days Iraq and Turkey conditions without load.....	56
Figure 4.29 Outlet temperatures of the wedge collector with different loads for the summer withload.....	56
Figure 4.30. Comparison mean temperature between the wedge collector and the cylindrical collector in spring day. ....	58
Figure 4.31. Comparison maximum temperature between the wedge collector and the cylindrical collector in spring day .....	58
Figure 4.33. Efficiency of the wedge collector (0.2 liters/day-Iraq and Turkey).....	62
Figure 4.34. Efficiency of the wedge collector (0.4 liters/min day-Turkey and Iraq) ..	63

## SYMBOLS AND ABBREVIATIONS

Some symbols and abbreviations used in this study are presented below, along with Descriptions.

Symbols	Description
$A_{col}$	Absorbed area of the inclined surface.
$Cp_w$	Specific heat of the water.
$I_{solar}$	Absorbed solar radiation on an inclined surface.
$m_w$	The total mass of the water inside the model.
$\dot{m}$	A mass flow rate of water.
$M_i$	Mass of specified slice.
$Q_{useful}$	Heat gain.
$T_{mean}$	The average water temperature inside the collector.
$T_{meanF}$	Mean water temperature at the end of the hour.
$T_{meanS}$	Mean water temperature at the beginning of the (without load).
$T_{OL}$	The outlet water temperature from the model.
$T_{IL}$	The inlet water temperature from the model.
$\eta$	Instantaneous collector efficiency.
$T$	Temperature



## 1. INTRODUCTION

The world has switched to alternative energy sources for science, environmentally sustainable emission mitigation from costly fossil fuels which is expected to be introduced in the coming years. The studies and experiments undertaken by scientists as a result of the rising need for energy. One of its most significant benefits is that it is available in all countries of the world, also does not require high technology as it is easily exploited. The study of solar energy was favored by researchers. If the use of solar energy is divided into three main sections: air conditioning, water heating, and electricity generation (Abdullah and Ahmed, 2019). The use of solar energy is gaining significant interest in the energy systems of different countries. The rapid depletion of fossil fuels and the combined pollution crisis and the dramatic rise in oil prices have contributed to a rapid increase in interest in solar energy.. Three appealing features are solar energy. In the first position, the sun is An infinite supply of electricity, basically. Secondly, all nations with varying amounts have access to this energy and, thirdly, it can be used with limited adverse effects on the climate (Arora and Domkundwar, 1981). The practical applications of solar energy, on the other hand, are not open. From difficulties. At night or during times when the local weather conditions obstruct the sun, solar energy is not available. Moreover, in its essence, solar energy is diffused. It is an energy resource dependent on time. The need for energy for a number of applications is also dependent on time, but in a different way from solar energy. Consequently, if solar energy is to be economically competitive it must be converted into a usable form of energy with maximum effectiveness.

Hot water is required for many purposes and the sun can be used effectively, efficiently, and economically to provide this heat. Solar water heaters generally employ a solar collector and a storage tank. The solar water-heating collector is by far the most widespread solar energy conversion device and there are several million in use around the world. Solar water heating reflects the use of solar energy at a low temperature. In two common device configurations, the basic elements in solar water heaters can be arranged (Duffie and Beckman, 1980). First, the framework of thermosyphons shown in (Figure 1.1). Where the tank is situated above the collector, and when solar energy in

the collector adds energy to the water in the collector leg, water circulates through natural convection and thus creates a density difference.

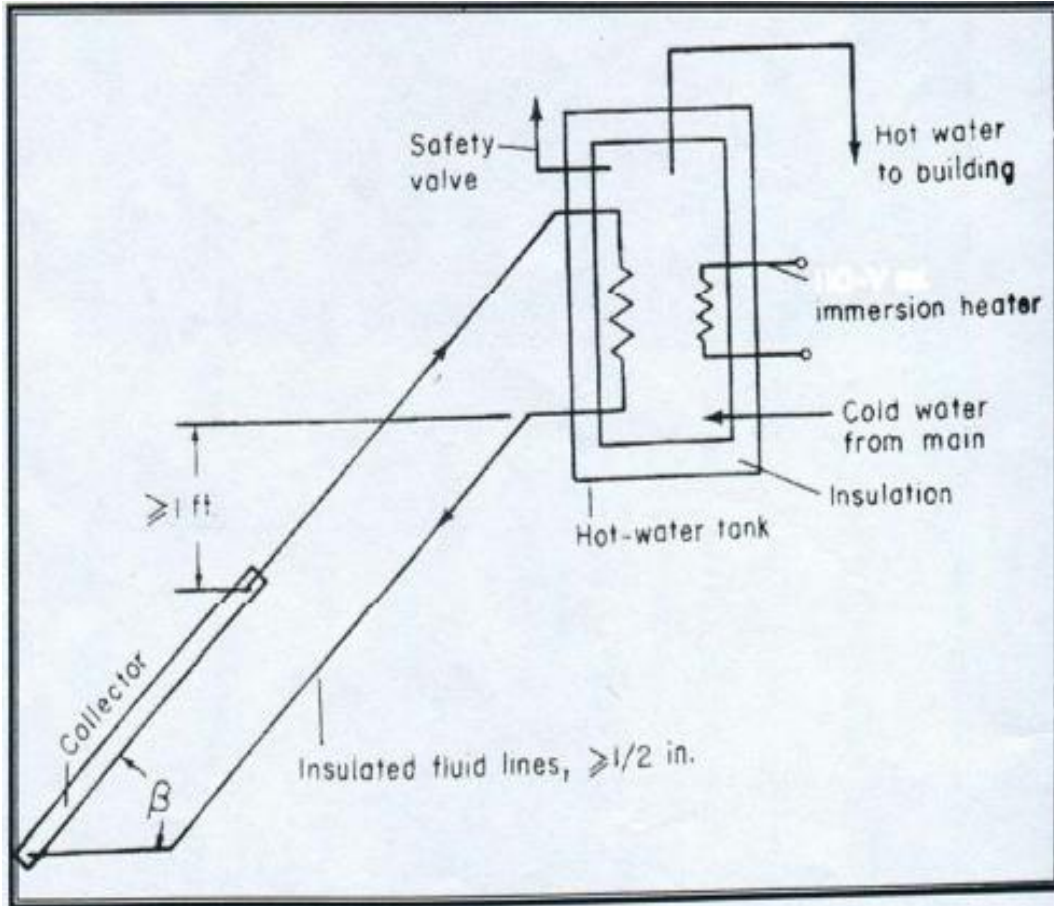


Figure 1.1. Thermosyphon system (Duffie and Beckman, 1980).

An electric immersion, to provide heat during long cloudy periods, it is possible to use the heater as a solar system backup. To improve stratification, the immersion heater is placed near the top of the tank, so that the heated fluid is at the appropriate distribution temperature. The second kind of solar heating system, which is a forced circulation system, is shown in (Figure 1.2). As this analysis deals with a three-dimensional model filled with water that reflects the models in this analysis. The sloping wall is exposed to solar radiation (Joudi, 2004). And the other walls were believed to be insulated in (Figure 1.3).

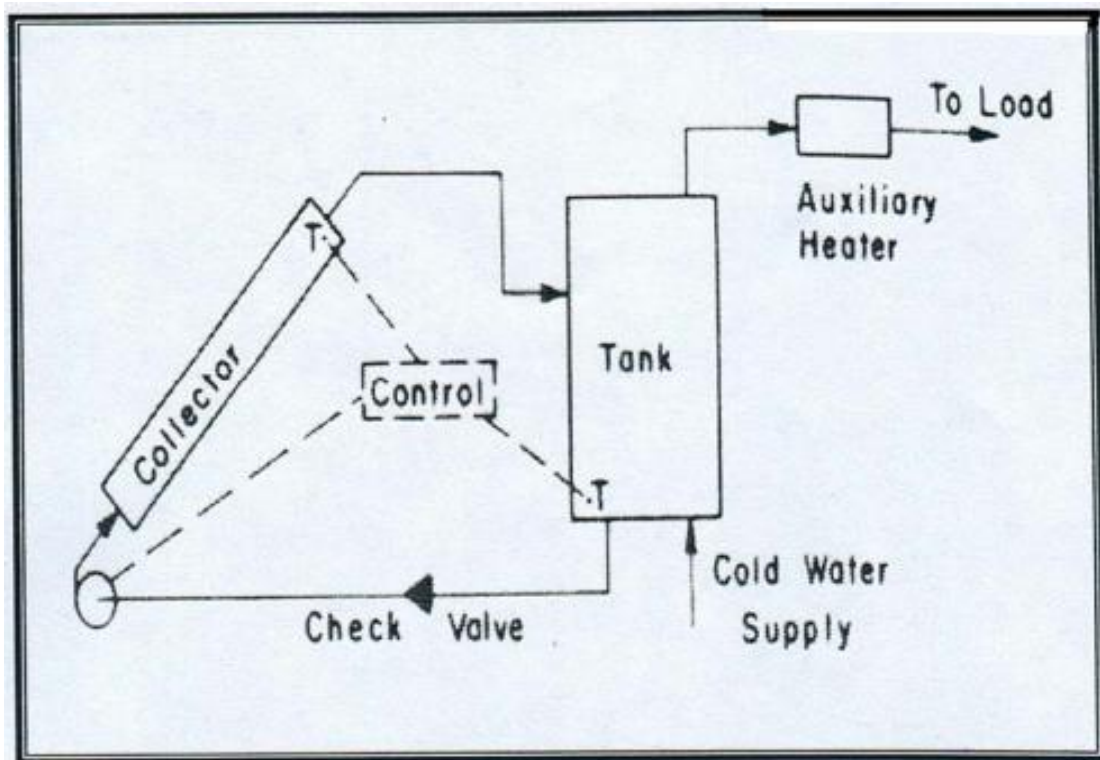


Figure 1.2. Forced circulation system (Duffie and Beckman, 1980).

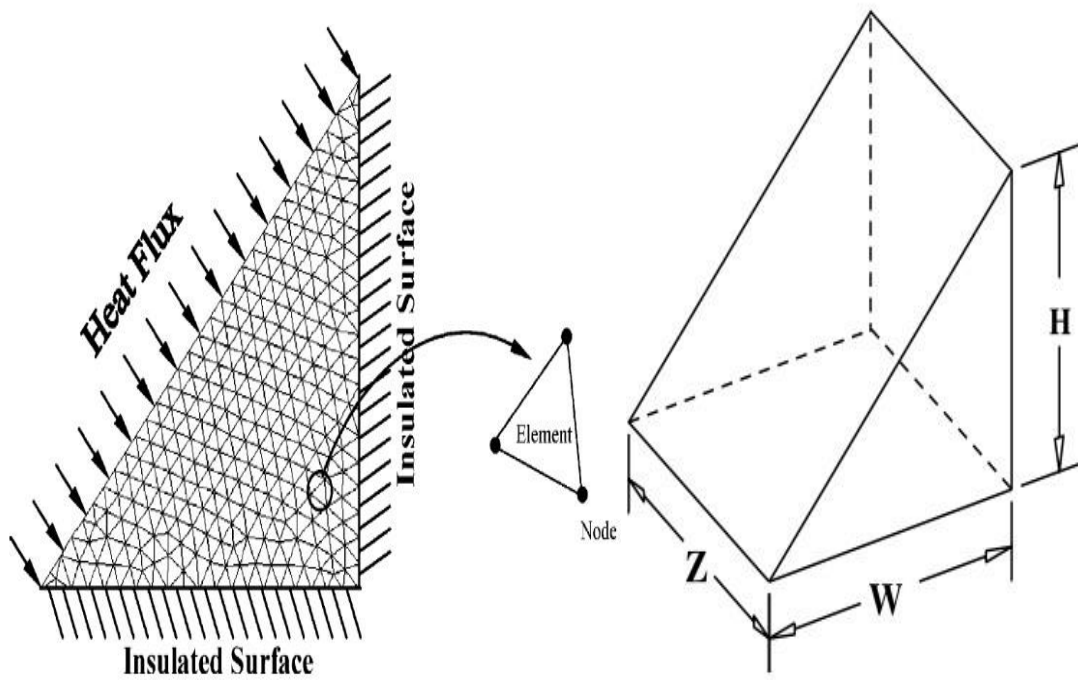


Figure 1.3. Rectangular storage collector (Joudi et al, 2004).

The researcher (Ahmed, 2018) created a new design, which is called the triple storage collector, which is in the form of a triangle, as in (Figure 1.4), which is a cubic piece with two levels, the first level in a vertical plane, and the second level at an angle of 45°. As the size can be controlled depending on the base and the height change. The face exposed to the sun is painted black and covered with a layer of glass to increase the absorption of solar radiation. Where results were obtained without a load in the summer at 57°C of storage water temperature. Efficiency 62%, while in winter, 41°C water temperature was obtained efficiency 48.7%. On continuous loading, he gained efficiency of 55.7% in winter and 65% in summer. The value of this ratio should be more than 12 to supply a sufficient amount of hot water for domestic applications. An energetic analysis of a Photovoltaicthermal integrated system was studied by (Radziemska, 2009).

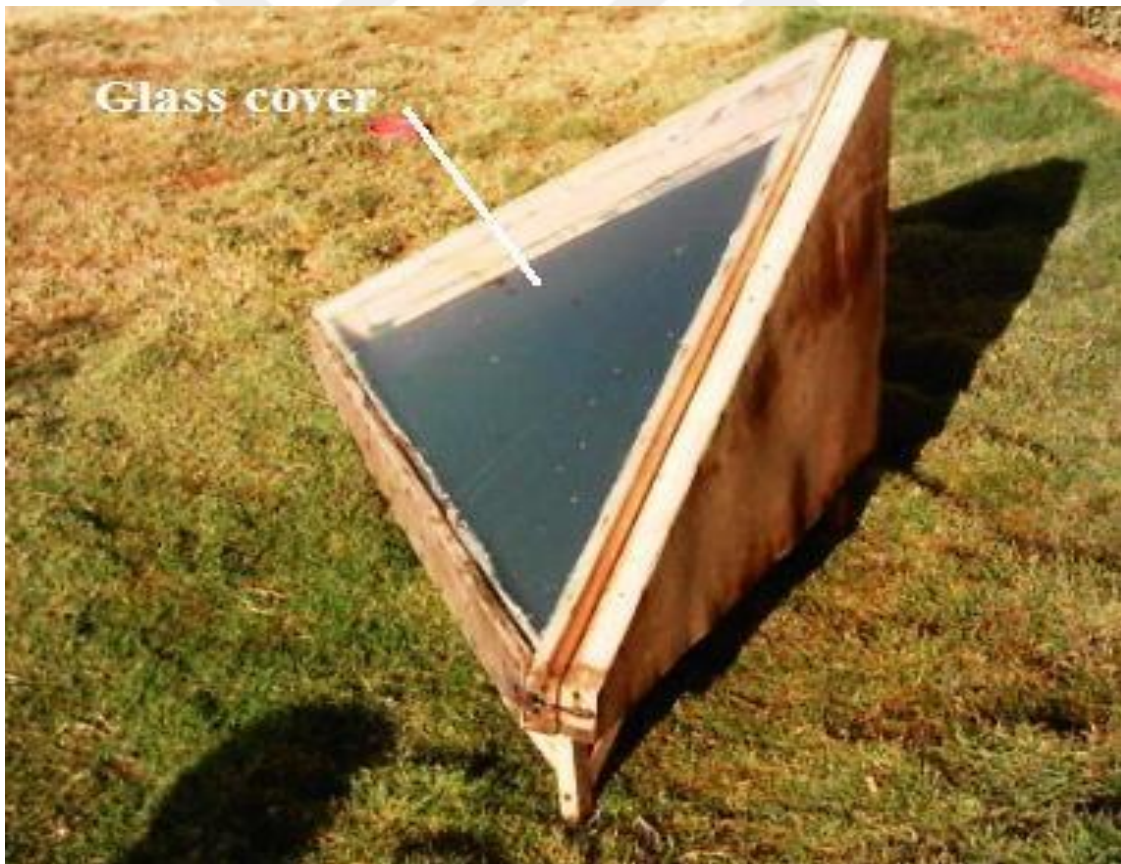


Figure 1.4. Triangular storage collector (Ahmed, 2018).

Where the researcher, (Ahmed, 2018), conducted a numerical study using the FLUENT program for a solar wedge-shaped as shown in (Figure 1.5). The analyzes were conducted, and the average water temperature was obtained at 18 °C on 21<sup>th</sup> December, as well as at 41 °C on 21<sup>th</sup> June. The researcher (Abdullah & Ahmed, 2019 ) studied the rectangular solar collector shown in (Figure 1.6), where cells were mounted on the surface exposed to the sun, where the water within the collector cools the solar cell, improving its efficiency, and the exhausted heat is used for domestic purposes to heat the water. As the results of this study revealed, the temperature of the water coming from the collector at 2 pm reached 42 ° C. It was found that this new design revealed that there is a 4.6 percent difference in temperature between the water inside and outside. When I find the load performance hits 63% in summer, and 37.7% without load.

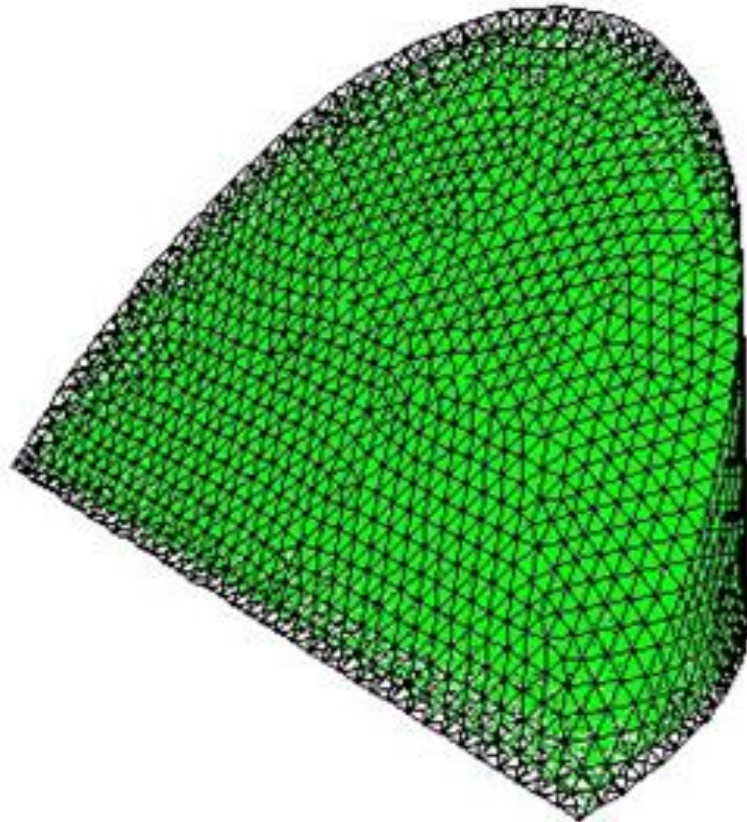


Figure 1.5. Numerical study of wedge collector (Ahmed, 2018).



Figure 1.6. PV/storage collector (Abdullah, 2019).

Thermal energy is needed for water heating, which is one of the basic elements of human beings. In ancient times, this energy was met by primitive methods such as wood burning. The principle of using solar energy to heat water goes back to about 200 b.c. When the Empire of Rome used it to heat public baths. Toward the end of the 19th century, solar water heating (SWH) was invented for industrial use in buildings. In the following years, this system was renovated through a series of upgrades such as antifreeze, thermosyphon, heating control, etc. Today 's environment makes heavy use of solar thermal technologies. An installed capacity of 410.2 GWth was in service worldwide at the end of (Mauthner F, 2014). The global share of solar thermal technologies is shown in (Figure 1.7). In Turkey, with 80.80 percent, water collectors such as flat plate collectors (FPCs) were predominant, followed by evacuated tube collectors (ETCs) with 19.17 percent, and air collectors occupied the remainder. Its inexpensiveness relative to the ETCs is considered the key problem why the FPCs are mostly used in the region.

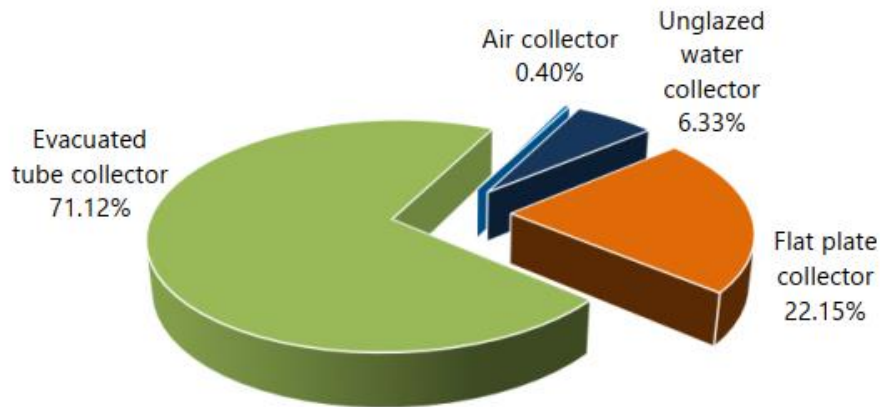


Figure 1.7. Distribution of the total installed capacity in operation by collector type (Mauthner F, 2014).

A variety of studies have been performed in Turkey to determine the optimum angle of tilt for solar collectors, such as zmir (Gunerhan and Hepbasli, 2007), Adana, Ankara, Diyarbakır, Erzurum, stanbul, zmir, Samsun and Trabzon (Bakirci, 2012). Based on the maximization of monthly average global radiation, these studies optimized the tilt angle for the related locations (Ertekin et al, 2008). A techno-economic study was carried out in which the optimal tilt angles were identified for Turkey's 129 geographical locations to optimize the usable heat gain of the SWH system. However, this research considered the determination of the energy requirements for water heating using the universal krigging spatial interpolation process in the ArcGIS software (ArcGIS, 2017). In the literature, the scale modeling of the SWH method for domestic supplies in Turkey is very limited. The modeling of a thermosyphon solar water heater in TRNSYS software[9] was proposed by (Akinoglu et al, 1999). Determine the optimum collector area in nine geographical locations in Turkey, including Iskenderun, Dalaman, Izmir, Istanbul, Sinop, Rize, Kayseri, Mardin, and Muş. Simulations transient (Çomaklı et al, 2012). A transient modeling was carried out for a SWH system operating under Erzurum's climatic conditions. For more economic and effective solar water heating systems, the optimum size for the volume of the storage tank to the collector area was suggested to be 50-70 liter/m<sup>2</sup>.

A collector of solar storage differs from the traditional collector because it combines, in one part, solar collectors and storage tanks. A theoretical and experimental evaluation of the integration of solar cells with the rectangular solar storage collector was performed in this paper. Introduced. Previous studies may show that it is less costly to use the solar collector and has proved its effectiveness. Since it has lower cost and performance, similar to conventional heaters' efficiency. Therefore, researchers have been interested in lowering costs, saving more space and lowering high-cost technology of this kind.



## **2. LITERATURE REVIEW**

A compact solar water heater, where some of the main parts were combined with some to reduce cost and space, as well as searching for improved performance and obtaining the largest amount of hot water stored, as the researchers studied several models and designs of different shapes to obtain the highest efficiency and the lowest cost.

### **2.1 History of solar water heating system for integrated collector storage**

The first solar water heater ICS was demonstrated in the southwest of the USA in the late 18th century. The water in the tank-type ICS (integral collector storage) systems was put out for heating at a few farms and ranches. On clear days, these systems have reportedly provided ample hot water (Smyth, Eames and Norton, 2006). In (Kemp, 1891). The first commercially produced "Climax" device was patented with the intention of implementing it as an ICS solar water heater. In this device, a metal tank was mounted inside a wooden box and a glass cover covered the top part of the box. The system provided hot water on sunny days, up to 38.8 C. Two Pasadena businessmen purchased Clarence's right to produce and sell it in California (Taylor, California Energy Commission. Public Interest Energy Research., & University of California Berkeley. Goldman School of Public Policy, 2007). Further in 1902, Walker (Heilig, 1994a) proposed that the tank be installed in the focal zone of a concentrating mirror. The system was also fitted with a standby gas-fired heater.

The first commercial ICS solar water heater had four cylindrical oval-shaped vessels facing the sun with a flattened surface. The vessel's size and shape had a major influence on solar energy collection (Heilig, 1994b). In addition, Haskell suggested replacing the tubular tanks, mounted within the hot case of the commercialized ICS system, with a flat tank to achieve a greater collector area per unit of tank volume. In order to achieve better heat removal from the absorbing panel, the tank was equipped with spacer elements and fins. In 1936, a closed and exposed single tank was studied in detail at the agricultural Experimental station at the University of California in the US

(A.F, 1936). In the early 1950s, a closed pipe ICS solar water heating system was commercialized and marketed in Japan. The concept was further improved by introducing cylindrical vessels (a combined collector and storage tank), which is still used in many commercial designs (Tanishita, 1970). Many researchers later demonstrated their interests in this field and developed, developed and analyzed many enhanced ICS systems in various parts of the world (Schmidt & Goetzberger, 1990). A few literature-based ICS designs have been discussed (Frid, Mordynskii, & Arsatov, 2012), and Devanarayanan and Murugavel. (Muneer et al, 2006) have also compared the thermal performance of two different designs of built-in storage water heaters. Studied the storage solar collector experimentally and numerically. Where the model was in the form of a prism triangle. They obtained close results between the experimental studies and numerical studies. Experimentally, the average storage temperature was 34 °C in February, when the initial water temperature was 16 °C.

Studied experimental and numerical of an integrated multiple-tank integrated-solar collector storage heater shown in (Figure 2.1). The created a 300-liter model and tested it experimentally. The results showed that the maximum temperature reached 48 °C in February. Where it was found that the results are close to numerical and practical results. Whereas, this integrated solar water heater is suitable for domestic needs in the winter in Iraqi condation (Alawi, 2004).

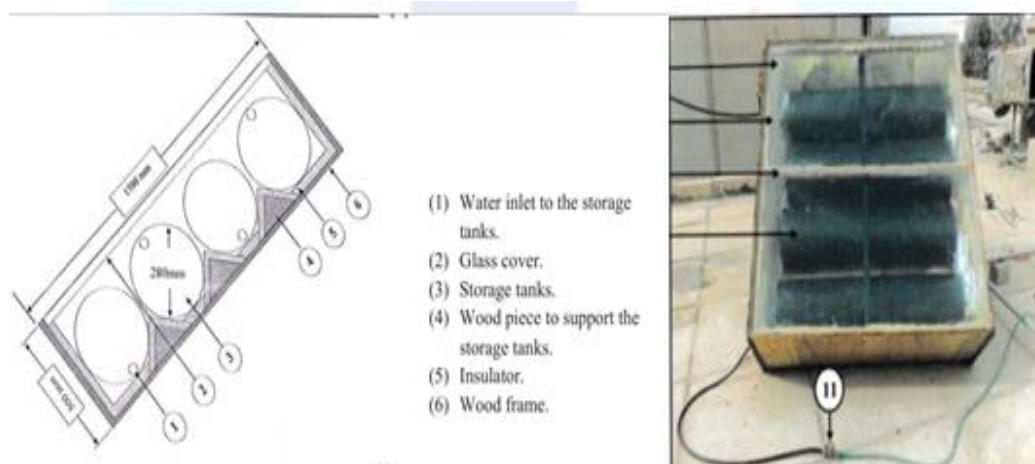


Figure 2.1. Photo and Schematic diagram of the integrated solar water heater (Alawi, 2004).

Where a different type of solar collector heater was studied, where the cylindrical tank was experimentally studied, as in (Figure 2.2), where it is 75 cm long, 50 cm in diameter and 147 liters. To collect the reflected rays, he mounted reflectors on both sides of the storage tank that reflected the rays to the the tank. The maximum temperature was 78.8 °C and the efficiency was 61%. It was noticed that the experimental analysis was similar to the numerical study (Zakariya, 2014).

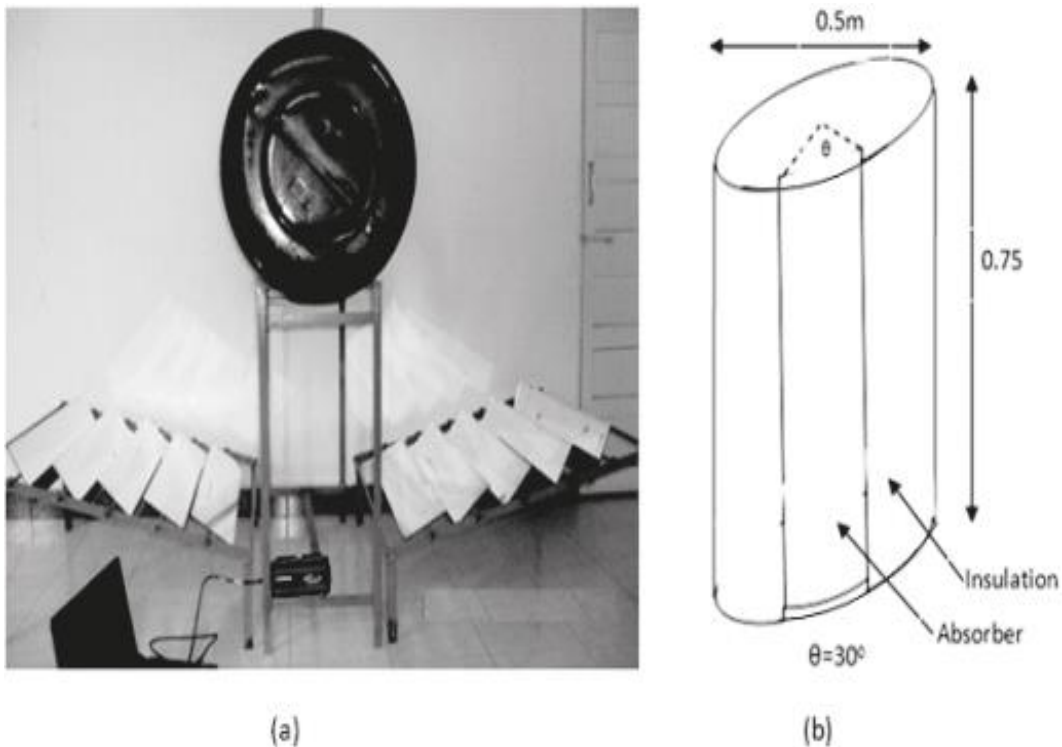


Figure 2.2. The experimental set up showing the central receiver cum storage tank along with the reflecting mirrors (Zakariya, 2014).

An experimental analysis of the storage solar collector has been studied, as this heater consists of a wooden box inside a 1.1 m long and 0.4 m diameter cylinder isolated with glass fibers other than the exposed side of the sun covered with glass as shown in (Figure 2.3). As the cylinder is painted black to increase absorption where it was found that the maximum temperature reaches 36.3 °C between the inlet and outlet of the water, which has a flow rate of 9 kg/hour and efficiency reached 52%, it was found that this system is well used with the lowest cost (Al-shamkhi, 2016).



Figure 2.3. Assembling cylinder of solar water heater (Al-shamkhi, 2016).

A numerical and experimental analysis of the cylindrical storage collector has been investigated shown in (Figure 2.4). It consists of cutting the cylinder by  $45^\circ$  to maximize absorption, the slanted surface is painted black and filled with glass. To prevent heat loss, all other components were insulated with glass fibers. An average temperature of  $25^\circ\text{C}$  was obtained, while a rectangular is  $23^\circ\text{C}$  was obtained under the same conditions in a spring day. when the temperature of the water inlet was  $12^\circ\text{C}$ . The cylindrical collector has been found to be comparable to conventional flat heaters in terms of performance. Also, he found the results of the experimental and numerical study similar (Ahmed, 2017).

Experimentally tested the built-in rectangular storage solar water heater ( $144 * 72 * 6$  cm). Where made of galvanized iron the front surface exposed to the sun is painted black to increase the absorption of solar radiation. Cover the front face with a 2 mm thick glass. the bottom and sides are insulated with glass fibers to reduce heat loss. Where the maximum temperature of  $76^\circ\text{C}$  in August in the bright days (Yassen et al, 2018).



Figure 2.4. Cylindrical storage collector (O.K.Ahmed, 2017).

The 90-liter solar water heater comprising a rectangular tank ( $1.12 * 0.8 * 0.1$  m) shown in (Figure 2.5) has been improved. Which performs the dual role of heat absorption and storage in Jodhpur at the same time that experiments were performed. Where a 70% performance factor has been achieved. The temperature was  $50-60$  °C in the winter and  $60-70$  °C in the summer. Tests indicate that an amount of hot water can be obtained in the early morning if the heater is covered with an insulating blanket overnight (Garg, 1975).

Studied an experimental study of a new design for a solar collector, whose dimensions ( $1.3 * 0.6 * 0.1$  m) are divided into three layers, as shown in (Figure 2.6). Approximate results were obtained for numerical results (Fraisseaet al, 2014).

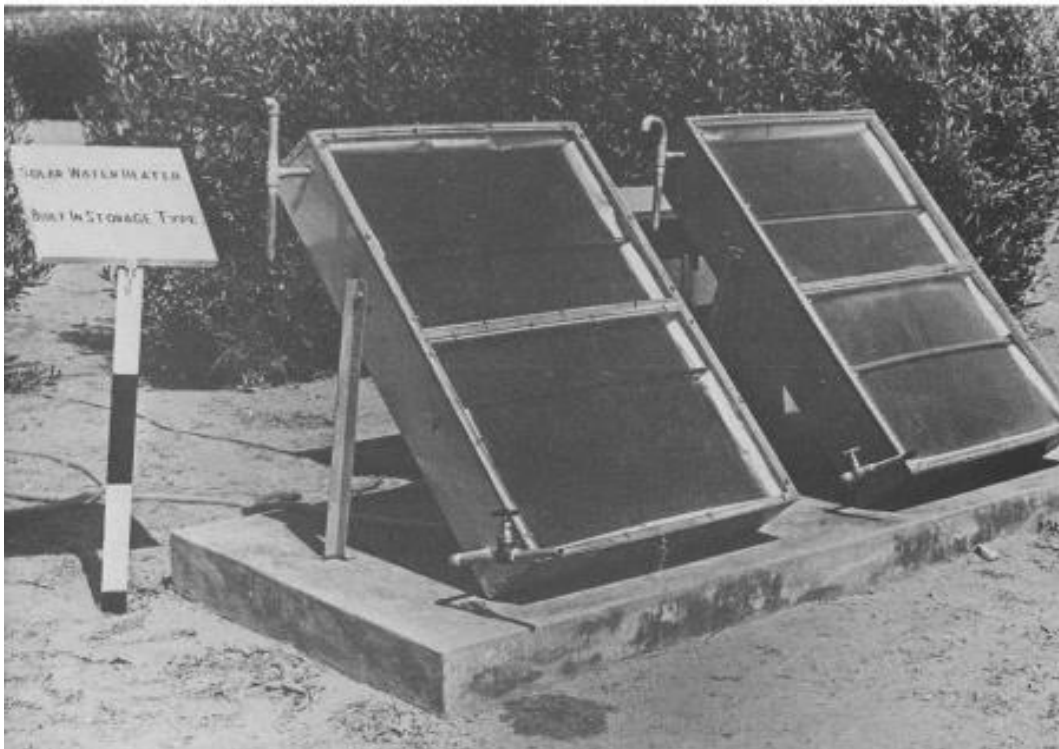


Figure 2.5. Photo of two units of built in storage type solar water heater suitable for urban use (Garg, 1974).

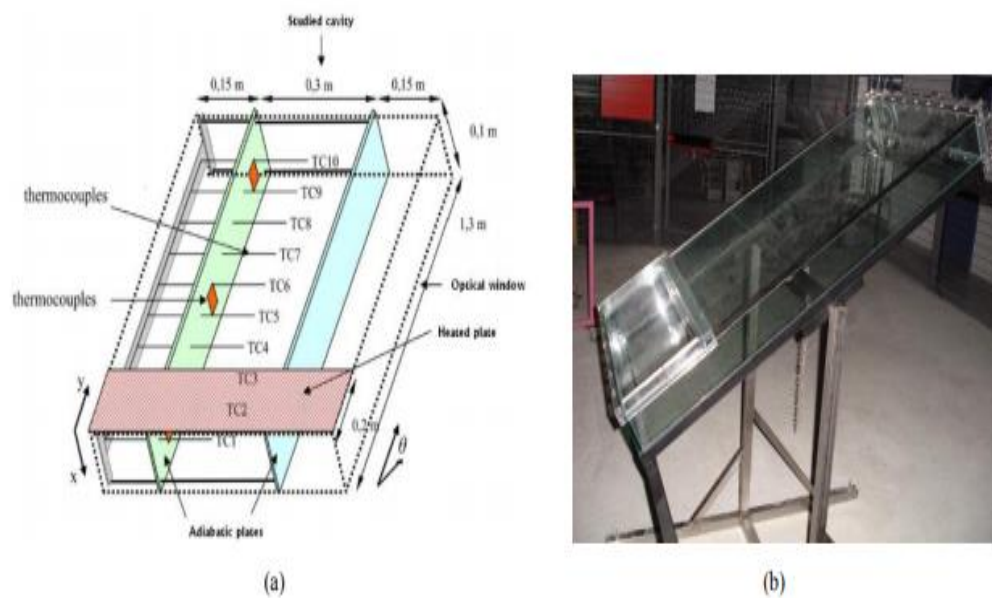


Figure 2.6. (A) Diagram of the positioning of the temperature sensors within the cavities; (b) photo of the device (Fraisae et al, 2014).

Studied an experimental and numerical study on solar energy collectors to heat water and its suitability for home use. This collector can be used to store and heat water simultaneously. It can replace the existing tank in the house. He conducted a study on the effect of the absorption plate surface shape on the performance of the solar energy storage collector. He built three compact storage collectors that are similar in shape and size, but the surfaces have different wavy and flat shapes, as in (Figure 2.7). Experiments were conducted in the summer and fall seasons. The results indicated a similar theoretical computation and could be used to provide hot water for domestic use. The results indicated that the heater with a winding surface is better to obtain a high temperature than other designs due to the increase in the surface area (Ahmad and Ali, 2014).



Figure 2.7. Three types of storage solar collector.

Where researchers studied on the storage of the integrated solar collector, which is a simple integrated composition of water heating by the sun. It combines the solar collector and storage tank in one unit. Previous studies have shown great requirements for hot water at the lowest possible cost. The design was studied as in (Figure 2.8) and good results were obtained at the lowest cost (Garnieret al, 2018).



Figure 2.8. Exploded view of new ICS-SWH design (Garnier et al, 2018).

Provided an enhanced storage solar collector analysis the solar water heater consisted of a rectangular insulated tank measuring with its top surface suitably blackened and coated with glass, (1.22 \* 0.9 \* 0.2) m. The collector serves as a holding tank in this system. They noticed that the heater could store a considerable amount of heat for an appreciable duration after collecting solar energy during the day if the top glass sheet is protected by sufficient insulation during the night. Analytical terms for transient water temperature have been derived and their findings were found to be in good agreement with the reported hourly results. Water temperature in the tank collector (Sodha et al, 1972).

Experimentally investigated the airflow of laminar convection in two-dimensional triangular enclosures with heated and cooled two-sided walls and an adiabatic bottom. The use of a Wollaston prism schlieren interferometer obtained both local and overall heat transfer results. The number of Grashofs ranged between  $2.9 * 10^6$  and  $9 * 10^6$ . Compared with previously collected isothermal inclined flat plate data and rectangular enclosure data, the results align with the results of the rectangular enclosure (Flach et al, 1979).

Experimentally investigated the airflow of laminar convection in two-dimensional triangular enclosures with heated and cooled two-sided walls and an adiabatic bottom. The use of a Wollaston prism schlieren interferometer obtained both local and overall heat transfer results. The number of Grashofs ranged between  $2.9 \times 10^6$  and  $9 \times 10^6$ . Compared with previously collected isothermal inclined flat plate data and rectangular enclosure data, the results align with the results of the rectangular enclosure (Flach et al, 1979).

As shown in (Figure 2.9), the built-in triangle solar water heater was studied. Where the galvanized iron gauge 20 was made, where the sun's exposed surface area is  $1 \text{ m}^2$ , where it was painted black, and where the glass was put over it was 3 mm thick. The tank is insulated by glass fibers on all sides to eliminate thermal losses. The tank was divided into two halves by means of a baffle baffle insulating plate, where the water is divided into two halves, and communication is made by means of holes in the parapet board, and it was found that the circular barrier reduces thermal losses during the night (Kaushik et al, 1995).

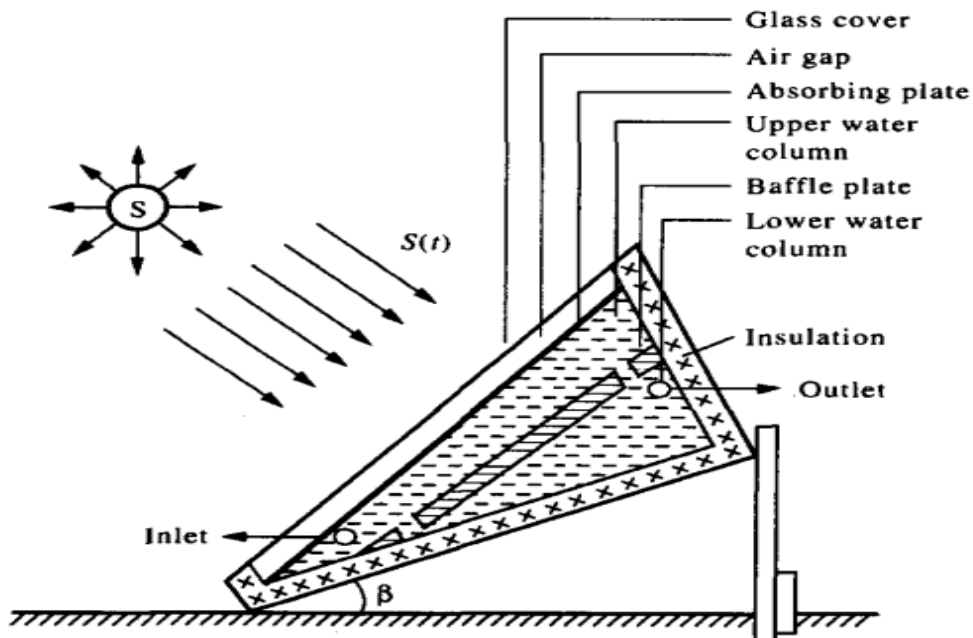


Figure 2.9. Schematic diagram of the triangular solar water heater built-in-storage with baffle plate (Kaushik, 1994).

A cubic galvanized steel tank (88 \* 88 \* 78 cm) was tested, as shown (Figure 2.10). Its walls face the southeast, the southwest, the northwest and the northwest. To improve absorption, the tank was painted black and was coated with a transparent insulating material to minimize heat loss. The bottom surface was made of insulation from polystyrene domestic use at a low cost has been discovered to meet (Atish, 2013).



Figure 2.10. Front view of the integrated collector storage solar water heater. (Atish, 2013).

An experimental study of a cubic water tank by Muhammad studied a piece at a 37-degree angle which is removed (0.5 \* 0.78 \* 0.5 m) as in (Figure 2.11). The front surface is painted black a glass was placed over the paint at a distance of 2.5 cm. All sides were insulated with insulation to reduce heat loss. Where 50% efficiency was obtained, the numerical and experimental studies have similar results (Mohamad, 1997).

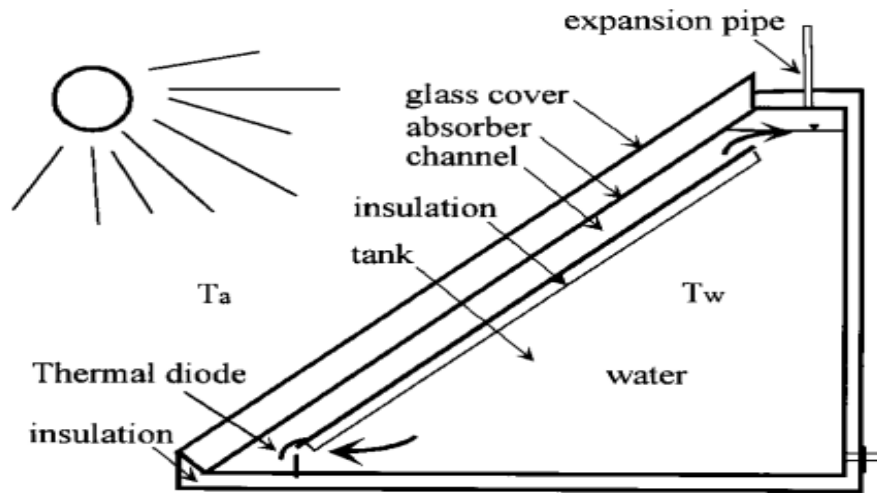


Figure 2.11. Schematic diagram of the integrated solar collector-storage tank (Mohamad, 1997).

Studied a numerical of a storage solar collector and heating water in the same time, that is, combining the storage reservoir and the collector, as in (Figure 2.12). He isolated the collector from all directions except for the exposed parts of the sun to reduce thermal losses, especially at night. A complete study was conducted to evaluate the heat transfer properties inside the heater as the tests were done numerically, good results were obtained and the cost was reduced (Sridhar and Reddy, 2007).

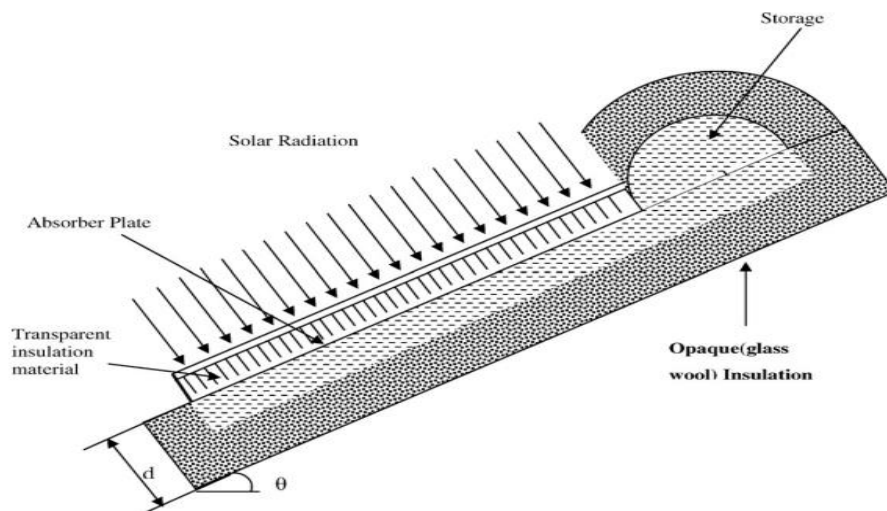


Figure 2.12. Modified cuboid solar integrated-collector-storage system.

Theoretically and experimentally, examined the influence of during cooling hours, use an insulation cover and also use an insulated baffle plate within the tank to the absorber plate, as shown in (Figure 2.13). The solar water heater was a  $1.12 * 0.8 * 0.1$  m rectangular galvanized steel tank with a capacity of 90 liters. In Delhi, the heater was inclined at  $45^\circ$  from horizontal and was focused in the winter season due south. In theoretical research, by solving the mathematical model consisting of energy balance equations written for different collector nodes, the transient output of the device was predicted. To make a theoretical model that can simulate the solar collector by using a computer, these equations have been transformed into the finite difference form. It was found that the efficiency of the collector could be improved by 70% by using the insulation cover. The use of a baffle plate enhances both daytime and night time efficiency also, if the device with the baffle plate was shielded, it was noticed that with night time insulation, it can supply ample hot water up to  $55^\circ\text{C}$  in the the early hours of the morning (Garge and Rani, 1982).

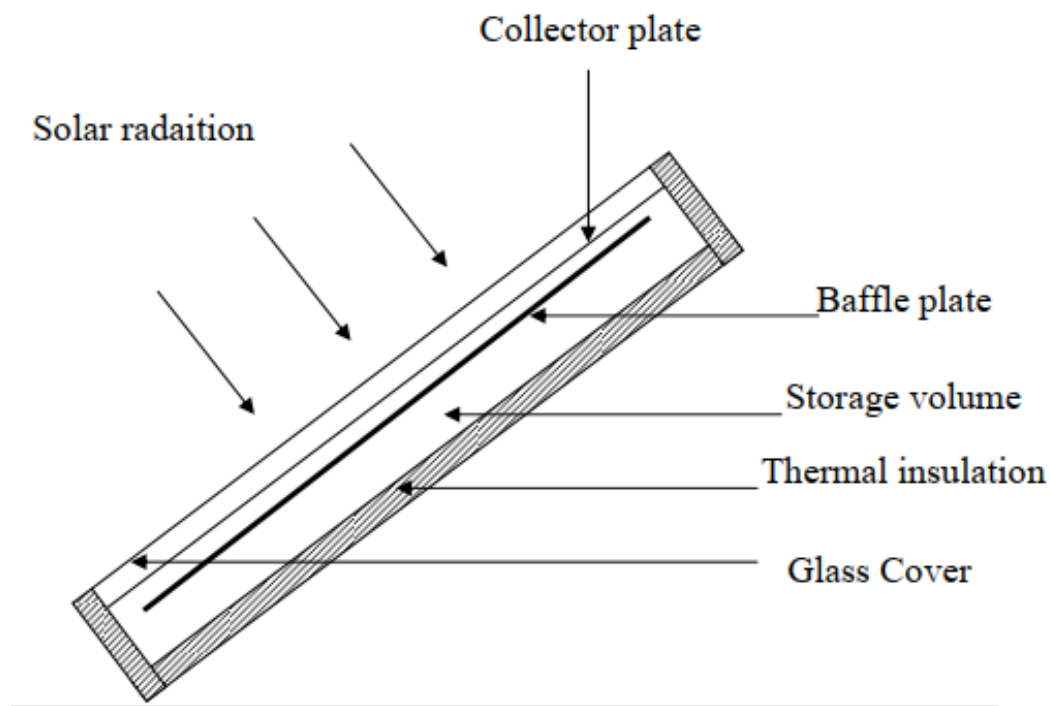


Figure 2.13. System with Baffle plate (Garge and Rani, 1982).

Has conducted practical experiments in hybrid solar (HyPV/T ) technology for that use solar thermal storage technologies shown in (Figure 2.14). It provides low-cost energy and also collects thermal energy for home use. He conducted the experiment at Ulster University where he patented the study. It warms the place or heating water for domestic purposes, as well as obtaining electrical energy through the cells at the front of the collector. Where efficiency was found lower compared to flat heaters (ICSSWH) in simulation conditions (Smyth et al, 2019).

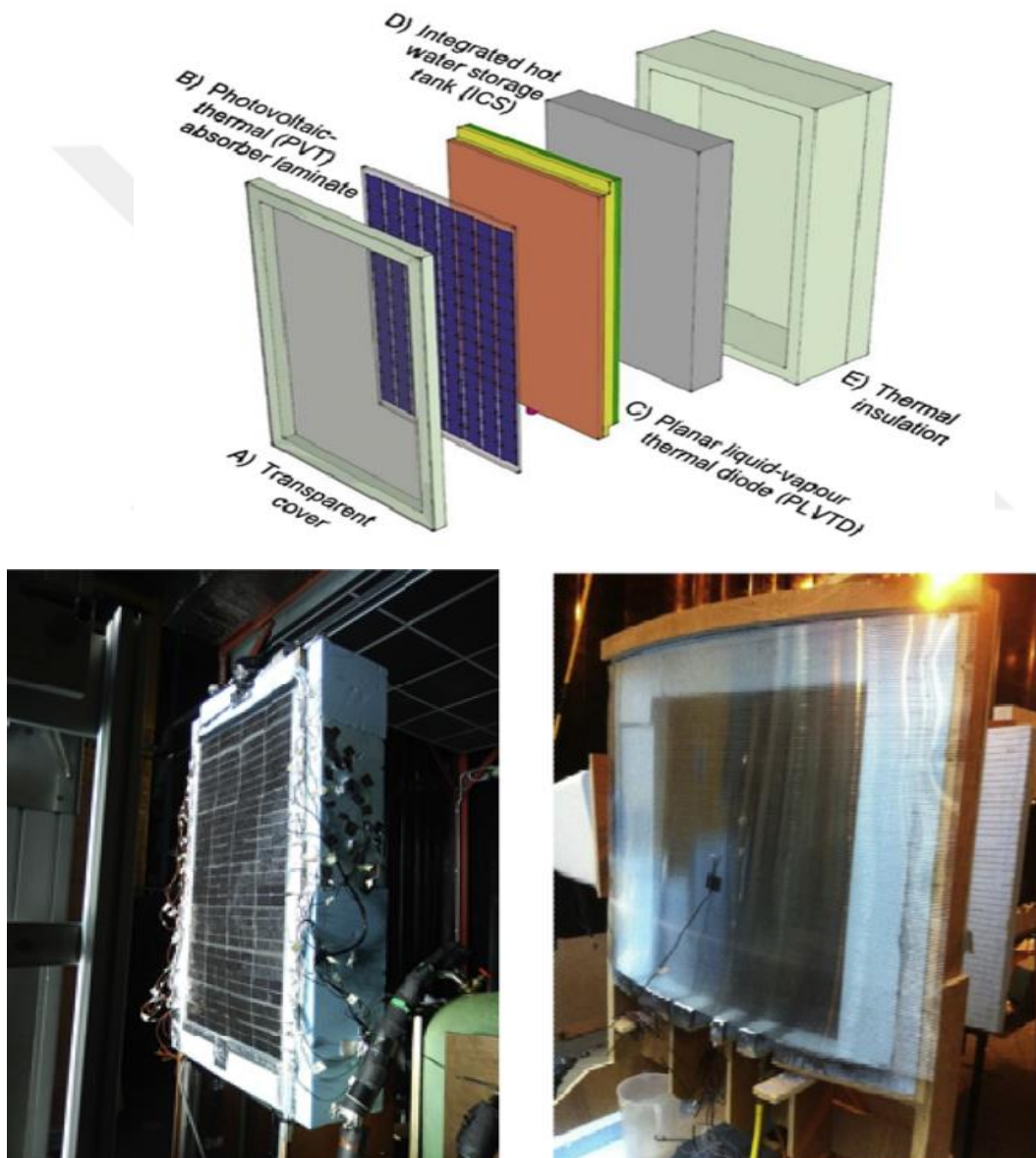


Figure 2.14. General arrangement of the Hybrid Photovoltaic/Solar Thermal (HyPV/T) module.

Transmission of heat into natural convection over a sinusoidal horizontal plate was conducted as a computational and experimental investigation. The topographical laser method was used to visualize the natural convection above the horizontal sinusoidal plate good information was provided on the flow structure. The equations were discretized by the finite volume method. The simple algorithm made sure the pressure and velocity fields were related. To stop solution oscillations and to track changes in the variable values between successive iterations and to avoid solution divergence, relaxation factors were used. Normal convection was significantly affected by the presence of protuberances compared with the case of a horizontal plane plate. A re-circulating motion of the fluid was found in the hollows of the sinusoidal profile of the plate. In both numerical and experimental visualization efficiency, this pattern was demonstrated (Pretot et al, 2000). The results of the average Nusselt number indicate a relatively strong dependence on the angle of inclination in an experimental study of three-dimensional natural convection heat transfer from isothermal inclined disks and rings facing upward and downward. With a choice of Rayleigh numbers, the experiments covered the laminar region of 106 orders in air (Abdul-lateef, 2002).

Numerical simulations of enhancement of heat transfer and pumping of a achieved the piezo-actuated diaphragm. The efficiency of a vibrating diaphragm as an air mover for convection cooling enhancement was assessed using an axi-symmetric finite volume simulation. For the steady state scenario, the commercial code Fluent was used with under relaxation to overcome. At 0.1 for pressure and 0.3 for momentum, the under relaxation was set. This was done to avoid diverging from the solution (Kramer, 2002).

It is important for us to study the issue of heat storage for its uses in solar energy many studies were conducted by the authors. Where most researchers model heat transfer by forced heat transfere, though interest in natural heat transfer is concerned. Therefore it is important to take a closer look at natural and forced thermal transfer. Investigated experimentally the performance of two types of home solar heaters, one under nutural heat transfere and the other under forced heat tranfer. The natural load system consists of a flat collector with an area of 1.5 square meters and a storage capacity of 125 liters (Abd-Alghani, 1983). The experiments were conducted in winter

and summer. The performance was evaluated for every hour during the day. The daily average temperature was taken, which allows calculating the solar energy taken during the day. Experiments were conducted in Iraq, Basra city (latitude  $30.76^\circ$  No). Experimenting in loading and non-loading conditions. The performance was evaluated and a maximum temperature of  $65^\circ\text{C}$  was obtained when the water entered  $35^\circ\text{C}$ . Carried out a mathematical investigation for the temperature field inside a hot water storage tank of a solar collector. The effect of the wall on the transient behavior of the storage tank was modeled by solving the energy equation in the fluid domain. Here, the effect of the wall was introduced as a modification to the energy equation in the fluid domain. The analysis takes into consideration the axial conduction of heat in both fluid and solid wall domains, the radial conduction of heat in the wall, and the heat capacity of the wall. Closed form expressions for the temperature field within the fluid domain were obtained. These expressions indicated that the wall tends to decrease the thermal stratification within the tank.

In this research, a different design has been studied from previous research. The form of the wedge, which is a half-cylinder cut at an oblique angle to the sun's angle of incidence, was studied. Throughout the seasons of the year, tests were performed on them, and various results were obtained. Two different places have studied the same model, the first in Iraq and the second in Turkey, and a comparison between them was conducted because there is a difference in temperatures between the two sites, and good results were obtained.



### 3. MATERIALS AND METHODS

The purpose of the study is to test the wedge storage solar collector under the Turkish and Iraqi weather conditions. The tests were performed in two locations, the one in the Iraqi Kirkuk city (35.47° No, 44.39° E), and the other in the Turkish van city (38.5° No, 43.33° E). For this reason, two identical models were constructed. From 9 am to 5 pm, where tests were performed and proof was taken. Modern storage solar collectors differ from the conventional solar water heating system by integrating the collector and the storage tank into one piece of equipment that acts as a solar collector and at the same time as the storage tank. This chapter lists the manufacturing process of these storage solar collectors, the instrumentation used for measurements, and the test procedure.

#### 3.1. Materials

The current research involves a pilot study to conduct a new form of solar collector, called wedge storage solar collector. In Turkey and Iraq, two identical experimental devices have been developed. As shown in (Figure 3.1) and (Figure 3.2), each experimental apparatus consists of a half-cylinder cut at an angle of 45 degrees where the area of surface exposed to the sun is 0.562 m<sup>2</sup>. The height of the tank is 0.5 m, while the radius of the tank was 0.5 m, where it gives a volume of 98.17 liters. Each model was manufactured from 2 mm thick ferrous metal sheets. The front face exposed to the sun is painted black to increase its absorption of solar radiation. To reduce thermal losses from the inclined surface, a glass layer of 4 mm thickness was installed at 3 cm from the inclined black surface within the optimum value for solar collectors (Deceased & Beckman, n.d.). Where the silicon material was put in place to prevent external air leakage from entering the space between the black surface and glass layer (Ahmed and Mohammed, 2017). The wedge solar collector is connected from the bottom to the entry of cold water and from the top of the exit of hot water. The base of the model and the sides for two models were isolated with good thermal insulation with a glass fibers (Ahmed et al, 2020).



Figure 3.1. The experimental model implemented in the city of Kirkuk - Iraq.



Figure 3.2. The experimental model implemented in the city of Van – Turkey.

### **3.1.1. Insulation**

Where glass fibers are used to reduce heat loss they were mounted on the sides with the exception of the side exposed to the sun and mounted in a wooden diaper box, as well as wood to improve insulation. As fiberglass (3 \*1) m and 3 cm thickness were used.

### **3.1.2. Glass**

Ordinary transparent glass that is used in homes is 2 mm thick. In order to improve the thermal insulation, it was used in the form of two layers and of 1 cm between of them. At a distance of 3 cm from the black face of the collector, the glass layer was located.

### **3.1.3. Iron material**

Iron with a thickness of 2 mm was used, where it was shaped like a wedge, where the front surface exposed to the sun was painted black to increase heat absorption.

### **3.1.4. Wood**

It was designed a box to increase the insulation and to protect the insulation content since it was mounted on all sides of the compound, with the exception of the sun-exposed front side.

### **3.1.5. Thermocouple**

Measurement of the performance of solar systems depends on the measurement of temperatures, therefore different thermocouples were installed and distributed in 9 locations. Five thermocouples distributed inside the tank were installed as shown in (Figure 3.3). Two thermocouples were utilized to sense the temperature of the inlet and outlet water from both systems. A thermocouple was used to measure the black surface another thermocouple was used to measure the temperature of the glass. The amount of

flowing water was measured using a rotameter before calibration, the flow meter was checked for scale formation inside the tube. Where a number of Digital Thermometer (tl 8009) were used as shown in the (Figure 3.4). Where all the readings were recorded throughout the day and for every hour. To measure weather conditions such as solar radiation, and temperature.

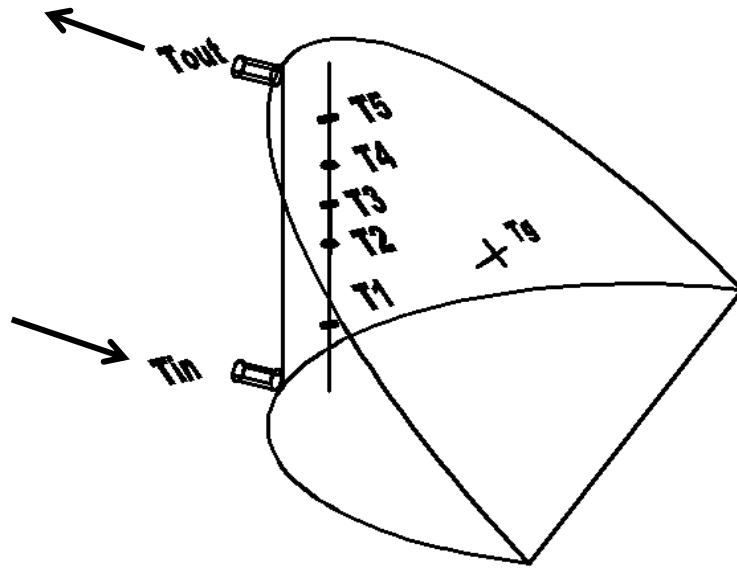


Figure 3.3. Locations of thermocouples inside the experimental set-up.



Figure 3.4. Digital Thermometer.

### 3.1.6. Solar radiation program

The solar radiation was calculated for each day of the experiment. The radiation was taken for every hour on that day through the solar radiation calculation program. And comparing it with the figures taken from the Meteorological Department in Iraq and Turkey. Where the results were found close to the program and the calculations were performed, the results were obtained.

In this program the solar radiation was calculated for each month, day and hour. By entering the latitude and longitude, as well as the month, day and hour. As well as inserting the angle of the solar collector, the solar radiation is obtained per hour, as shown in the (Figure 3.5).

## Determining Solar Versus Local Time

**Step 1:** In the table to the right, enter the local **latitude** and **longitude** angles of the location in degrees. For example, Las Cruces, NM, is at latitude 32.32 degrees north from the Equator and at longitude 106.75 degrees west from the Prime Meridian.

**Step 2:** In the same table to the right, enter the **month** and **day** for which you want to calculate the corresponding **Julian Day** (1–365) of the year, with 1 being Jan 1st and 365 being Dec 31st.

**Step 3:** In the green cells below, enter the local time in the green "Enter the *local* time" cell. Enter the value for the hour using 24-hour time—for example, 2:30 pm would be 14 hours (Hr) and 30 minutes (Min). Finally, enter whether or not Daylight Saving Time is active, along with the corresponding Time Zone

Location's <b>Latitude</b> Angle in degrees	35.46	degrees
Location's <b>Longitude</b> Angle in degrees	106.75	degrees
44.39		
Enter the month and day to calculate the Julian day number:		
<i>Month</i>	<i>Day</i>	<b>Julian Day</b>
December	12	346

	Hr	Min	Time in decimal	
Enter the <i>local</i> time: (hours and min)	10	0	12.00	
Are you in Daylight Saving Time (Y/N)?	N			
Time Zone (use drop-down menu)	Mountain			

Julian Day Number for the 1st Day of Each Month					
Month	n =	Month	n =	Month	n =
January	1	May	121	September	244
February	32	June	152	October	274
March	60	July	182	November	305
April	91	August	213	December	335

Calculations:		
Longitude Correction (B)	262.09	degrees
Equation of Time (E)	5.21	minutes
Local Meridian (degrees West of Greenwich)	45	degrees
Hours before (+) or after (-) solar noon	0.00	hours or <b>0:00 BEFORE solar noon</b>

Time Conversion		
Longitude Correction (B)	262.09	degrees
Equation of Time (E)	5.21	minutes
Local Meridian (degrees West of Greenwich)	45	degrees
Hours before (+) or after (-) solar noon	0.00	hours or <b>0:00 BEFORE solar noon</b>

Local Time Zones		
Eastern	75	degrees West
Central	90	degrees West
Mountain	105	degrees West
Pacific	120	degrees West

Figure 3.5. Solar radiation program.



## 3.2. Methods

### 3.2.1. Irradiance calculation

On the collector surface, the solar radiation incident was measured since, for this reason, a solar meter was currently unavailable at the test site. The sum of solar radiation for each month was therefore taken from the meteorological department for the calculation of hourly incident solar radiation on a tilted surface with a angle of 45° for each day of the year. There was the use of the clear day model. Details the analytical protocol for the assessment of solar intensity under the above-mentioned conditions. As solar radiation hits the surface of the collector, the majority of it is transmitted through the glass, while the glass cover reflects and absorbs the remainder. The absorber plate then absorbs much of the emitted radiation, with the remaining portion being reflected upwards.

Where the software was used to validate the findings taken from the meteorology of solar radiation. As the software in its calculations depends on mathematical equations. It is a general program for any location and any day of the year for measuring the hourly solar radiation. This software relies on the input data the user provides to the program in order to enforce the program and measure the radiation needed.

### 3.2.2. Measurement flow rate

A floating style flow meter was determined by the volumetric flow rate of the water supply through the test rigs. The flow meter was tested for scale formation within the tube previous to the calibration. The flow meter calibration is done using the stopwatch and the graduated container. The volume of liquid flowing from the solar collector was measured by means of a vessel of known size and contains graduations. While measuring the volume of the liquid, the time required for this volume to pass is calculated. If the volume of the passing fluid is  $v$  ( $m^3$ ), and time is  $T$  (min), then the passing flow is  $Q$  ( $m^3/min$ ) “Eq 3.5”.

$$Q = \frac{V(m^3)}{T(min)} \quad (3.5)$$

### 3.2.3. Uncertainty

Analysis of experimental uncertainty is a methodology that analyzes a derived quantity based on the uncertainties in experimentally calculated quantities that are used to calculate that derived quantity in some sort of quantitative relationship. Generally, the model used to translate the measurements into the derived sum is based on fundamental concepts of a discipline of science or engineering. There are two elements of uncertainty, namely bias (related to precision) and the inevitable random variance that occurs when repeated measurements are made (related to accuracy). There may be biases in the calculated numbers, and they certainly have random variation, but what needs to be discussed is how these are 'propagated' through the derived number variability. Detection of uncertainty is also referred to as the "propagation of error."

To evaluate the uncertainty in the experiments is very significant for the check the validity of the performance, the results is calculated by the following relation is given by Kline and McClintock the following relation "Eq 3.6"

$$\omega_R = \sqrt{\left(\frac{\partial U}{\partial x_1} \times \omega_1\right)^2 + \left(\frac{\partial U}{\partial x_2} \times \omega_2\right)^2 + \dots \dots \dots + \left(\frac{\partial U}{\partial x_n} \times \omega_n\right)^2} \quad (3.6)$$

Where uncertainty is one of the tools used in the experiments

Table 1. Uncertainty of the experimental device.

<b>Equipment</b>	<b>Measurement</b>	<b>Error (%)</b>
Solar meter (SM206)	Solar meter (SM206)	(±10 W/m <sup>2</sup> )
Rotameter	Flow rate of water	( ± 1 m <sup>3</sup> /min)
Thermometer (tl 8009)	Temperature	(±1 °C)

### 3.2.4. Performance Calculations

As the heat is lost from the front face of the collector is very important. Which causes a loss of heat absorbed from the air. It is lost by radiation, convection, and outward by the glass segment.

#### 1. No-load conditions

In this process, the compound is filled with cold water in the morning and water is not drawn from it. The heat load of the collector is calculated in the event that no water is drawn from it without a load by the “Eq 3.1”.

$$Q_{useful} = m cp (T_{meanF} - T_{meanS})/3600 \quad (3.1)$$

#### 2. Load conditions

In this case amount of flowing water of load water was controlled by a globe valve at the inlet of the design. The flow rate of the water flow rate is measured by the collected water cylinder over time. The energy collected during with load is calculated by the following “Eq 3.2”.

$$Q_{useful} = [m cp (T_{meanF} - T_{meanS})/3600] + \dot{m} (T_{OL} - T_{IL}) \quad (3.2)$$

#### 3. Average temperature

$T$  It is the average temperature of the water inside the tank and is calculated by the following “Eq 3.3”.

$$T_{storage} = \frac{\sum_{i=1}^n M_i T_i}{M_{total}} \quad (3.3)$$

#### 4. Efficiency

The hourly system efficiency of a novel design is simple the ratio of the useful energy to the total incoming solar energy as “Eq 3.4”.

$$\eta = \frac{Q_u}{A_c I} \quad (3.4)$$

From the experiments conducted on the wedge solar collector, the values were obtained as follows:

$$I_s = 0.79467 \text{ kW/m}^2$$

$$T_{\text{average}} = 28.2 \text{ }^\circ\text{C}$$

$$T_{\text{in}} = 11.3 \text{ }^\circ\text{C}$$

$$A = 0.562 \text{ m}^2$$

$$C_p = 4.18 \text{ kJ/kg }^\circ\text{C}$$

$$m = 97 \text{ kg ( 1 liter of water was taken equal to 1 kg of water)}$$

If these values are substituted in the above formula,

$$Q_u = m \cdot c_p \cdot (T_{av} - T_i) / t$$

$$Q_u = \frac{97 \cdot 4.18 \cdot (28.2 - 11.3)}{9 \cdot 3600} = 0.21219 \text{ kW}$$

$$\eta = \frac{Q_u}{I_s \cdot A_c}$$

$$\eta = \frac{0.21219}{0.79467 \cdot 0.562} = 0.47$$

## **4. RESULTS AND DISCUSSION**

To assess the performance of the proposed collector, two laboratory models were built; one of them was tested under Iraqi weather conditions and the other was under Turkish weather conditions. The two models were directed to the southeast to absorb the most significant amount of solar energy. At the beginning of each day, the glass cover is cleaned of dust, and readings are recorded every hour from 9 p.m in the morning until 6 p.m in the evening. The results were divided into two parts, the first part is test results in the Iraqi Kirkuk city (35.47° N, 44.39° E), and the second part is test results in the Turkish Van city (38.5° N, 43.33° E). The solar collector is located in a southeast direction, so the most appropriate direction is to get the longest time exposed to the sun, to get the higher amount of solar radiation.

### **4.1. Results of the Storage Collector**

#### **4.1.1. Under Iraqi Weather Conditions**

The solar radiation quality for the city of Kirkuk for winter, spring and summer is shown in (Figure. 4.1). For the summer season, the maximum solar radiation amount was 890 W/m<sup>2</sup> at noon, although it was 786 W/m<sup>2</sup> for the spring and 690 W/m<sup>2</sup> for the winter. Due to the clear dust-free weather that diffuses solar radiation, the radiation value was found to be high in the summer season. The amount of solar radiation has a noticeable effect on the rate of temperature rise, as the solar radiation is directly proportional to the increase in temperature. The amounts of solar radiation differ from one region to another, as it depends on the location in terms of longitude and latitude. Where the solar radiation is affected by the dust in the atmosphere as the dust scatters the solar radiation. It is a group of electromagnetic waves, part of which can be seen by the human eye, which is called visible light, while the other parts are not visible, so it is called invisible light. The amount of this energy varies according to the frequency of the wave that makes up the beam, as the amount of this energy increases as the amount of the wavelength increases. Electromagnetic waves have thermal energy it is probable that solar radiation is classified as the amount of solar rays falling in a particular location or

area, so that these rays are capable of producing electricity, since only a small part of the millions of parts of the sun's rays are reaching the Earth, and that small part is responsible for all of the Earth's surface and atmospheric thermal energy. Where we observe the extent of the change in the weather temperature during the experiments, as the air temperature increases with the increase in the amount of solar radiation.

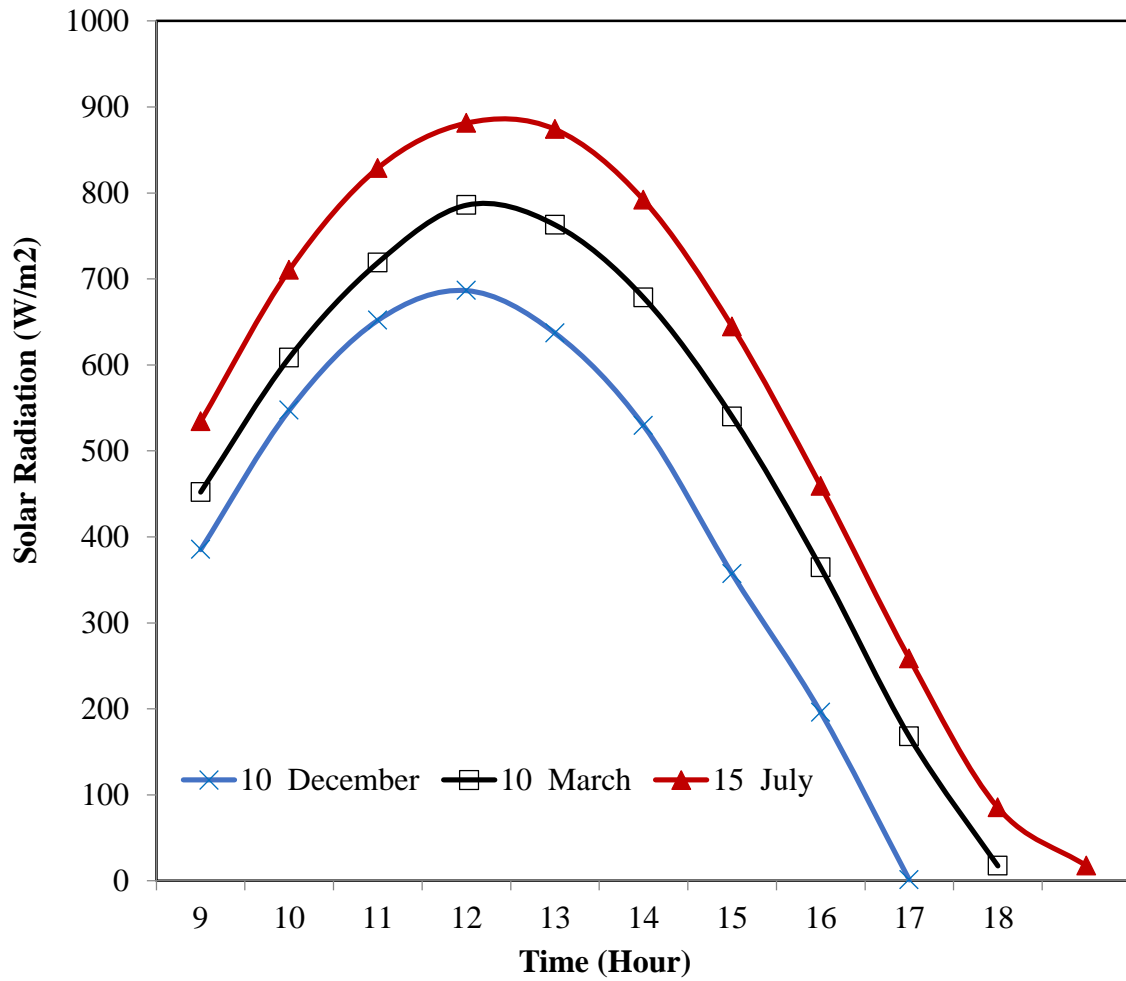


Figure 4.1. Variation of solar radiation for Kirkuk city.

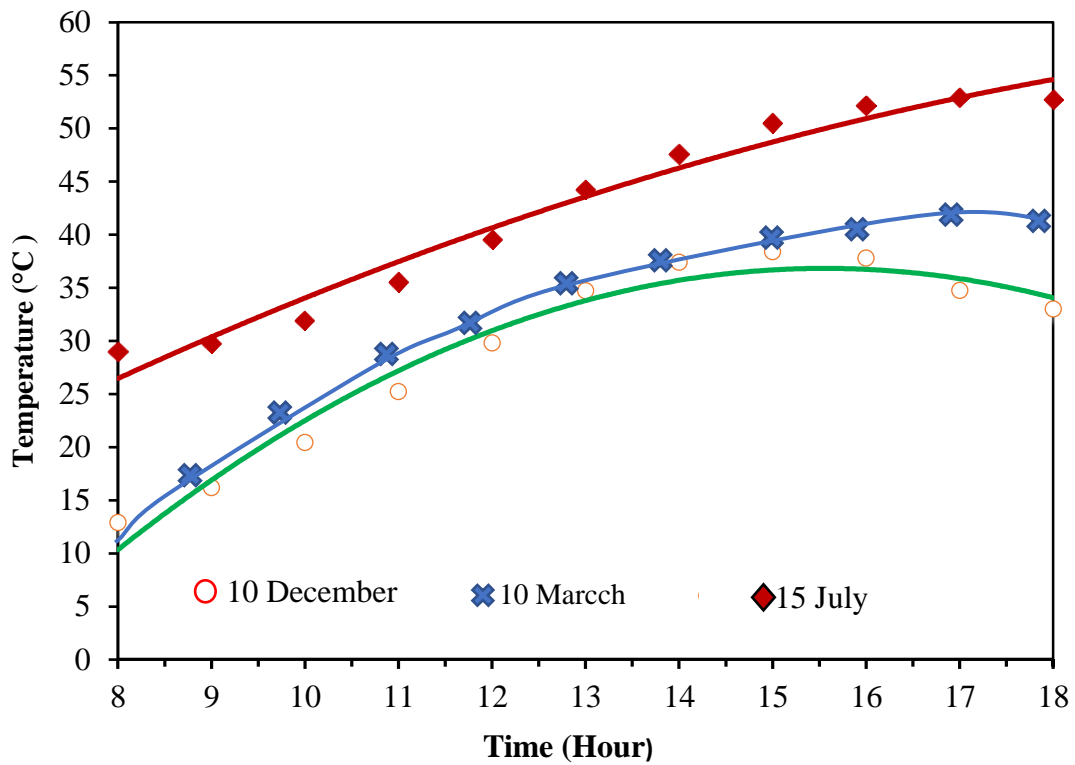


Figure 4.2. Variation of storage average temperature of the collector without load under Iraqi weather conditions.

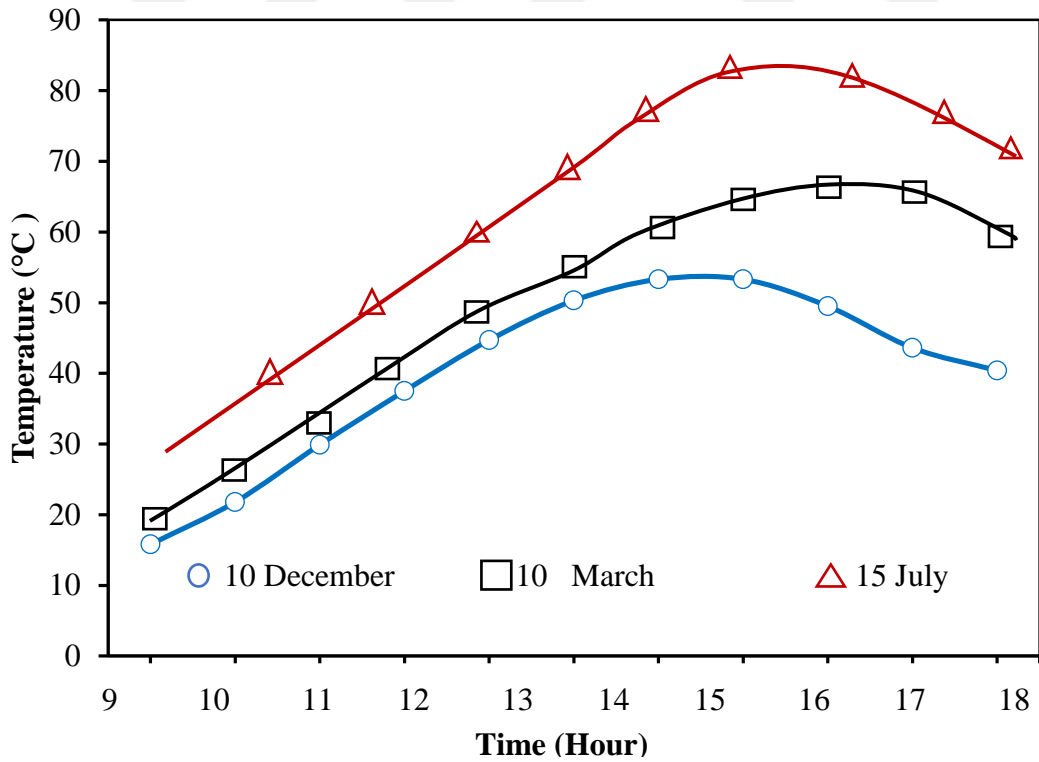


Figure 4.3. Variation of maximum water temperature of the collector without load under Iraqi weather conditions.

Under the Iraqi weather conditions for without load, it is observed that the average storage water temperature changes from the early morning hours to reach its highest value of 53 °C at 5 p.m of 15<sup>th</sup> July. While the maximum average water temperature of storage reached 35 °C on 10<sup>th</sup> December, and 42 °C for 10<sup>th</sup> March under without load conditions (Figure 4.2). It is also observed that, due to the increase in the amount of absorbed solar radiation, the storage water temperature increases during the first half of the day, and then decreases afterwards due to the decrease in the value of solar radiation and the increase in thermal losses from the front side of the collector (Ahmed, 2018). As for the maximum temperature of the solar heater, on 15<sup>th</sup> July, at 4 pm, it reached its highest level of 83 °C. As for the month of 10<sup>th</sup> March, the maximum temperature reached 63 °C at 2 pm, and. While the lowest temperature in 10<sup>th</sup> December reached 48 °C at 12 noon, as shown in the (Figure 4.3).

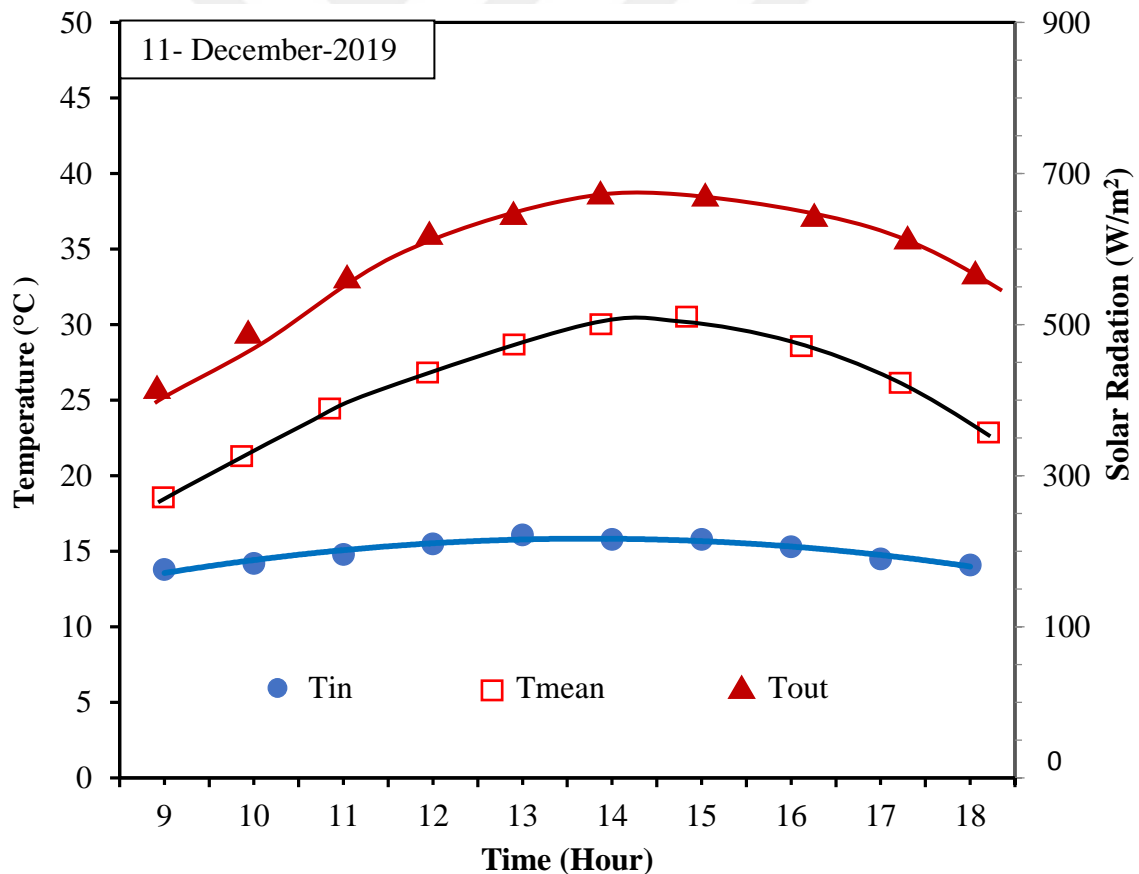


Figure 4.4. Effect of load (0.2 liters/min) on the system temperature under Iraqi weather conditioning.

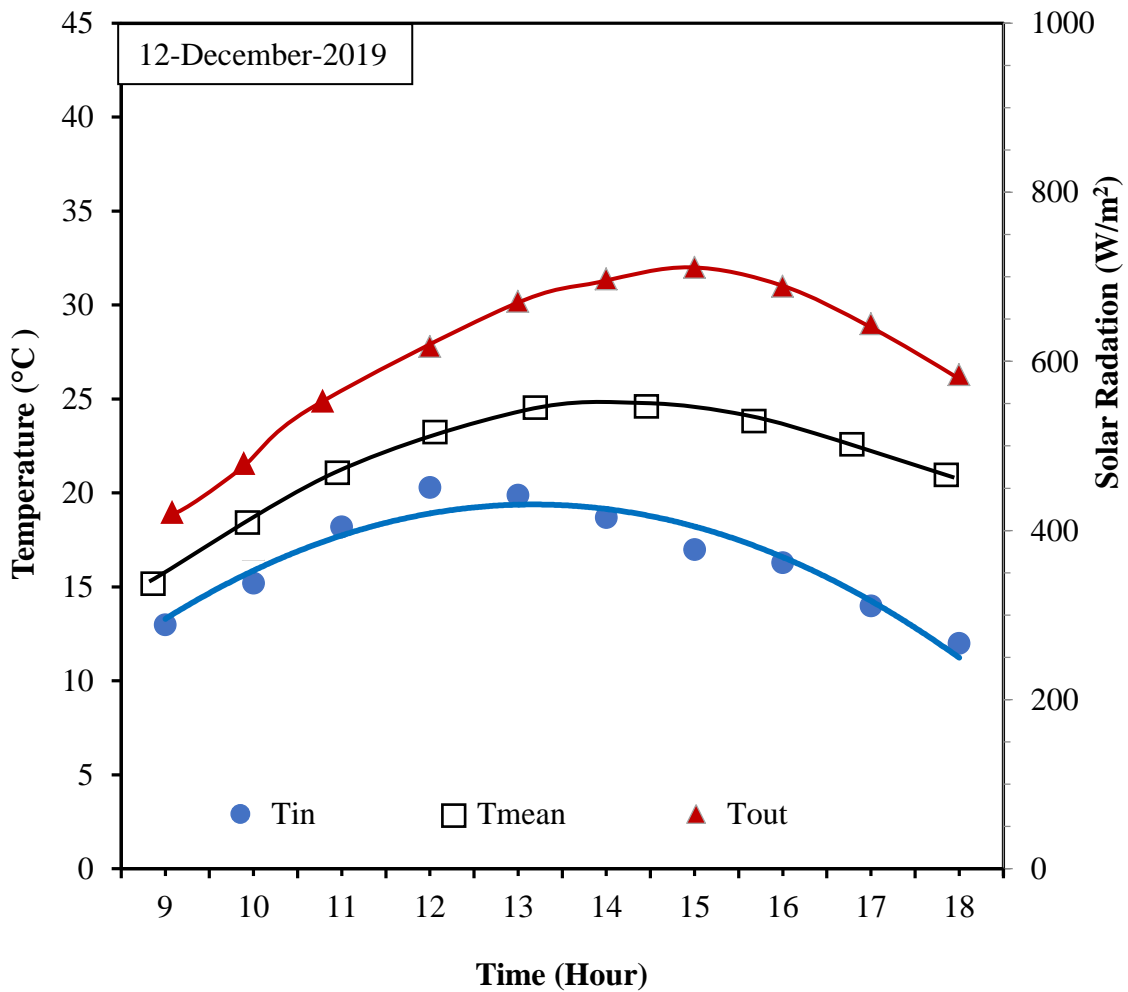


Figure 4.5. Effect of load (0.4 liters/min) on the system temperature under Iraqi weather conditioning.

Some experiments were carried out with hot water being drawn from the collector during the day. Take hot water that is drawn continuously at two different rates (0.2 liter/min and 0.4 liter/min). The mass flow rate and the temperature of the water were both measured. This was achieved by allowing the collector at its bottom to join cold water, and hot water was drawn from the top of the collector. The outlet water temperature was 37 °C, while the mean temperature of the water inside the collector was 28 °C, as the degree of entry of water 15 °C where each flow rate was 0.2 liters/min (Figure 4.4). The maximum temperature was 31 °C and the average water temperature inside the tank was 25 °C when the flow rate was 0.4 liters/min, as in (Figure 4.5).

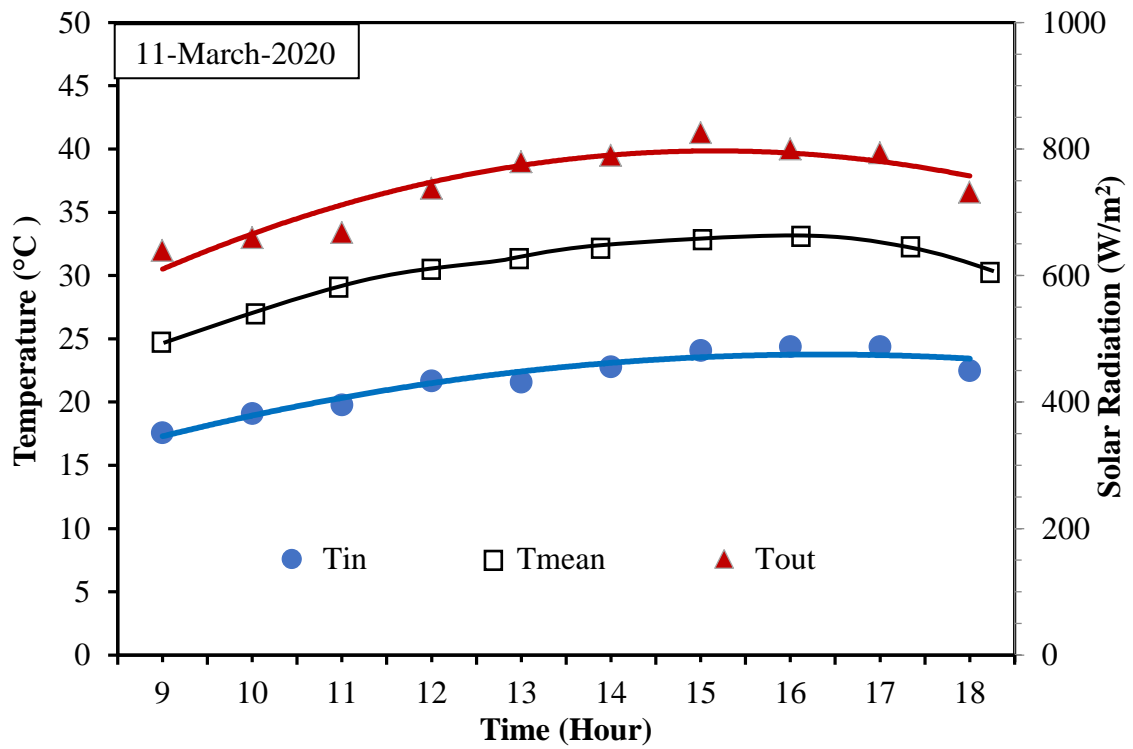


Figure 4.6. Effect of load (0.2 liters/min) on the system temperature under Iraqi weather conditioning.

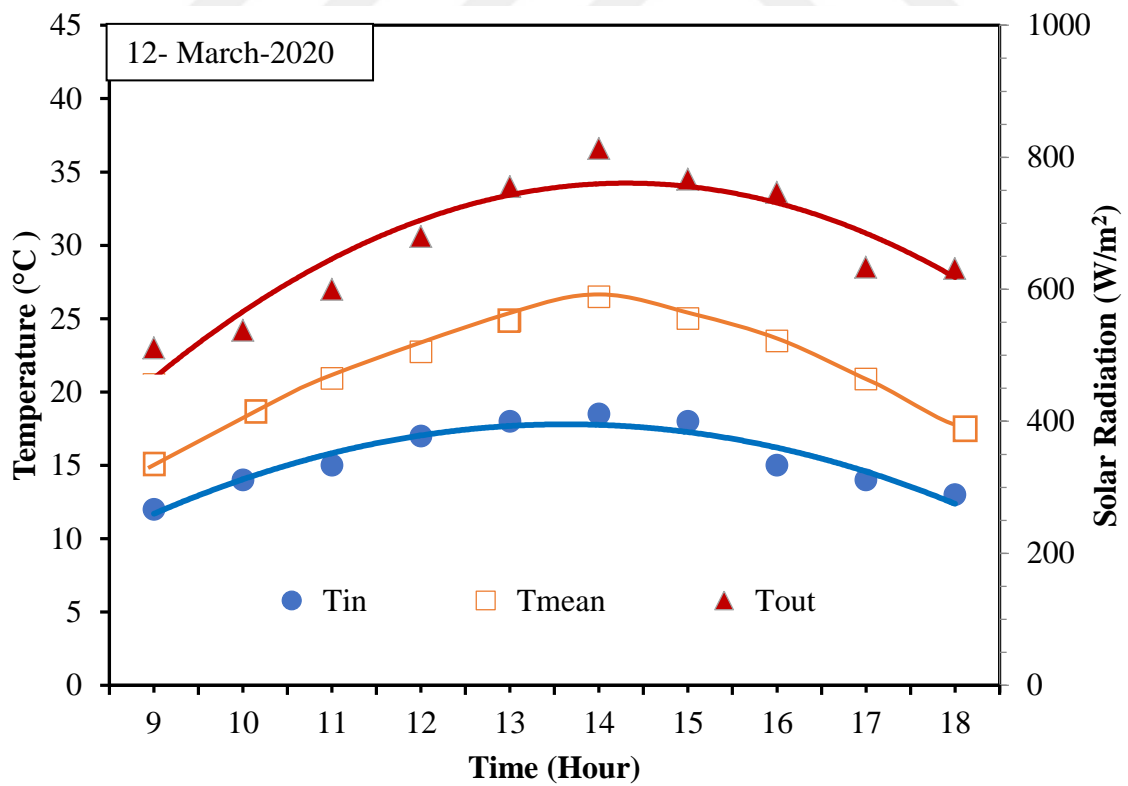


Figure 4.7. Effect of load at (0.4 liters/min) on the system temperature under Iraq weather conditioning.

For the different months of the year, experiments were conducted in the month of 11<sup>th</sup> March, an experiment. The difference of system temperatures with a mass water flow rate was 0.2 liters/min different results were obtained. It is noted that the mean temperature of storage and outlet water increases between 9 a.m and 3 p.m during the day. That confirmed that the solar energy absorbed is higher than that of the outlet hot water. These temperatures start to decrease after 4 p.m. due to lower solar radiation absorbed than the energy drained by the hot water. As in (Figure 4.6) the maximum temperature of the water leaving the collector was 41 °C at 3 p.m. and the mean temperature on 11<sup>th</sup> March was 32 °C. The experiment was also carried out at a flow rate of 0.4 liter/min, with a mean temperature of 27 °C and outlet water temperature is 35 °C as the inlet water temperature is 18 °C shown in (Figure 4.7).

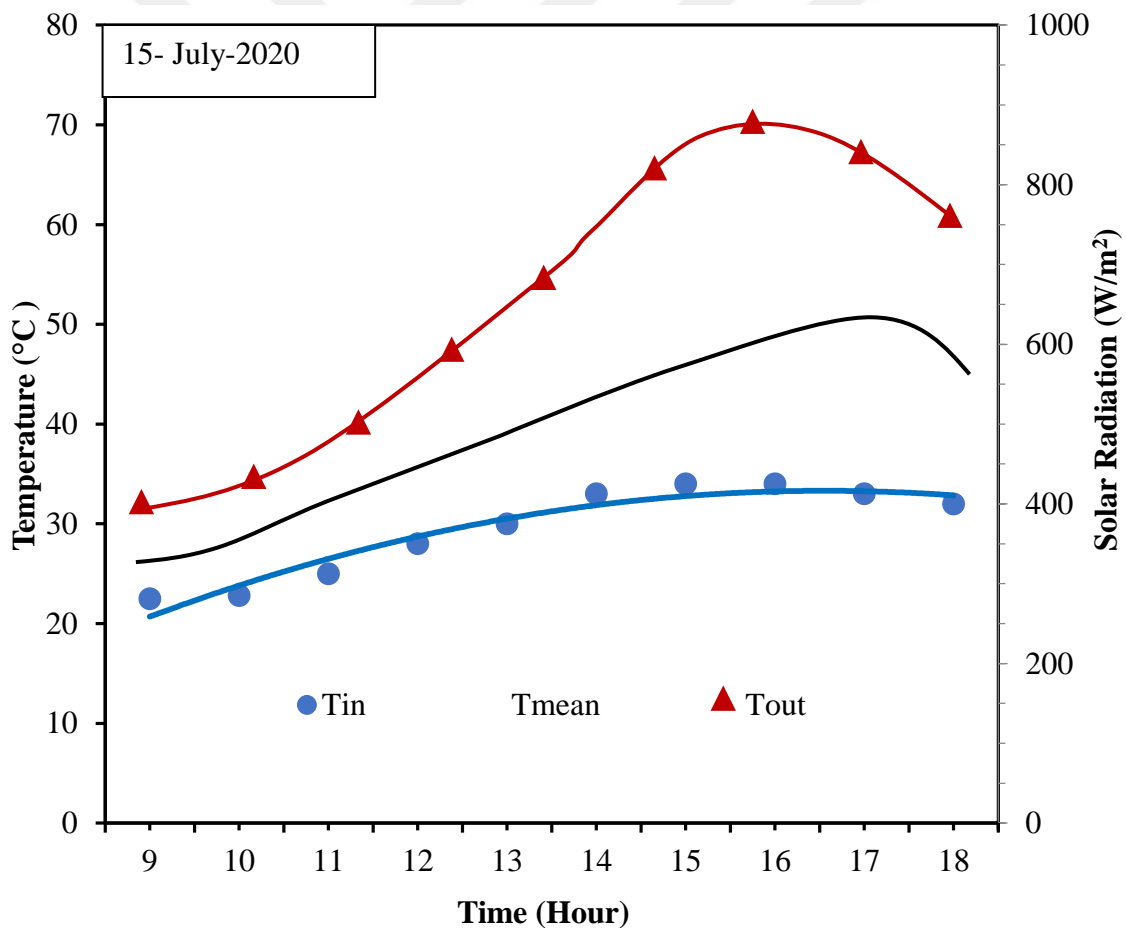


Figure 4.8. Effect of load at (0.2 liter/min) on the system temperature under Iraq weather conditioning.

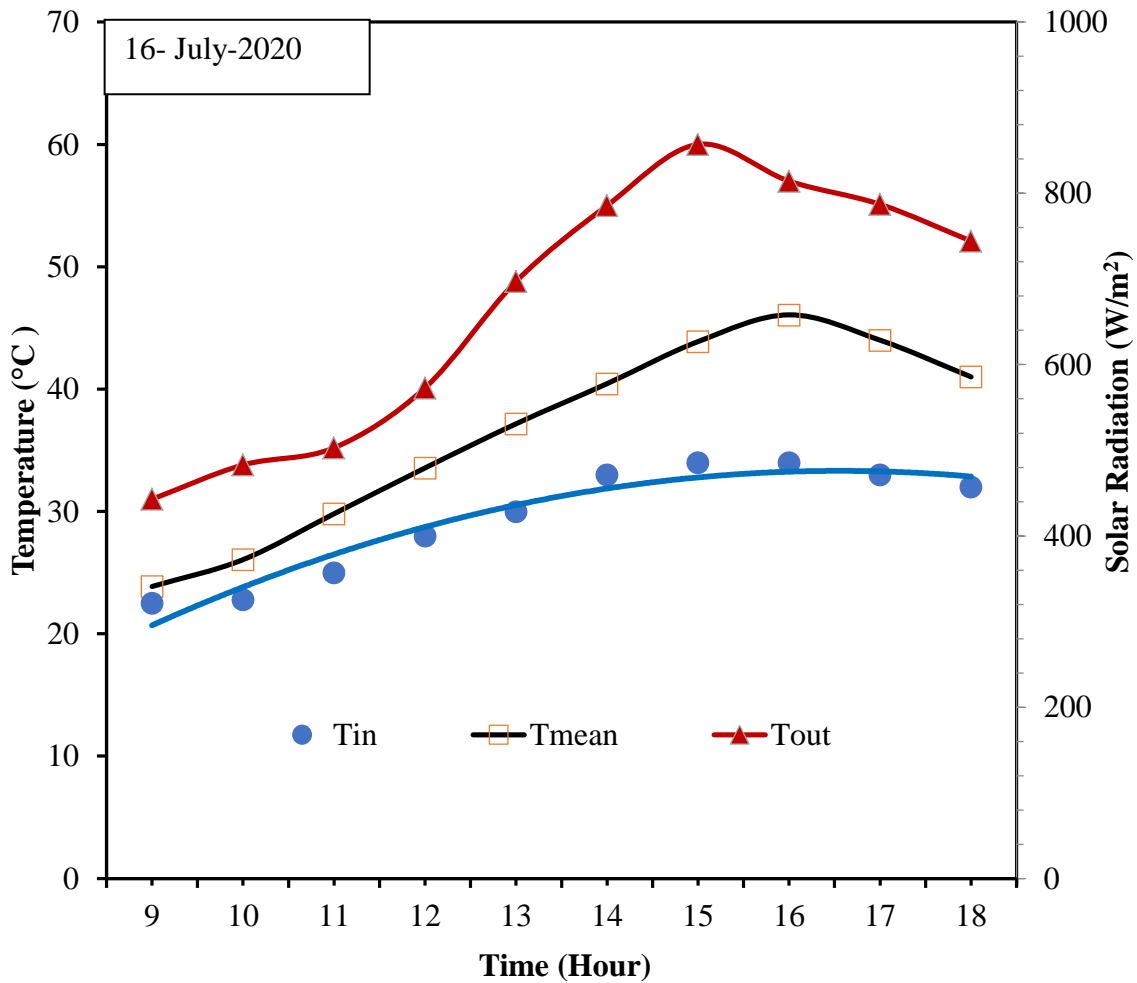


Figure 4.9. Effect of load at (0.4 liter/min) on the system temperature under Iraq weather conditioning.

The same experiment was carried out during 15<sup>th</sup> July; when the flow rate was 0.2 liter/min, the average water temperature of 48 °C was obtained when the outlet water temperature was 68 °C at 2 pm because the solar radiation is at its highest levels as shown in (Figure.4.8). In comparison, when the flow rate was 0.4 liter/min as the outlet water temperature of 58 °C, the average water temperature was 46 °C note that the inlet water temperature was between 27-33 °C (Figure 4.9).

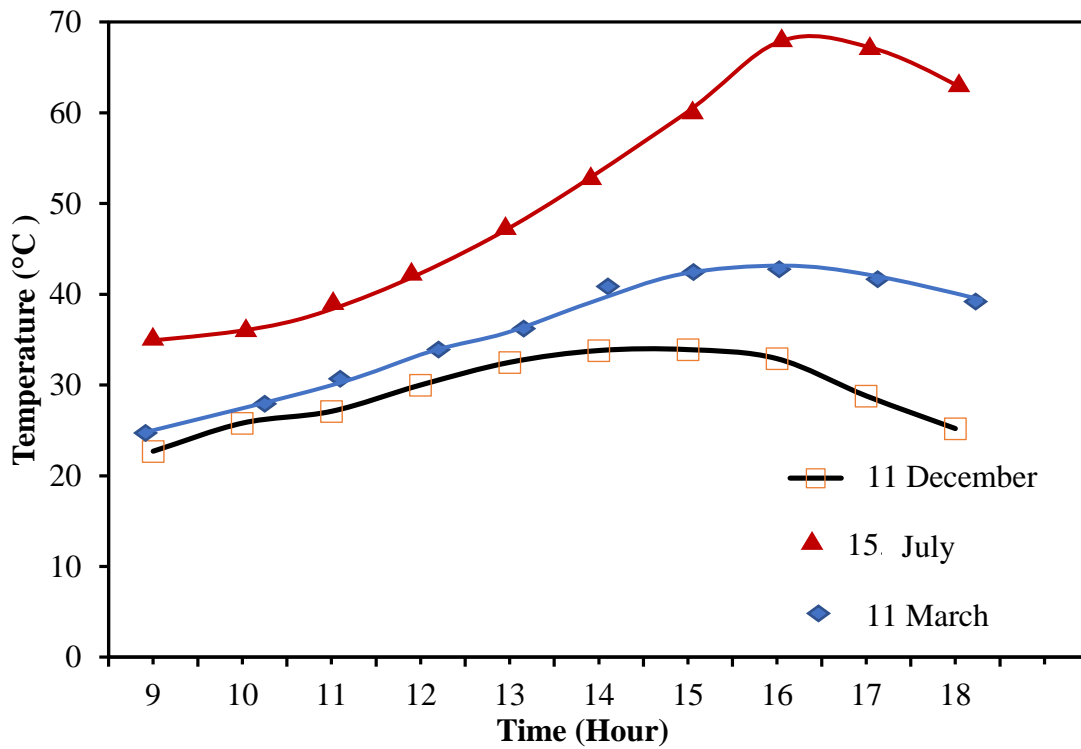


Figure 4.10. Variation of outlet temperature of the wedge collector on typical winter, spring and summer days with load 0.2 liter/min.

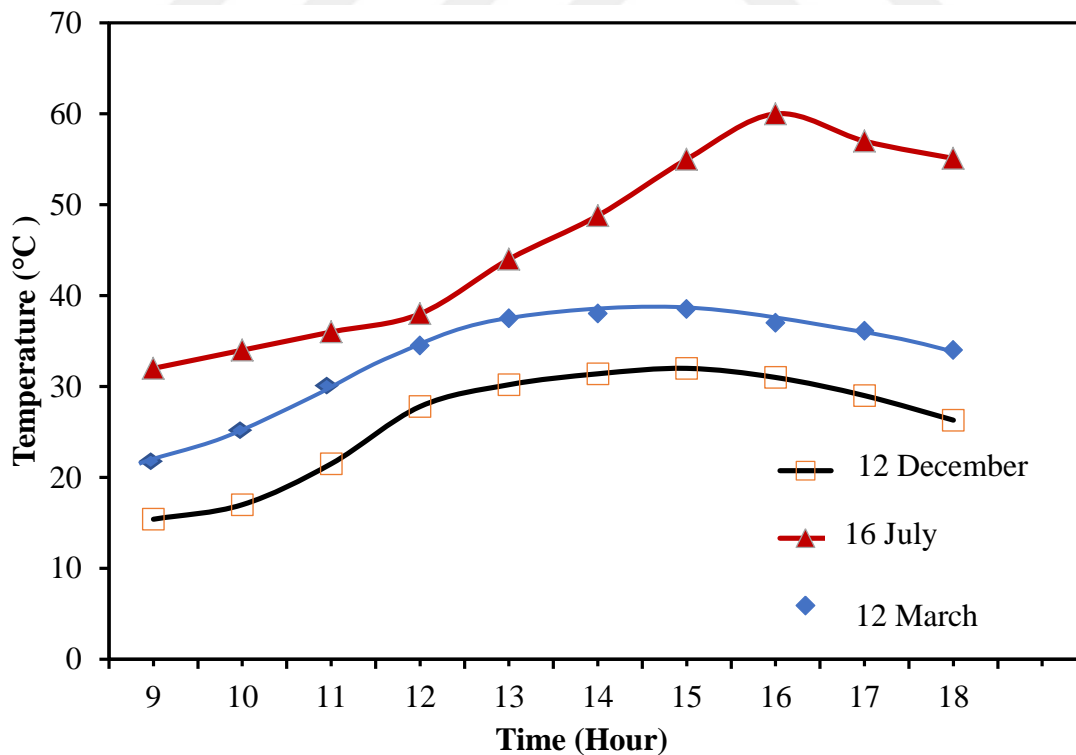


Figure 4.11. Variation of outlet temperature of the wedge collector on typical winter, spring and summer days with load 0.4 liter/min.

Water temperatures in the collector have been measured for the different seasons of the year with continuous loading the load in the first experiment was 0.2 liters/min. So the outlet water temperature coming from the solar collector was 68 °C in the summer for the spring season, we had a temperature of 41 °C, and for the winter, 32°C (Figure 4.10). But increased the rate of water flow to 0.4 liters/min, we obtained in summer a temperature of 61 °C we obtained a temperature of 36 °C in the spring and of 28 °C in the winter. The temperature of the water flowing from the solar collector increased as the more solar radiation, as it was found that the maximum temperature we received was at 2 pm because the amount of radiation is high, as in( Figure 4.11).

#### 4.1.2. Results of the Storage Collector under Turkish Weather Conditions

The solar collector was directed to the southeast to receive the longest exposure to the sun and to obtain the maximum amount of solar radiation. The solar collector's angle of inclination was 45°, which is the best angle for the sun's rays incidence.

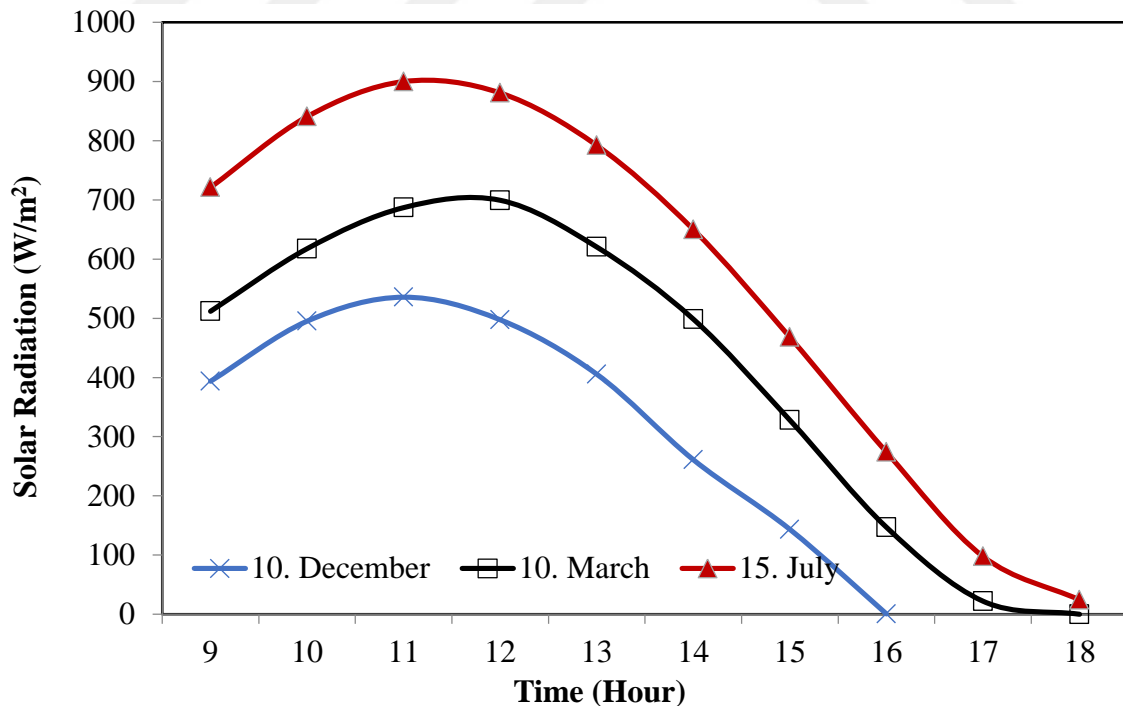


Figure 4.12. Variation of solar radiation for Van city.

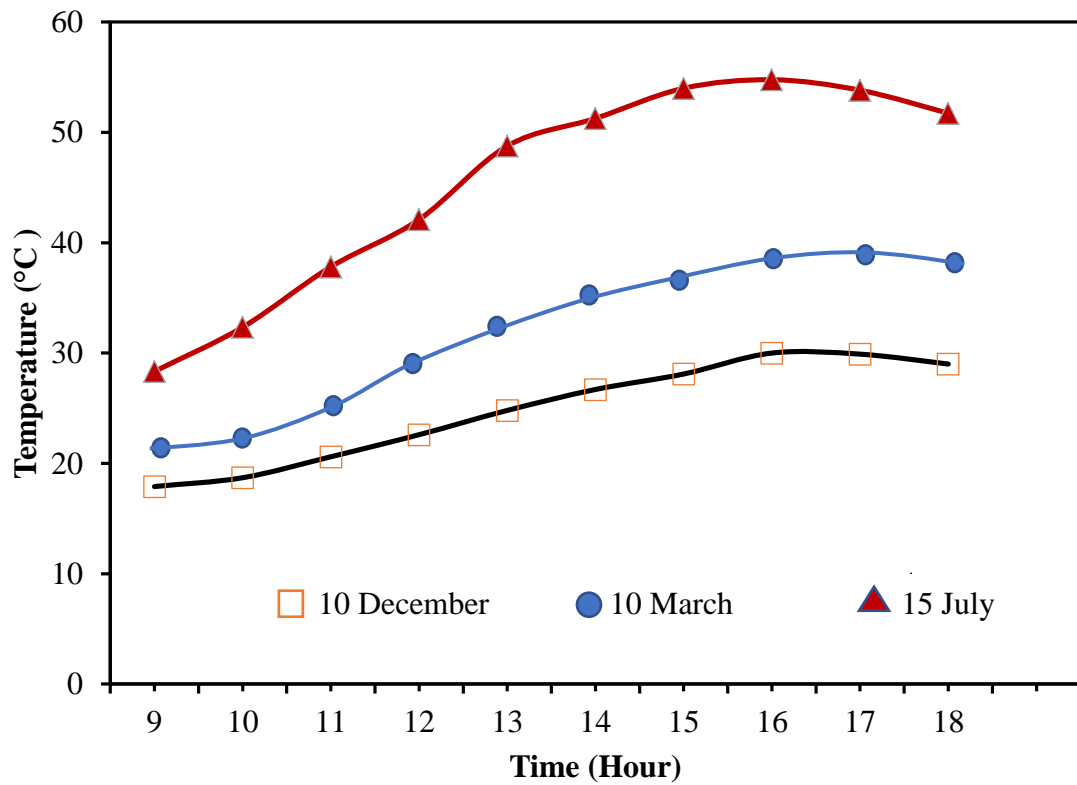


Figure 4.13. Variation of mean water temperature without load under Turkish weather conditions.

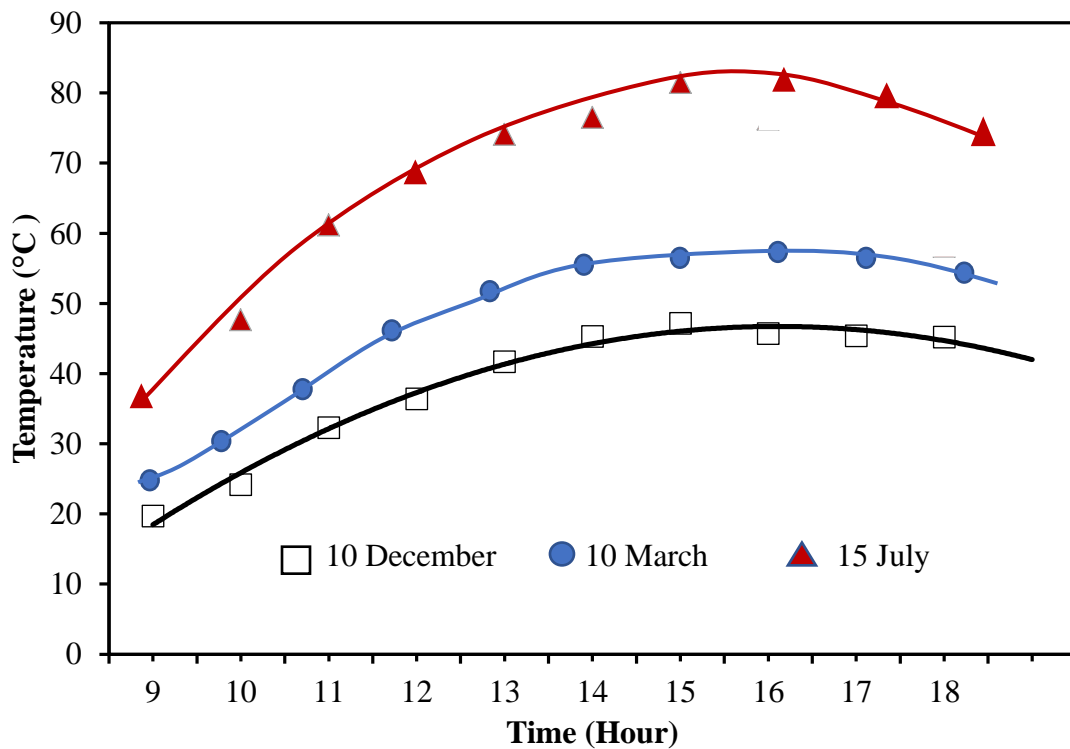


Figure 4.14. Maximum water temperature changes without load within Turkey weather conditions.

The solar radiation amount for Van City was shown in the winter, spring and summer (Figure 4.12) The maximum solar radiation value was  $900\text{W/m}^2$  in the summer at noon. The increase in average water temperature during the day under the Turkish weather conditions for without load conditions indicates as solar radiation  $701\text{W/m}^2$  in spring and  $536\text{W/m}^2$  in winter. The average storage water temperature varies from the early morning hours to its maximum value of  $28\text{ }^\circ\text{C}$  at 5 p.m at 10<sup>th</sup> December,  $36\text{ }^\circ\text{C}$  10<sup>th</sup> March and  $54\text{ }^\circ\text{C}$  15<sup>th</sup> July, respectively for the two variants, (Figure. 4.13) The maximum temperature for the collector is  $81\text{ }^\circ\text{C}$  on 15<sup>th</sup> July,  $53\text{ }^\circ\text{C}$  in 10<sup>th</sup> March and  $46\text{ }^\circ\text{C}$  10<sup>th</sup> December indicates a difference between the water temperature at the top of the tank and time. Owing to the high levels of solar radiation in Iraq, the temperature in Iraq is higher than Turkey (Figure 4.14).

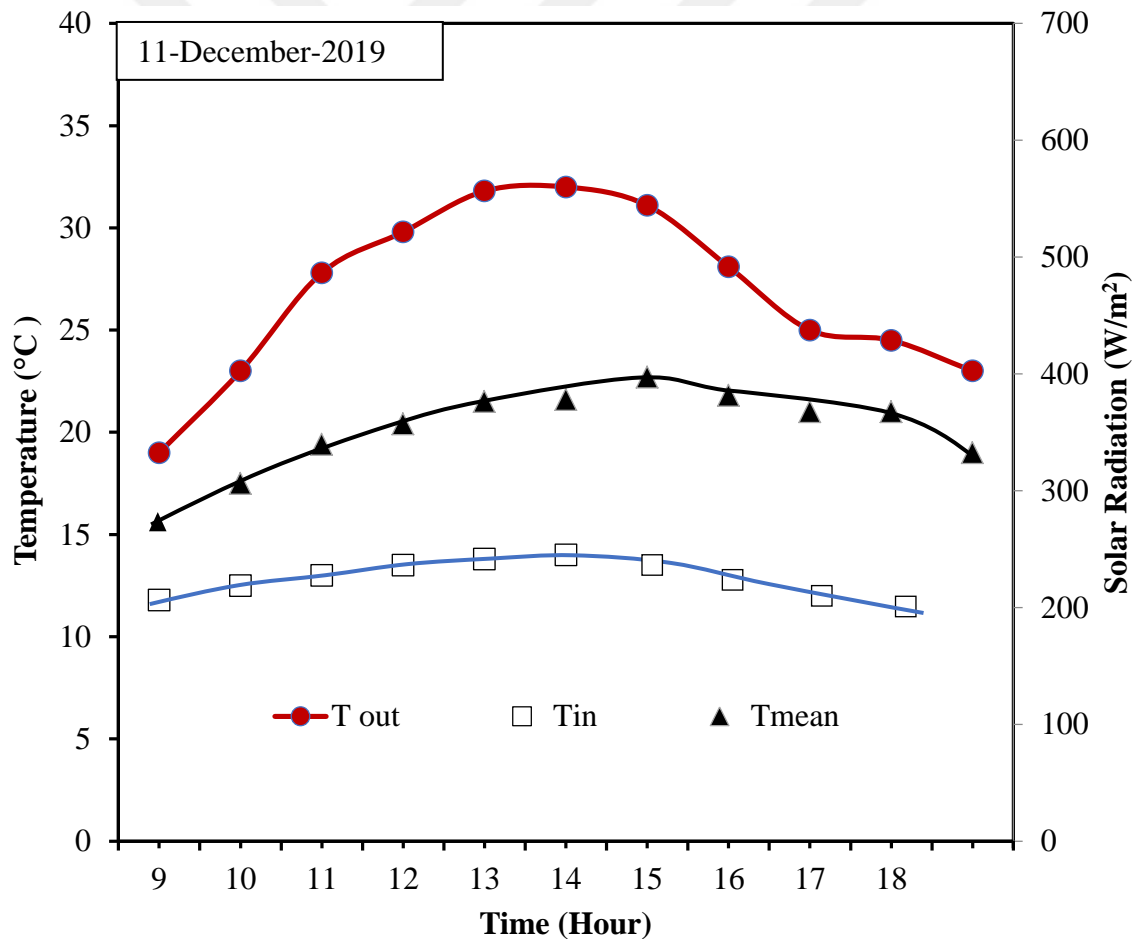


Figure 4.15. Effect of load (0.2 liters/min) on the system temperature within Turkey weather conditions..

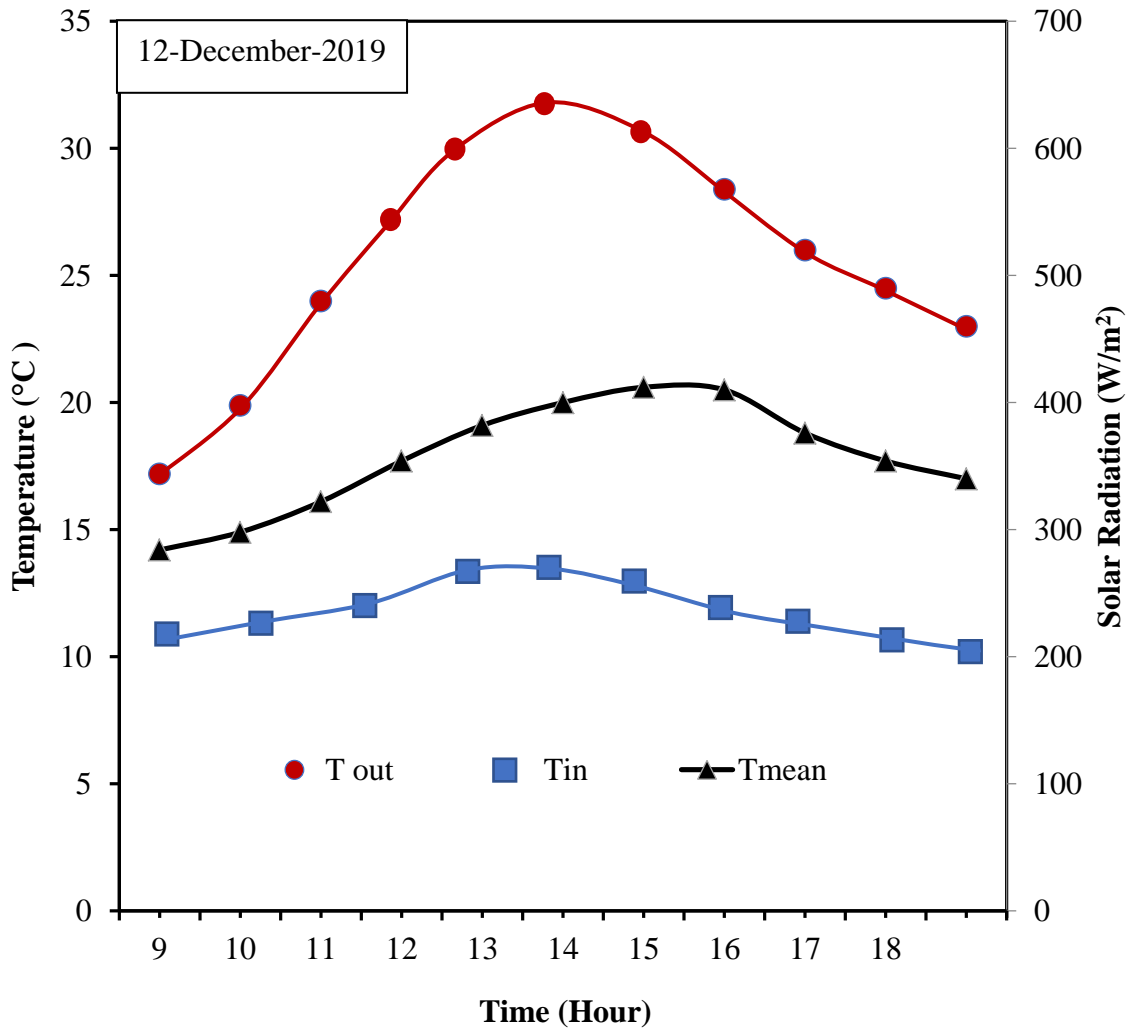


Figure 4.16. Effect of load (0.4 liters/min) on the system temperature under within Turkey weather conditions.

The comparison of system temperatures with a water mass flow rate under Turkish weather conditions of 0.2 liter/min. The mean storage water temperature 24 °C and maximum temperature of the outlet water 34 °C was observed to increase between 9 a.m. And 2 p.m, which confirmed that the solar energy absorbed is higher than that of the hot water exhausted (Figure 4.15). These temperatures begin to decrease after 4 p.m. due to the lower solar energy absorbed than the energy exhausted by the hot water. At 2 p.m., the maximum water temperature leaving the collector was 32 °C and mean water temperature 23 °C. When the volume flow rate was (0.4 liters/min) for the Turkish model as in (Figure 4.16), the same behavior of system temperatures was recorded at 3pm.

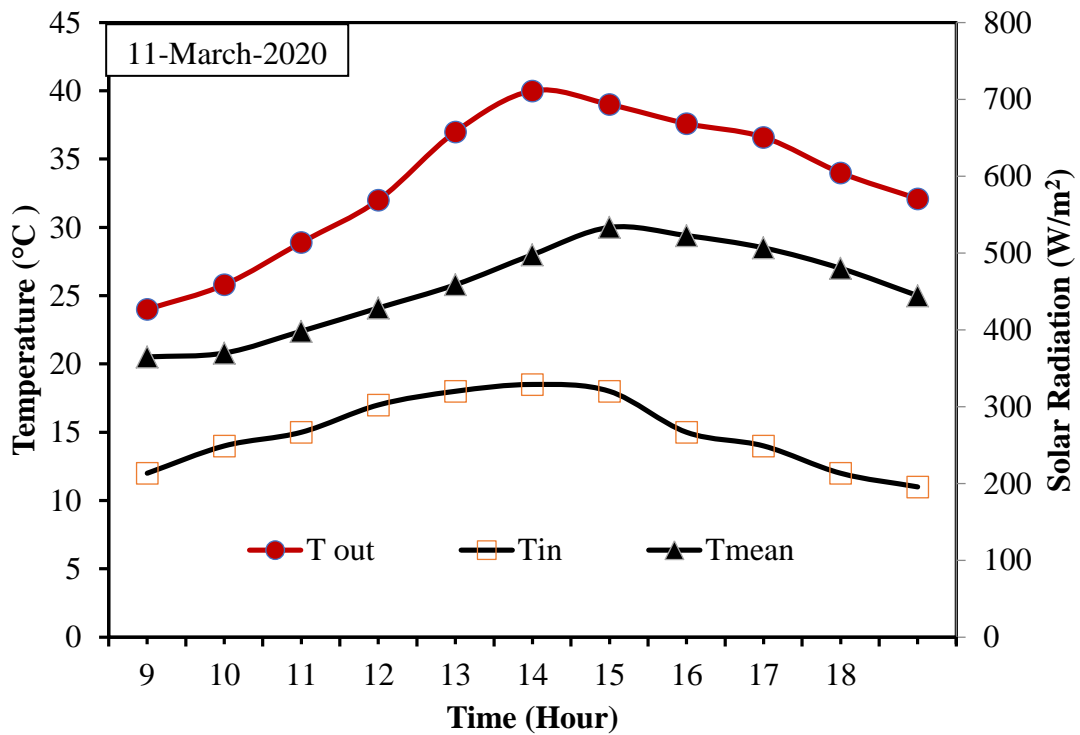


Figure 4.17. Effect of load at (0.2 liters/min) on the system temperature within Turkey weather conditions.

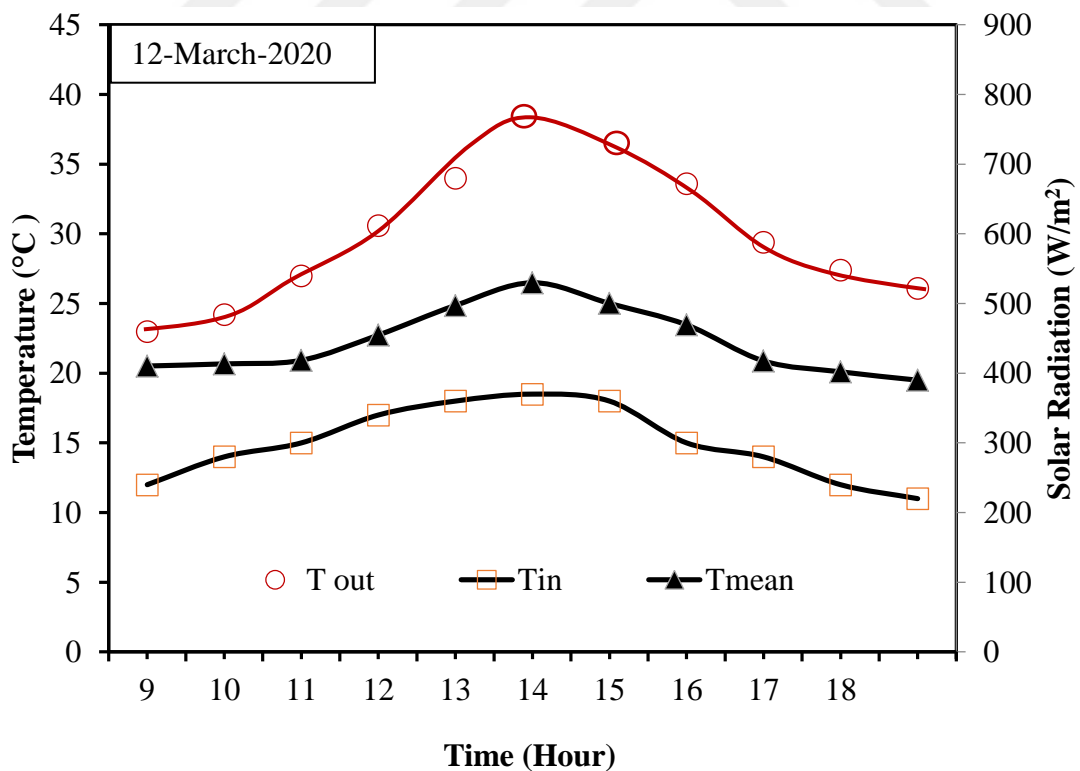


Figure 4.18. Effect of load (0.4 liters/min) on the system temperature within Turkey weather conditions.

The maximum value of the average water temperature 30 °C in 11<sup>th</sup> March, and outlet water temperature of 42 °C. When the water flow rate is 0.2 liter/min seen in (Figure 4.17). But high the flow rate water is 0.4 liter/min, the average water temperature of 26 °C and the outlet water temperature of 37 °C is obtained in (Figure 4.18).

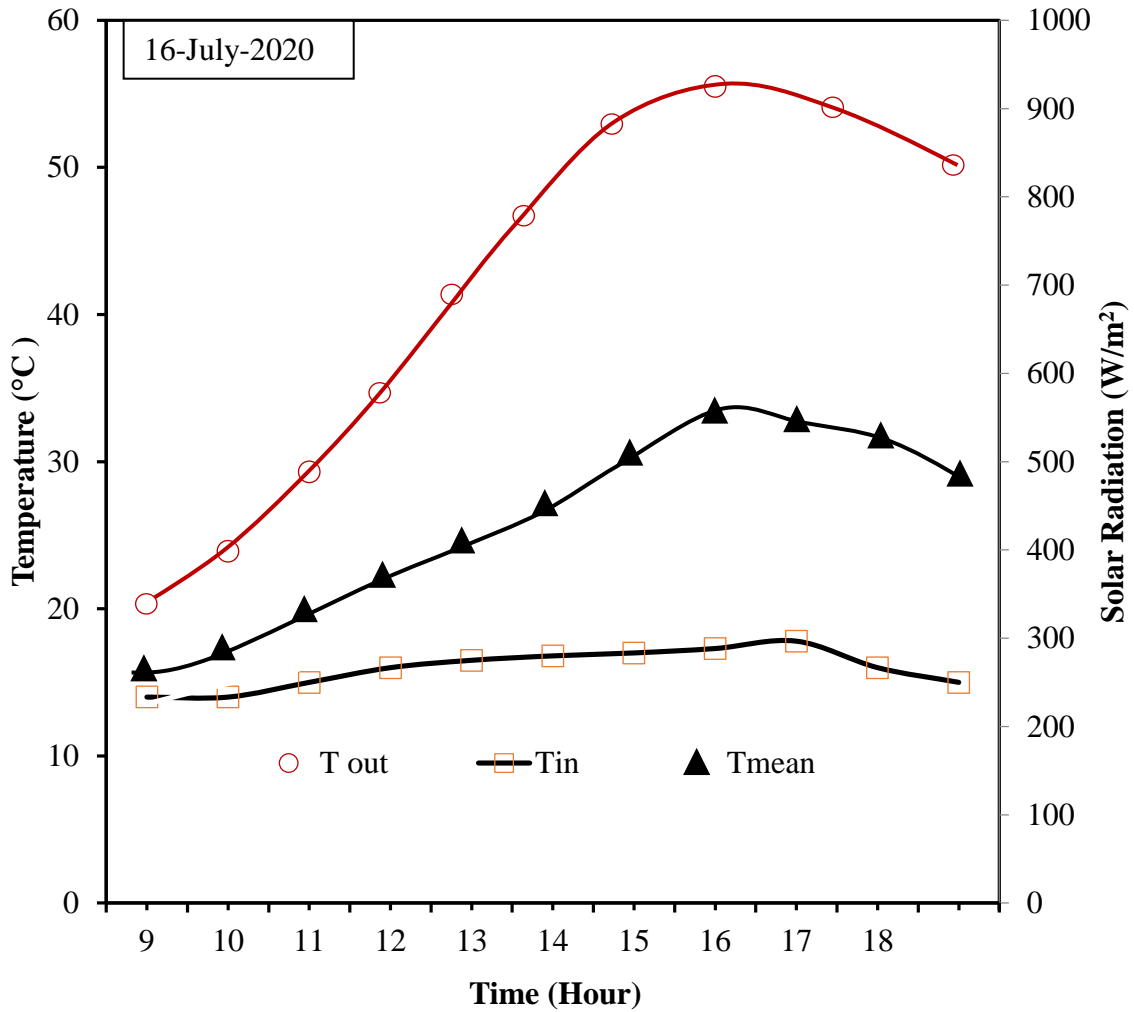


Figure 4.19. Effect of load (0.2 liters/min) on the system temperature within Turkey weather conditions.

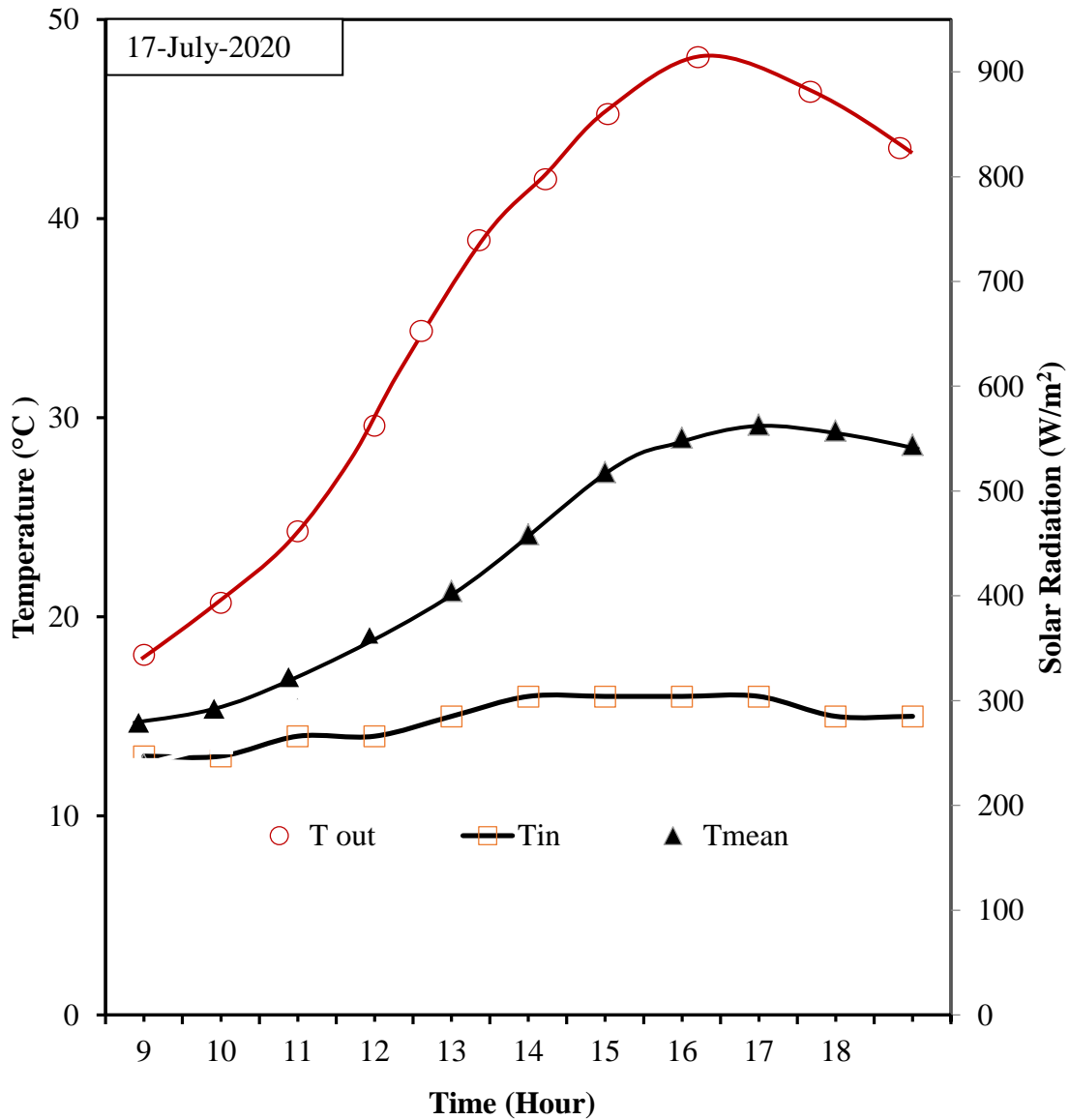


Figure 4. 20. Effect of load (0.4 liters/min) on the system temperature within Turkey weather conditions.

The same experiment was carried in the month of 16<sup>th</sup> July, and the mean water temperature of 48 °C and the outlet water temperature of 55 °C as inlet water temperature 14 °C were obtained when the flow was 0.2 liter/min. When the flow is 0.4 liter/min, the outlet water temperature of 47 °C and the mean water temperature of 29°C are obtained, as in the two (Figures 4.19 and (Figure 4.20). The high temperatures were observed in the solar collector at 3 pm, and the reason was due to the high solar radiation.

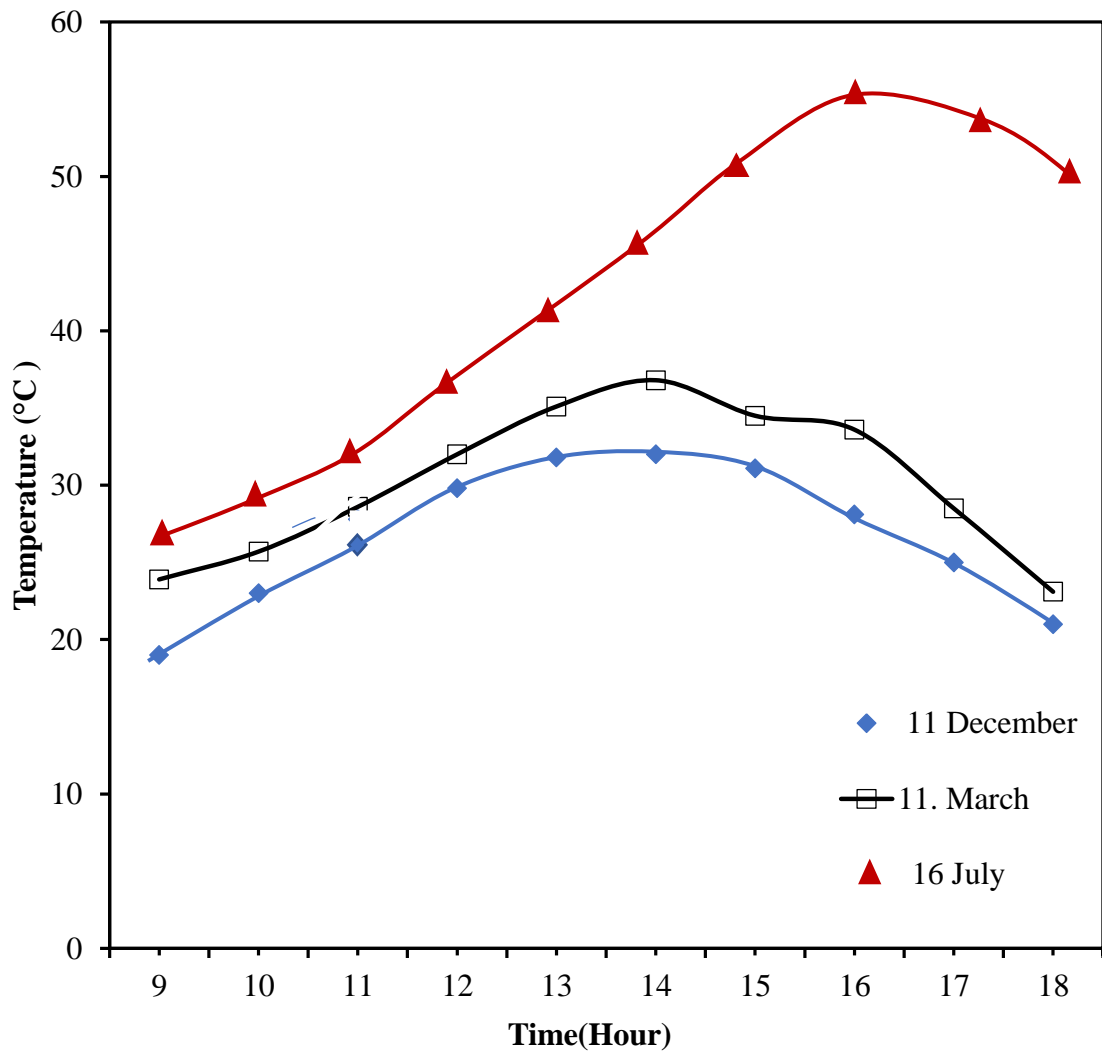


Figure 4.21. Variation of outlet temperature of the wedge collector on typical winter spring and summer days with load 0.2 liter/min.

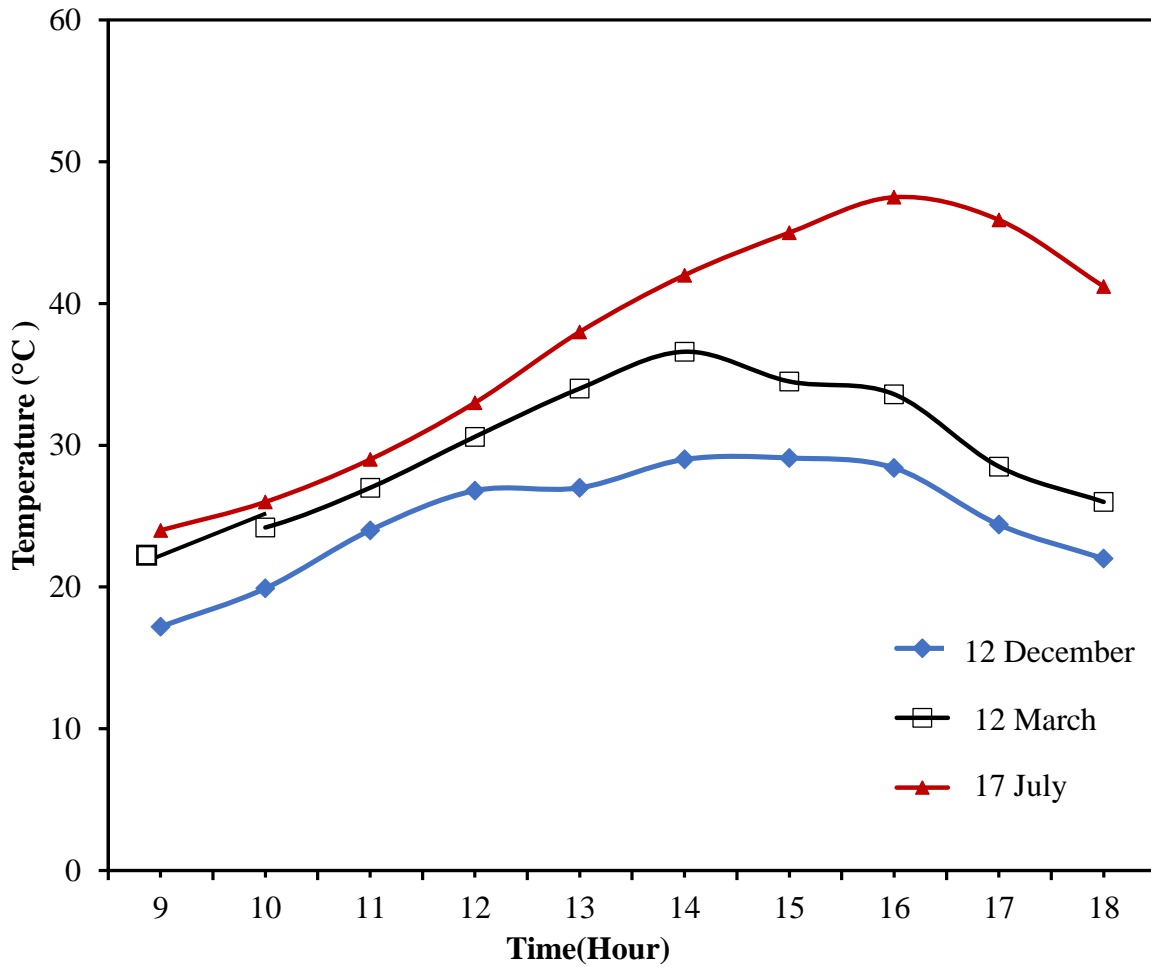


Figure 4.22. Variation of outlet temperature of the wedge collector on typical winter, spring and summer days with load 0.4 liter/min.

Also experiments were conducted by continuous load on this type of solar collector. Where a continuous load was carried out at a rate of 0.2 liter/min, as it was noticed that the temperature of the water leaving the compound was 56 °C in the summer and it was above the maximum temperature at 3 pm. As for the spring season, the temperature of the water outlet of the collector was 36 °C at 2 pm. The temperature outlet the collector was obtained at 31 °C at 2 pm during winter, as in (Figure 4.21), because at this hour solar radiation is at its maximum levels. But we got a maximum temperature of 47 °C at 3 pm in the summer when we increased the load to 0.4 liter/min and ran during the same seasons of the year. Whereas we have a mean temperature of 29 °C at 2 pm in the spring and a temperature of 25 °C at 1 pm in the winter, as in (Figure 4.22).

#### 4.1.3. The Comparison Between Iraq and Turkey

Where a comparison was made between the average water temperatures between the Iraqi and Turkish weather for the different seasons of the year without load. Likewise, a comparison was made with load of two different loads, the first is 0.2 liter/min and the second load is 0.4 liter/min, where the difference between the water temperature outlet the solar collector was found for the Iraqi and Turkish models.

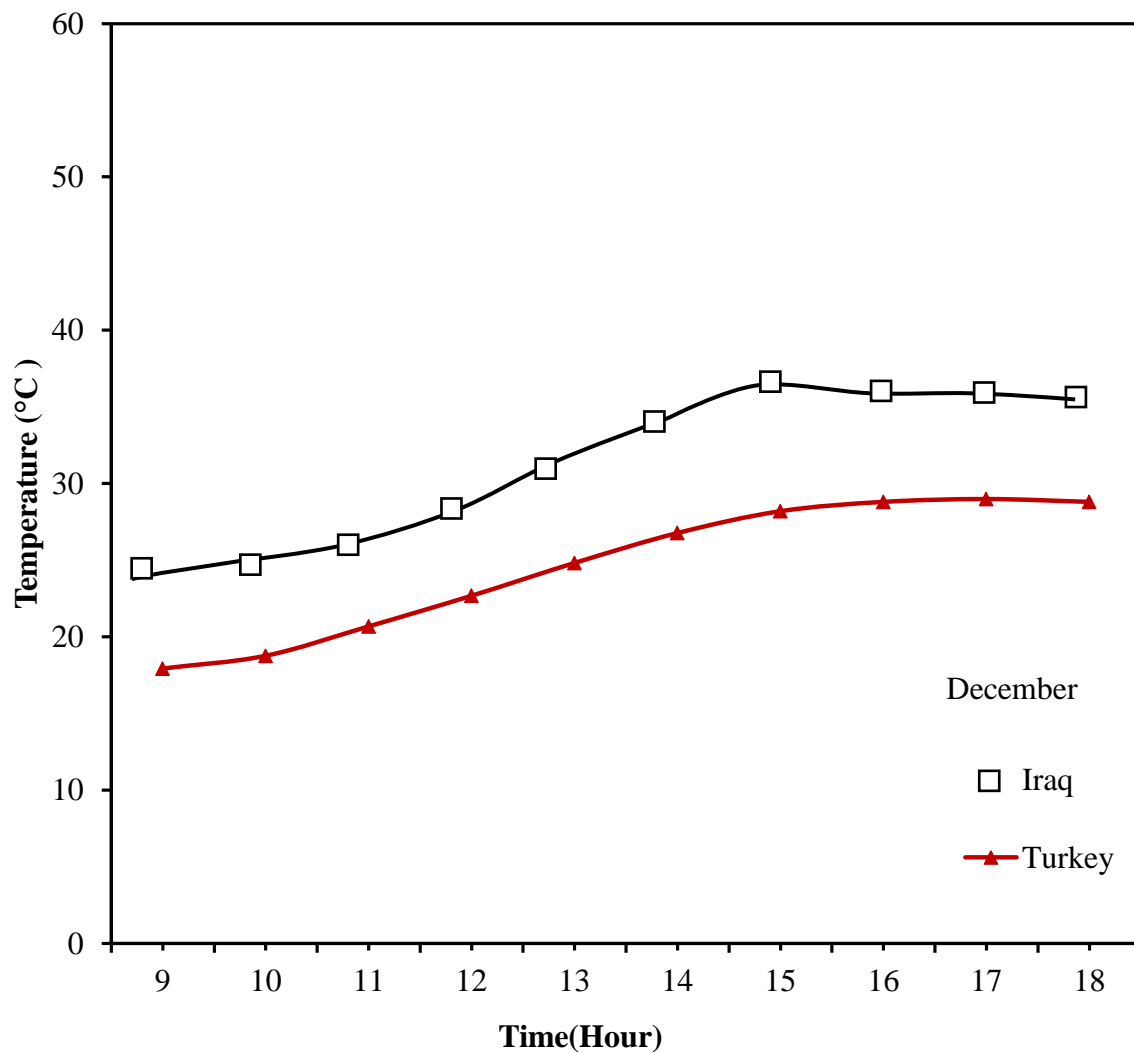


Figure 4.23. A comparison of the mean temperature for the winter between the Turkey and Iraq conditions without load.

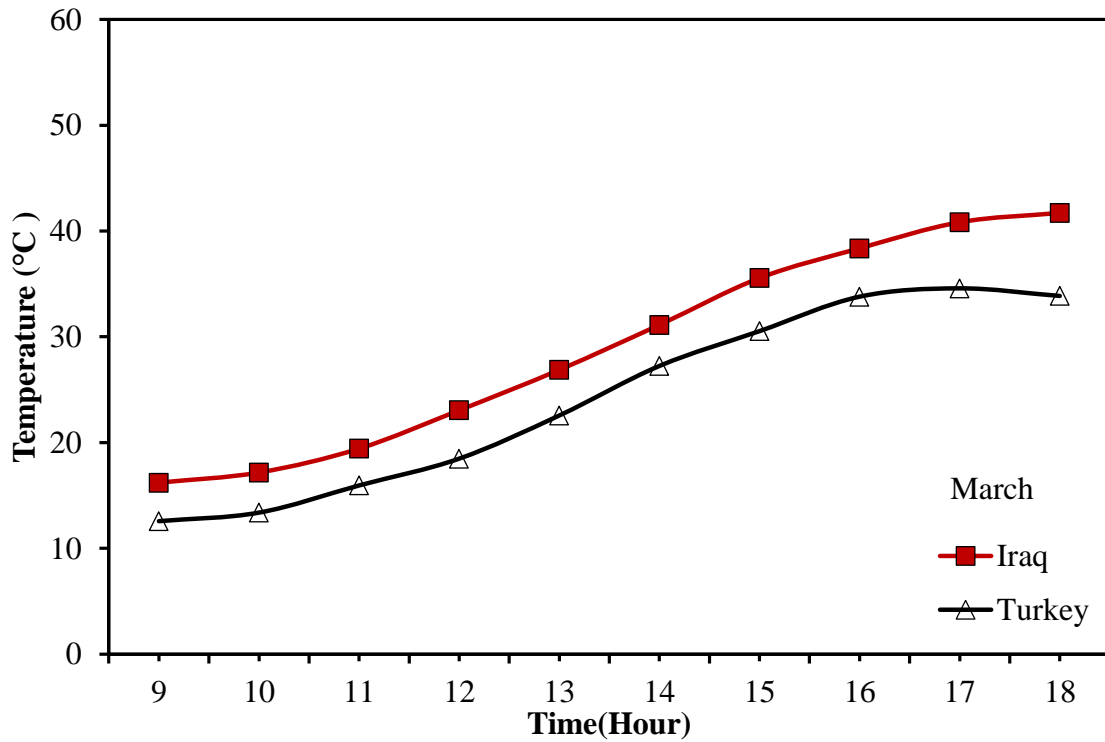


Figure 4.24. A comparison of the mean temperature for the spring between the Turkey and Iraq conditions without load.

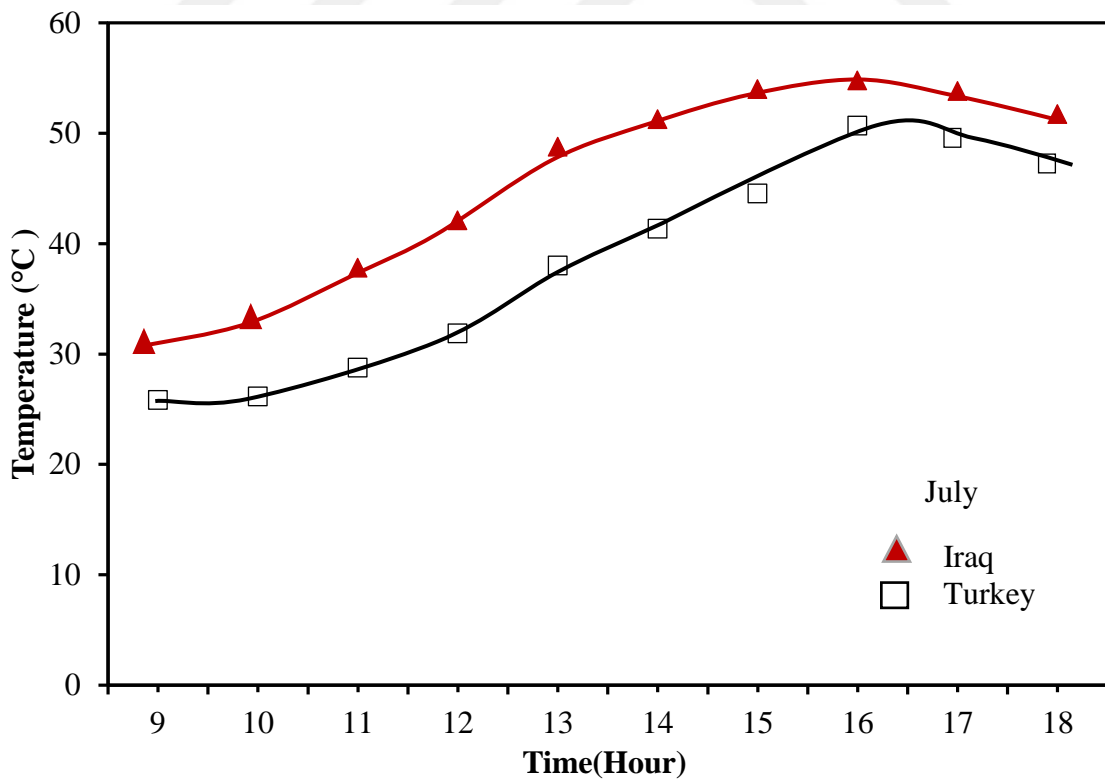


Figure 4.25. A comparison of the mean summer temperature between Turkey and Iraq conditions without load.

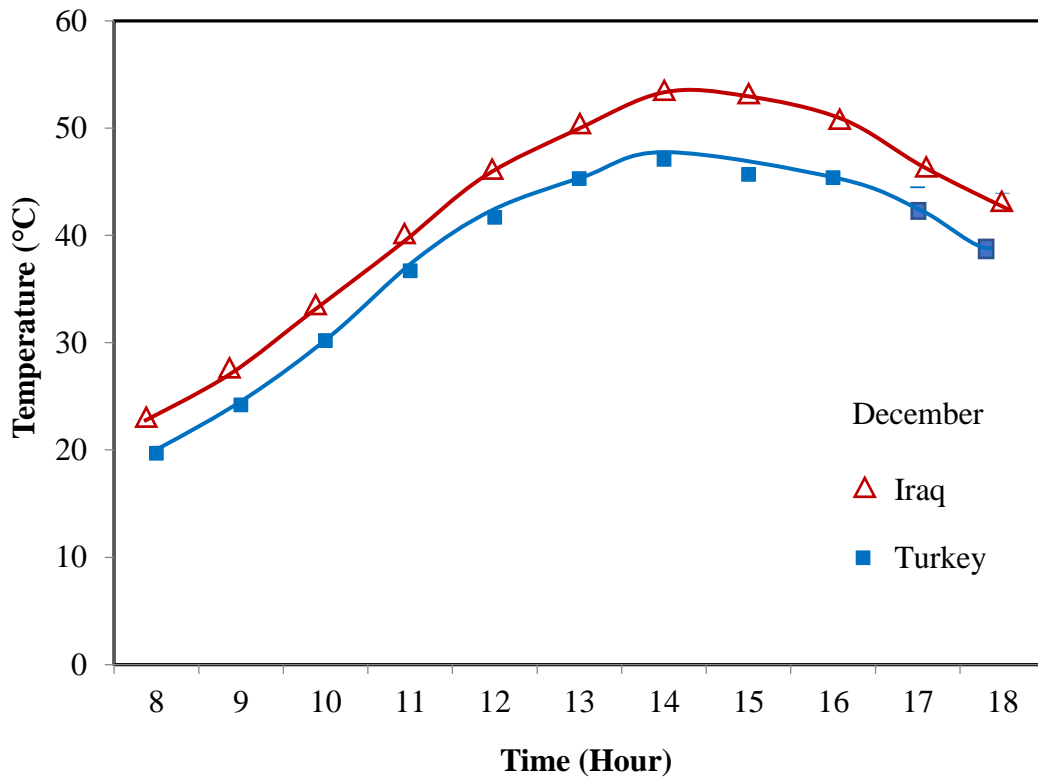


Figure 4.26. Variation of maximum storage temperature of wedge collector on winter days Iraq and Turkey conditions without load.

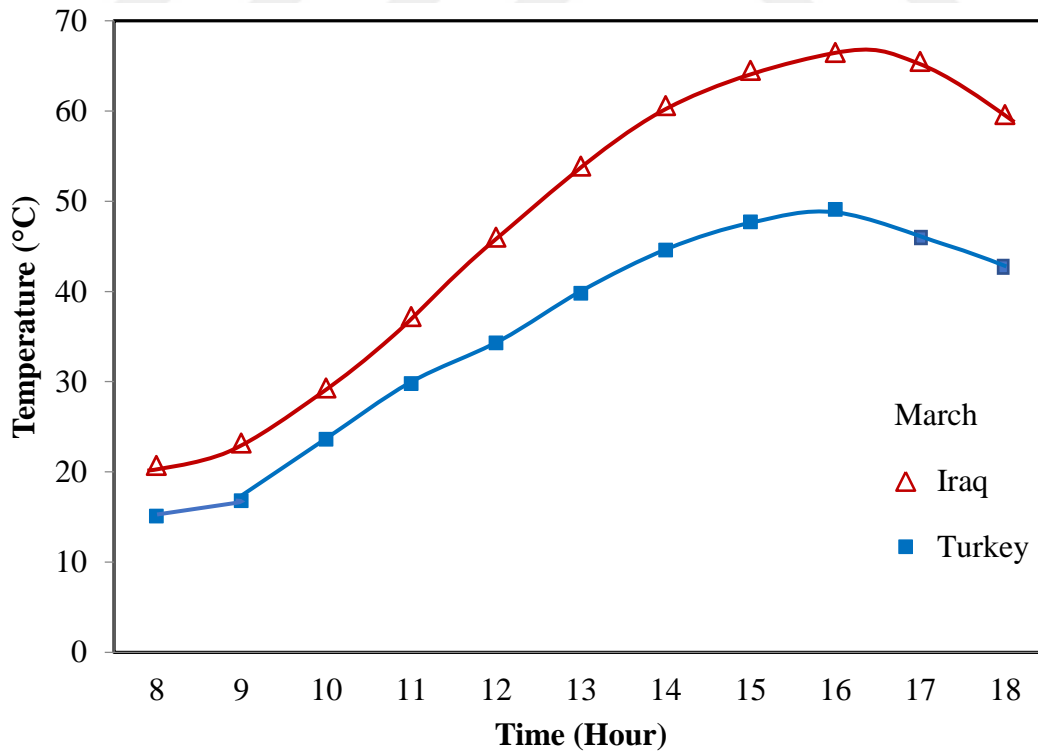


Figure 4.27 Variation of maximum storage temperature of wedge collector on spring days Iraq and Turkey conditions without load.

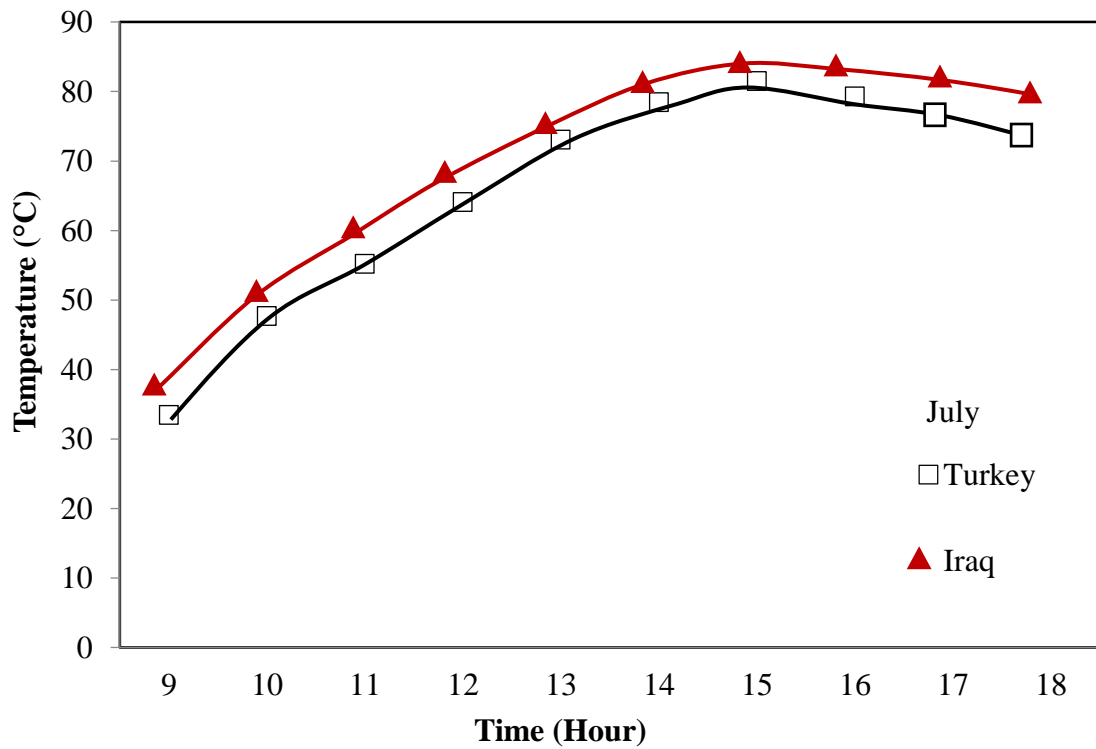


Figure 4.28. Variation of maximum storage temperature of wedge collector on summer days Iraq and Turkey conditions without load.

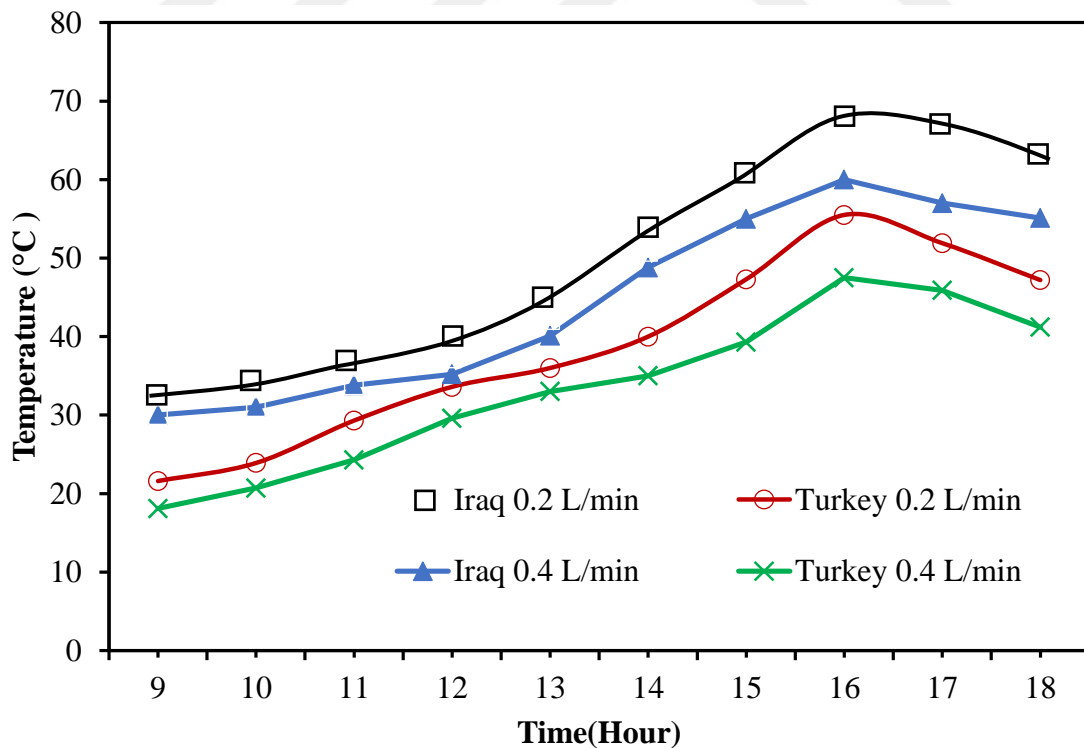


Figure 4.29 Outlet temperatures of the wedge collector with different loads for the summer with load.

For the Turkish and Iraqi weather, a comparison was made between the average water temperature in summer. If the water temperature in Iraq was 55 °C, than the water temperature in Turkey was 50 °C shown in (Figure 4.23). The average water temperature of 43 °C in Iraqi weather conditions was obtained in the spring, while the water temperature of 34 °C in Turkish weather conditions was obtained (Figure 4.24). As for the winter season, in Iraqi conditions, the average water temperature was 33°C but the water temperature of 28 °C was obtained while in Turkish weather, as in (Figure 4.25).

The maximum water temperatures in winter for Iraq and Turkey under the weather conditions. Where a water temperature of 53 °C was obtained under Iraqi weather conditions but under Turkish weather conditions, the maximum water temperature of 47 °C was obtained (Figure 4.26). The weather conditions in Iraq and Turkey weather conditions for the spring where 65 °C was obtained in Iraqi weather conditions, but in Turkish weather conditions, the maximum water temperature of 50 °C was obtained in (Figure 4.27). The maximum water temperature in Iraq and Turkey weather conditions for the summer. Where water temperature 83 °C was obtained in Iraqi weather conditions, but in Turkish weather conditions, the maximum water temperature of 81 °C (Figure 4.28). We made a comparison of the water temperatures at different loading of 0.2 liter/min leaving the solar collector. In summer, we had a temperature of 68 °C in Iraqi weather, when in Turkish weather, we had a temperature of 54 °C as for the load to 0.4 liter/min when we increased, In Iraqi weather, we have the water temperature outlet of the collector at 58 °C, while in Turkish weather, we have the water temperature at 45 °C. Iraq's water temperatures have been shown to be higher than Turkish weather, which is why Iraq is defined by the hot weather shown in (Figure 4.29).

Whereas, the new design of the wedge collector is better in performance than the cylindrical collector (Ahmed, 2017). Where we got an average water temperature of 41 °C while the maximum water temperature is 66 °C for the Wedge collector, but we got cylindrical collector in 32 °C average water temperature while the maximum water temperature is 58 °C in Iraq for a spring day in (Figure 4.30) (4.31)

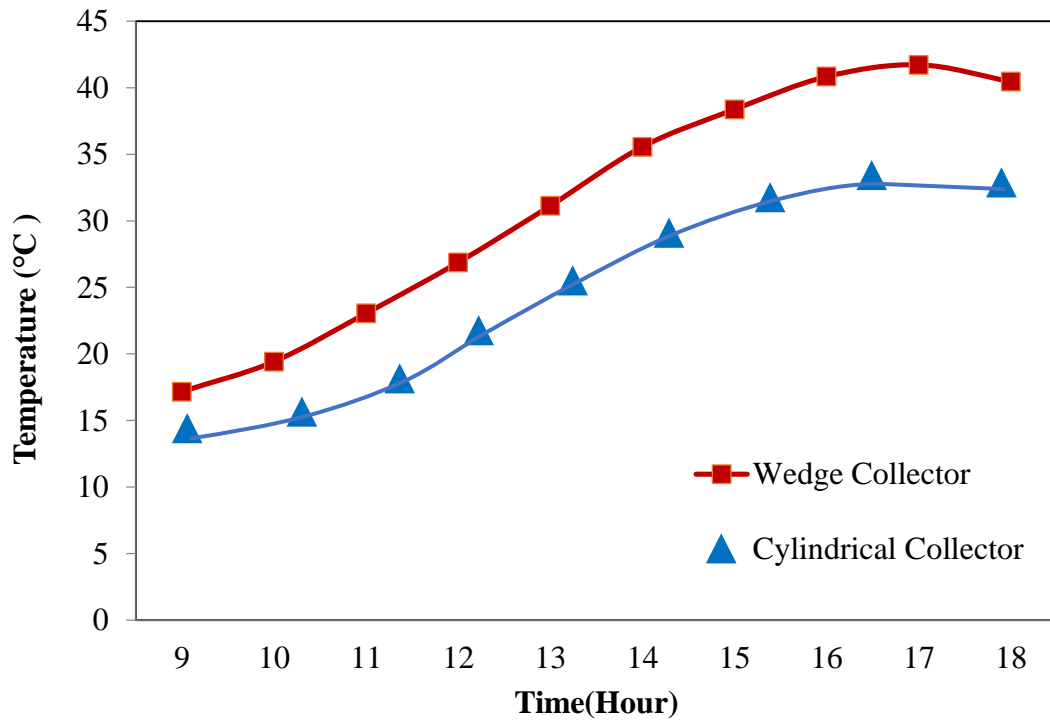


Figure 4.30. Comparison mean temperature between the wedge collector and the cylindrical collector in spring day.

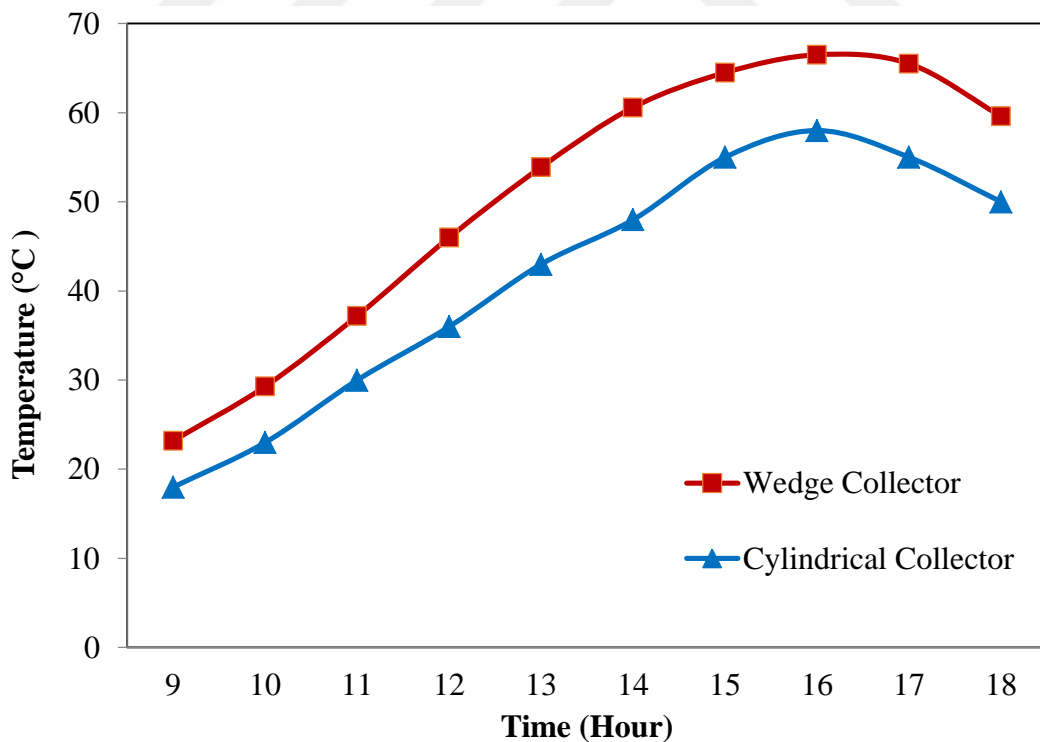


Figure 4.31. Comparison maximum temperature between the wedge collector and the cylindrical collector in spring day

## 4.2. Efficiency of the Proposed Storage Collector

Where calculations were made to assess the efficiency of the wedge solar collector, as calculated using "Eq 4.2". In which the studies were carried out at various seasons of the year under different weather conditions. In load variations the first experiment was conducted at the first location in Iraq and the second location in Turkey. Where the first experiment was conducted without load in December, 41% was obtained in Iraq, while 26% was obtained in Turkey on the same day. Similarly, in March, the same experiment was conducted, where 46% efficiency was achieved in Iraq, while 32% was achieved in Turkey. We conducted the experiment during the summer season in July, as the efficiency in Iraq is 62%, while in Turkey it is 55%. The solar collector has been shown to be more effective under Iraqi conditions than in Turkish conditions, but there is little difference, as shown in (Figure 4.32). This is based on the fact that, as shown by the measurements and the solar radiation in Table 4.1, the solar radiation between them is very similar.

$$\eta = \frac{\int Q_u dt}{A \int I dt} \quad (4.1)$$

The instantaneous thermal efficiency of the collector is:

$$\eta = \frac{Q_u}{AI} \quad (4.2)$$

Tabel 4.1. Calculate the efficiency of the wedge collector without load (Iraq-Turkey)

Experiments	Experiment (1) 19-12-2019		Experiment(2) 10-03-2020		Experiment(3) 15-07-2020	
Location	Iraq	Turkey	Iraq	Turkey	Iraq	Turkey
$T_{average}$	28.2	24.8	38.3	27.2	45.8	40
$T_i$	18.3	20	13.8	20.2	24.5	23.8
$Q_u$ (W)	123	60.26	173.40	88.17	276.12	202.1
Solar radiation ( $W/m^2$ )	529	405.19	678	498.5	791	650
$\eta = \frac{Q_u}{A * I_s}$	0.41	0.26	0.46	0.32	0.62	0.55

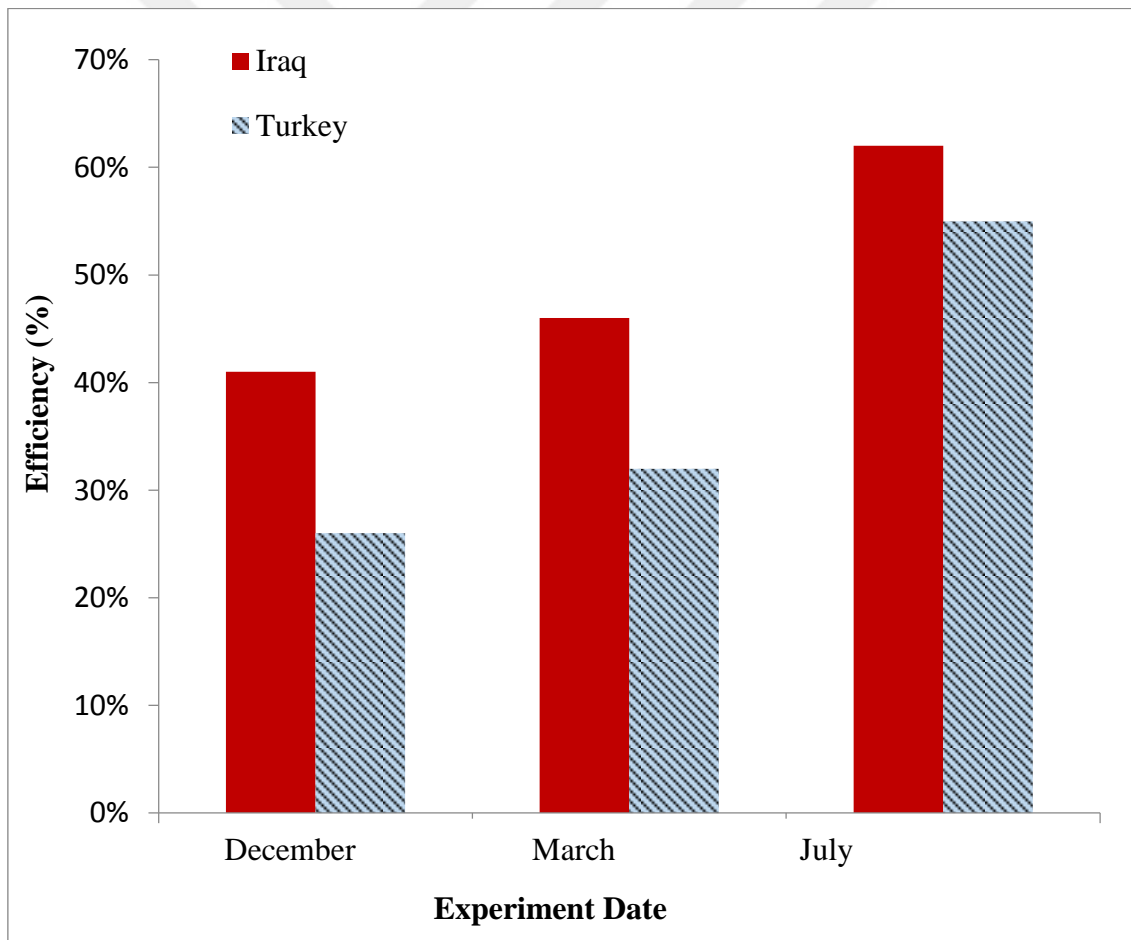


Figure 4.32. Efficiency of the wedge collector (without load-Turkey and Iraq)

We tested a continuous load on the solar wedge collector and set out the same experiments and in different seasons of the year and for the first location in Iraq and the second location in Turkey. When we put continuous load at a rate of 0.2 liter/min where we obtained 56% in Iraq, and obtained 49% in Turkey in December. We obtained 62% in Iraq and 53% efficiency in Turkey when we did the same experiment and the same load for the two locations in the spring season in March. Also we did the same experiment in the summer season in July, when we obtained 65% efficiency in Iraq, when we obtained 57% efficiency in Turkey. As we increase the load, as in (Figure 4.33), it has been found that there is a very near in efficiency between the two locations. Increases can be seen in the same direction as in Table 4.2.

Table 4.2. Calculate Efficiency of the wedge collector (0.2 liters/day-Iraq and Turkey).

Experiments	Experiment (1) 20-12-2019		Experiment(2) 11-03-2020		Experiment(3) 16-07-2020	
	Iraq	Turkey	Iraq	Turkey	Iraq	Turkey
$T_{\text{average}}$	23.1	19.4	26.8	23	43.8	19.6
$T_i$	18.5	18.7	16.2	22.5	30	18
$Q_u$ (W)	146.23	150.31	273.65	208.65	280.41	285.13
Solar radiation (W/m <sup>2</sup> )	686.2	535.23	785.2	699.5	767.62	899.1
$\eta = \frac{Q_u}{A * I_s}$	0.56	0.49	0.62	0.53	0.65	0.57

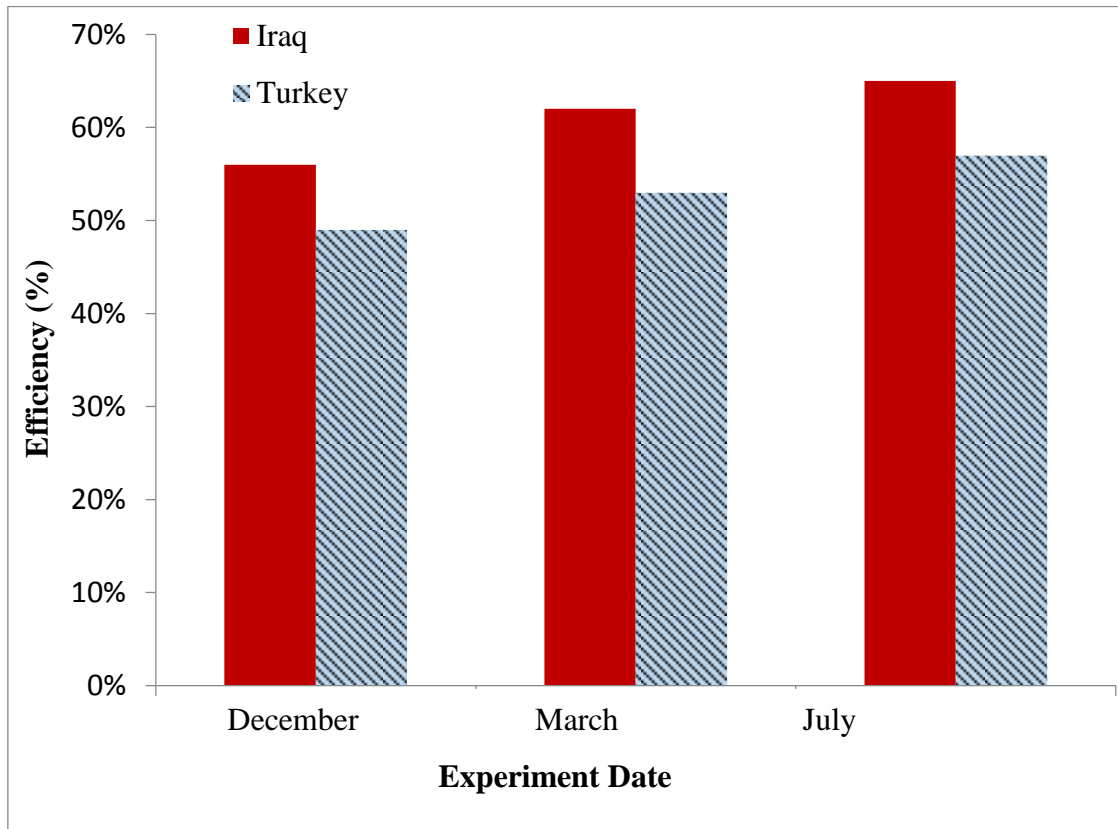


Figure 4.33. Efficiency of the wedge collector (0.2 liters/day-Iraq and Turkey).

The same experiment was conducted with an increase in load to 0.4 liter/min. During the winter season, the experiment was conducted at two locations in December, where 58% efficiency was obtained in Iraq while 61% was obtained in Turkey. And when we conducted the same experiment in the spring season in March, we took efficiency of 64% in Iraq, but in Turkey, we obtained 65%. And we obtained 73% production in Iraq and 76% in Turkey in the summer season shown in July (Figure 4.34). Experiments and analysis into the operation of efficiency have shown that increase the flow rate, the efficiency increases in Turkey in Table 4.3. It was also noted that by increasing in the mass flow rate contributes to an increase in the compound's efficiency due to a reduction in the temperature rates of the system when the volumetric flow rate increases,, which leads to a decrease in thermal losses in the proposed collector. Also, because the difference between the temperature of the water inlet and

outlet in Turkey is higher than the difference between the temperature of the water inlet and outlet in Iraq.

Table 4.3. Efficiency of the wedge collector (0.4 liters/min day-Turkey and Iraq)

Experiments	Experiment (1) 21-12-2019		Experiment(2) 12-03-2020		Experiment(3) 17-07-2020	
Location	Iraq	Turkey	Iraq	Turkey	Iraq	Turkey
$T_{\text{average}}$	22.3	15	25.1	26.2	33.5	18
$T_i$	20.5	12.8	17	17.5	31	16.2
$Q_u$ (W)	223.6	169.85	258.245	317.08	361.43	383.4
Solar radiation ( $W/m^2$ )	686.3	495.64	718.74	686.14	881.96	899.81
$\eta = \frac{Q_u}{A * I_s}$	0.58	0.61	0.64	0.65	0.73	0.76

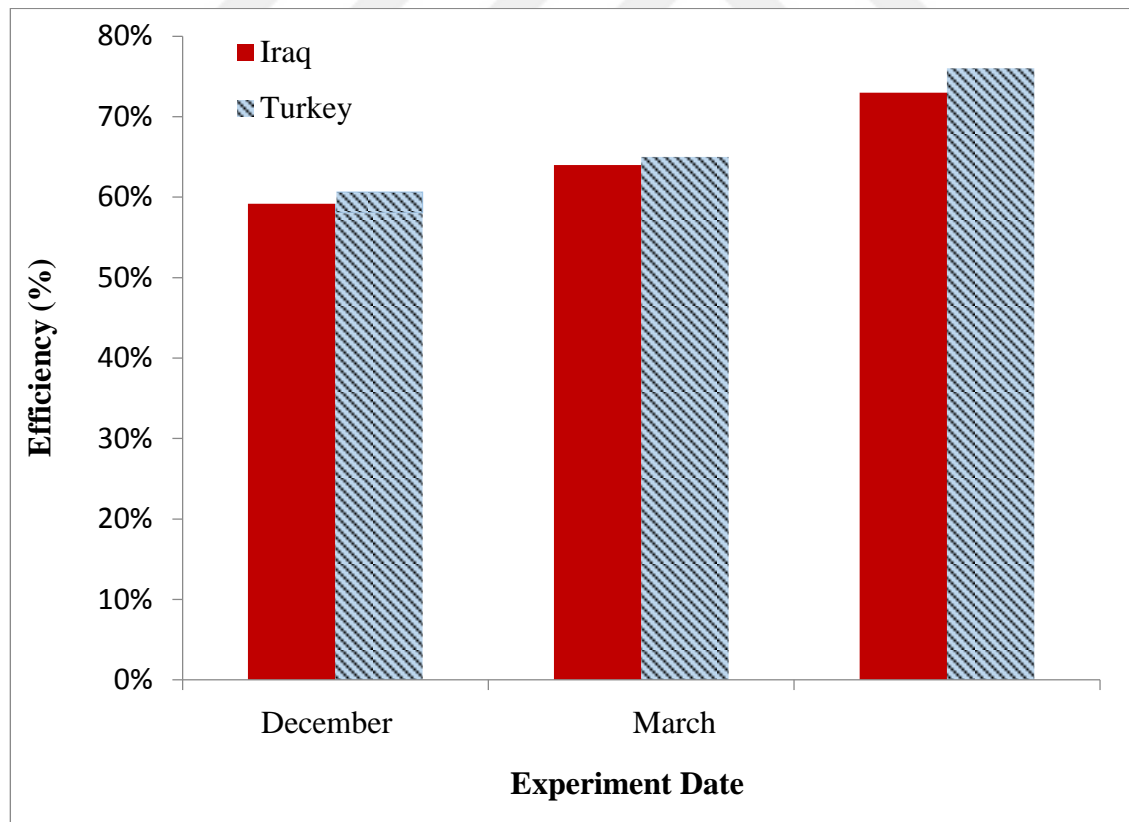


Figure 4.34. Efficiency of the wedge collector (0.4 liters/min day-Turkey and Iraq)



## 5. CONCLUSIONS AND RECOMMENDATIONS

From the results presented in the previous paragraphs, the following can be observed and concluded:

- Use the wedge solar collector as a water tank and a solar heater at the same time in homes.
- The temperature of the outlet water and stored water increases from 9 a.m. until 4 p.m, which confirmed that the absorbed solar energy is higher than that exhausted by the hot water..
- For the month of December, the average water temperature in Iraq is 33 °C, when in Turkey, it is 28 °C without load. The efficiency in Iraq reached 41%, while it reached 26% in Turkey.
- For March, where the average water temperature is 43 °C in Iraq, while in Turkey it is 34 °C without load. As the efficiency in Iraq reached 46%, while in Turkey it reached 32%.
- When the average water temperature without load in Iraq was 55 °C ius for the month of July, in Turkey it was 50 °C. Because Iraq's efficiency reached 62%, while Turkey's efficiency reached 55%, since solar radiation is near to each other even though Iraq is characterized by high temperatures due to its geographical position close to the equator, Iraqi weather contains large amounts of desertification dust contaminants. Where the dust scatters to reduces solar radiation. As well as because of the thermal losses in Iraq, more than in Turkey. Where the Turkish weather is less desertified, the green areas are large and highly humidified. It is for this reason that we see that the efficiency in Turkey in the summer season started to high rise.
- When we increased the flow rate to 0,2 liter/min for the months of December, March and July efficiency, 56%, 62% and 65% respectively in Iraq. While in Turkey we got the efficiency of 49%, 53% and 57% respectively.

- When the flow increased to 0.4 liter/min, the efficiency for December, March and July was 58%, 64% and 73%, respectively, in Iraq. While in Turkey for the same months, the efficiency was 61%, 65% and 76% respectively.
- It has been observed that there is an increase in efficiency in Turkey as flow rate increased compared to Iraq, and that is why the difference between the temperature of water entering and leaving it in Turkey is higher than the difference from inlet-outlet of temperature in Iraq. Likewise, the higher the flow rate, the lower the temperature, which reduces the heat losses and Likewise, the humidity is higher in Turkey than in Iraq, which is characterized by dry weather. As well as because of the solar radiation very near between them, but the weather of Iraq contains many pollutants and dust that lead to the dispersion of solar radiation.
- As the wedge collector turned out to be more efficient than the cylindrical one, where an average temperature of 41 °C and a maximum temperature of 66 °C were obtained, while in the cylindrical collector, an average temperature of 28 °C and a maximum temperature of 58 °C were obtained for a spring day.
- The performance of the new solar collector was, in general, similar to the performance of the conventional thermosyphon flat plate solar water heaters.

## REFERENCES

- Al-Jubori, Ahmed., 2006. *Numerical and Experimental Performance Analysis for a Novel Design of Storage Solar Collector* (Doctoral thesis), Baghdad-Iraq.
- Abdullah, A. H., & Ahmed, O. K., 2019. Performance analysis of the new design of photovoltaic / storage solar collector. *Enregy Storage*, **10** (1): 1-13.
- Ahmad, O. K., Ahmed, A. H., & Ali, O. M., 2014. Effect of the shape surface of absorber plate on performance of built-in-storage solar water heater. *Sciencepub*, **3** (5): 58-65.
- Ahmed, Omer K., Hamada, K. I., Salih, A. M., & Daoud, R. W., 2020. A state of the art review of pv-trombe wall system: design and applications. *Environmental Progress and Sustainable Energy*, **39**(3): 1-16.
- Ahmed, Omer K, Daoud, R. W., & Mahmood, O. T., 2019. Experimental study of a rectangular storage solar collector with a numerical analysis. *IOP Publishing*
- Ahmed, Omer Khalil., 2017. Case studies in thermal engineering experimental and numerical investigation of cylindrical storage collector ( case study ). case studies in *Thermal Engineering*, **10**(6): 362-369.
- Ahmed, Omer Khalil., 2018. A numerical and experimental investigation for a triangular storage collector. *Solar Energy*, **171**(6): 884-892.
- Ahmed, Omer Khalil., 2018. Assessment of the performance for a new design of storage solar collector. *Reserch Gate*, **8**(1): 5-16.
- Ahmed, Omer Khalil., 2018c. Assessment the performance of the triangular integrated collector. *Science Journal*, **6**(4):171-176.
- Ahmed, Omer Khalil, & Mohammed, Z. A., 2017. Dust effect on the performance of the hybrid pv/thermal collector. *Thermal Science and Engineering Progress*, **3**(7): 114-122.
- Al-shamkhi, D. M. H., 2016. Experimental study of the performance of low cost solar water heater in najaf city. *International Journal*, **16** (01): 1-18.
- Alawi, W. H., 2004. *Numerical and Experimental Study of the Solar Collector Storage Pyramidal with right angle* (M.Sc. Thesis), University of Technology, Baghdad.
- D. Faiman., 1985. Towards a standard method for determining the efficiency of integrated 410 collector-storage solar water heaters. *Sol Energy*, **33**(5): 459-463.
- Duffie, J. A., Beckman, W. A., & McGowan, J., 1985. Solar engineering of thermal processes. *In American Journal of Physics*, **4**( 53): 762- 767.
- Frid, S. E., Mordynskii, A. V., & Arsatov, A. V., 2012. Integrated solar water heaters. *Thermal Engineering*, **59**(11): 874-880.
- Garg, H. P., 1975. Year round performance studies on a built-in storage type solar water heater at jodhpur. *Solar Enerergy*, **17**(3): 167-172.
- Garnier, C., Muneer, T., & Currie, J., 2018. Numerical and empirical evaluation of a novel building integrated collector storage solar water heater. *Renewable Energy*, **5**(12): 281-295
- Heilig, M. L., 1994. United states patent office. *ACM SIGGRAPH Computer Graphics*, **28**(2): 131-134.

- Kaneesamkandi, Z., 2014. Performance evaluation of a low cost integrated collector storage solar water heater with independent plane reflectors. *Bcsir*, **49**(3): 147-154.
- Kaushik, S. C., Kumar, R., & Garg, H. P., 1995. Effect of baffle plate on the performance of a triangular built-in-storage solar water heater. *Energy Conversion and Management*, **36**(5): 337-342.
- Kemp, C. M., 1891. *Patent No. 451384*. USA.
- Mohamad, A. A., 1997. Integrated solar collector – storage tank system with thermal diode. *Solar Energy*, **61**(97): 211-218.
- Mozumder, A., & Singh, A. K. 2013. An Integrated collector storage solar water heater and study of *Temperature Stratification*, **63**(92): 189-195.
- Muneer, T., Maubleu, S., & Asif, M., 2006. Prospects of solar water heating for textile industry. *Renewable and Sustainable Energy Reviews*, **10**(1): 1-23.
- Radziemska, E., 2009. Performance analysis of a photovoltaic-thermal integrated system. *International Journal of Photoenergy*, **9**(2): 1-9
- Saied, R. O., 2014. Experimental study on the performance of built-in storage tank solar water heater climate. *Physical Sciences Research International*, **2**(3): 54-61.
- Schmidt, C., & Goetzberger, A., 1990. Single-tube integrated collector storage systems with transparent insulation and involute reflector. *Solar Energy*, **45**(2): 93-100.
- Smyth, M., Eames, P. C., & Norton, B., 2006. Integrated collector storage solar water heaters. *Renewable and Sustainable Energy Reviews*, **10**(6): 503-538.
- Smyth, M., Pugsley, A., Hanna, G., Zacharopoulos, A., Mondol, J., Besheer, A., & Savvides, A., 2019. Experimental performance characterisation of a hybrid photovoltaic / solar thermal façade module compared to a flat integrated Collector storage solar water heater module. *Renewable Energy*, **137**(8): 137-143.
- Sridhar, A., & Reddy, K. S. 2007. Transient analysis of modified cuboid solar integrated-collector-storage system. *Applied Thermal Engineering*, **27**(2): 330-346.
- Tanishita, I., 1970. Numerical and experimental study of the solar collector storage pyramidal with right angle. In 5092813 (Ed.), *Conference: International Solar Energy Society Conference*,
- Taylor, M. R., 2007. California energy commission public interest energy research., & University of California Berkeley. goldman school of public policy.. Government actions and innovation in clean energy technologies : the cases of photovoltaic cells, solar thermal electric power, and solar water heating., *In California Climate Change Center report series*.
- Yassen, T. A., Waes, M. M., Ahmed, O. K., Tahseen, T. A., & Baharom, M. B., 2018. Performance investigation on an integrated multi-stage cylindrical-tank solar water heater. *In AIP Conference Proceedings* . AIP Publishing LLC.
- Mauthner, F., Weiss, W., & Spörk-Dür, M., 2016. Solar heat worldwide: markets and contribution to the energy supply, *IEA Sol. Heat. Cool. Program*, **6**(2): 270-265.
- Gunerhan, H., & Hepbasli, A., 2007. Determination of the optimum tilt angle of solar collectors for building applications. *Building and Environment*, **42**(2): 779-783.
- Bakirci, K., 2012. General models for optimum tilt angles of solar panels: Turkey case study. *Renewable and Sustainable Energy Reviews*, **16**(8): 6149-6159.
- Ertekin, C., Kulcu, R., & Evrendilek, F., 2008. Techno-economic analysis of solar water heating systems in Turkey. *Sensors*, **8**(2): 1252-1277.

- Sodha, M.S.; Nayak, J.K.; Kaushik, S.C.; Sabberwal S.P.; and Malik, M.A.S., 1972. *Performance of a collector/storage solar water heater*, J. of energy conversion, **1**(19) : 41-47
- Flack, R.D; Konopnicki; T.T and Rooki, J.H., 1979. The measurements of natural convection heat transfer in triangular enclosures, Trans. of the ASME, J. *Of heat transfer*, **1**(101): 648-653
- Pretot, S.; Baily, Y.; Zeghmati, B.; Mieriel, J., 2000. Visualization and simulation of the natural convection heat transfer over a sinusoidal horizontal plate, *Laboratories de thermique des batiments, France*, **2**(1): 520-550.
- Kramer, Alex, M., 2002. Numerical simulation of heat transfer enhancement and pumping of a piezo actuated diaphragm, Mechanical engineering department, Purdue University, *West Lafayette*, **2**(3): 180-19





## GENİŞLETİLMİŞ TÜRKÇE ÖZET (EXTENDED TURKISH SUMMARY)

### DAİRESEL DILIM KESİTE SAHIP GÜNEŞ DEPOLAMA KOLLEKTÖRÜNÜN PERFORMANS DEĞERLENDİRMESİ

JASSIM, Marwan Rija  
Yüksek Lisans Tezi, Makine Mühendisliği Anabilim Dalı  
Tez Danışmanı : Dr. Öğr. Ü. Altuğ KARABEY  
Ocak 2021, 71 sayfa

#### 1.ÖZET

Bu çalışmada, bir güneş kolektörüne ait yeni bir tasarımın deneysel bir incelemesi amaçlanmıştır. Bu tasarım, silindirik tankın iki seviyede kesilmesiyle elde edilmiştir; öncelikle silindirik tank, enine ortadan ikiye kesilmiş, ardından 45° eğimli olacak şekilde tekrar kesilerek yeni bir geometri oluşturulmuştur. Deneylerin, ilki Kerkük-Irak (35.47 °K, 44.39 °D) diğeri ise Van-Türkiye ilinde (38.5 °K, 43.33°D) olmak üzere iki farklı ortamda gerçekleştirilmiştir. Bu amaçla iki benzer deneysel model oluşturulmuştur.

Yeni tasarıma ait araştırma sonuçları, genel olarak, modelin farklı iklimlerdeki ölçümleri göz önüne alındığında, Irak şartlarındaki ortalama su sıcaklığının, Türkiye şartlarındaki ortalama su sıcaklığından daha yüksek olduğu gözlemlenmiştir.. Çalışmanın ikinci aşamasında, farklı mevsimlerde çalışmanın ilk aşamasıyla eş zamanlı olacak şekilde, tasarımın 0.2 l/dk ve 0.4 l/dk'lık yük durumu altındaki davranışı incelenmiştir. Tasarımın ölçüm sonuçlarına göre, 0.2 l/dk yük durumu altında yeni kolektörden çıkan ortalama su sıcaklığı Kerkük'te Aralık, Mart ve Temmuz aylarında saat 15:00'de sırasıyla 34°C, 42°C, 68 °C olarak ölçülmüştür. Tasarımın ölçüm sonuçlarına göre, 0.4 l/dk yük durumu altında yeni kolektörden çıkan ortalama su sıcaklığı Kerkük'te Aralık, Mart ve Temmuz aylarında saat 15:00'de sırasıyla 31°C, 38°C, 61 °C olarak ölçülmüştür. Türkiye'de ise ortalama su sıcaklığı saat 14:00'de sırasıyla 28°C, 33°C, 55°C olarak ölçülmüştür. Sonuçlar, kolektörden çıkan ortalama su sıcaklığının suyun debisine ve çevredeki iklim koşullarına bağlı olduğunu göstermiştir.

**Anahtar kelimeler:** Güneş, Depolama, Toplayıcı, Dairesel dilim kesiti

## 2. MATERYAL VE YÖNETEM

### 2.1. Deney Sisteminin Kuruluşu

Çalışmanın amacı, farklı tasarıma sahip güneş enerjili depolama kolektörünü Türkiye ve Irak koşullarında karşılaştırmaktır. Bu nedenle iki özdeş model oluşturularak sabah 9'dan akşam 5'e kadar, deneyler yapıp sonuçlar saatlik olacak şekilde kayıt altına alınmıştır. Modern ısı depolamalı güneş kolektörünü ve depolama tankını tek bir ekipmana indirgeyen sistem, bu yönüyle geleneksel güneş enerjili su ısıtma sisteminden farklıdır. Bu bölüm, güneş enerjisi depolama kolektörlerinin üretim sürecini, ölçümler için kullanılan enstrümantasyonu ve ölçümlerle ilgili hesaplama metotlarını kapsamaktadır.

Oluşturulan deneysel sistemde, güneşe maruz kalan yüzey alanının  $0.562 \text{ m}^2$  olduğu  $45$  derecelik bir açıyla yarım silindirik bir kesimden oluşmaktadır. Tankın yüksekliği  $0,5 \text{ m}$ , tankın yarıçapı  $0,5 \text{ m}$  ve tank hacmi  $98,17$  litre olarak ölçülmüştür. Her model  $3 \text{ mm}$  kalınlığında sac levha kullanılarak üretilmiştir. Güneşe maruz kalan ön yüz, güneş radyasyonu emilimini artırmak için siyaha boyanmıştır. Eğimli yüzeyden ısı kayıplarını azaltmak için, eğimli siyah yüzeyden  $3 \text{ cm}$  uzağa güneş kolektörleri için optimum değer dahilinde  $4 \text{ mm}$  kalınlığında bir cam tabaka yerleştirilmiştir (Deceased & Beckman, n.d.). Isıtıcının siyah yüzeyi ile dış cam tabaka arasındaki boşluğa harici hava sızıntısının girmesini önlemek için silikon malzemenin kullanıldığı alan oluşturulmuştur. Cam levhanın kırılma indisi ve sönme katsayısı sırasıyla  $1.53 \text{ m}^{-1}$  ve  $0.025 \text{ mm}^{-1}$  olarak alınmıştır (Ahmed ve Mohammed, 2017). Sisteme alttan soğuk su girişi ve üst kısımdan sıcak su çıkışı olacak şekilde bağlantılar yapılmıştır. Modelin tabanı ve iki modelin yanları  $0,8 \text{ W/m}^2 \text{ }^\circ\text{C}$  ısı iletkenliği ile ısı yalıtımı ile izole edilmiştir (Ahmed et al, 2020).



Figure 1. Kerkük-Irak için üretilen deneysel model.



Figure 2. Van-Türkiye için üretilen deneysel model.

### 3. BULGULAR VE TARTIŞMA

#### 1. Radyasyon Hesaplama Programı

Geliştirilen program aracılığıyla deneylerin yapıldığı her gün için güneş radyasyonu hesaplanmıştır. Güneş radyasyonu hesaplama programı ile ölçüm yapılan günde 09:00-17:00 saatleri arası radyasyon ölçümleri kayıt altına alınmıştır. Buna ek olarak, Irak ve Türkiye'deki Meteoroloji Müdürlükleri'nden alınan ışınım değerleriyle karşılaştırma yapılmış ve sonuçların birbirine yakın olması nedeniyle hesaplamalarda programa ait sonuçlar kullanılmıştır.

İlgili programda güneş ışınımı her ay, gün ve saat için hesaplanabilmektedir. Enlem ve boylamın yanı sıra; ay, gün ve saat değerleri ile Güneş kolektörünün açısı girilerek ışınım değeri hesaplanabilmektedir.

Determining Solar Versus Local Time																																																									
<b>Step 1:</b> In the table to the right, enter the local <b>latitude</b> and <b>longitude</b> angles of the location in degrees. For example, Las Cruces, NM, is at latitude 32.32 degrees north from the Equator and at longitude 106.75 degrees west from the Prime Meridian.			Location's <b>Latitude</b> Angle in degrees: <b>35.46</b> degrees Location's <b>Longitude</b> Angle in degrees: <b>106.75</b> degrees																																																						
<b>Step 2:</b> In the same table to the right, enter the <b>month</b> and <b>day</b> for which you want to calculate the corresponding <b>Julian Day</b> (1-365) of the year, with 1 being Jan 1st and 365 being Dec 31st.			44.39 Enter the month and day to calculate the Julian day number:																																																						
<b>Step 3:</b> In the green cells below, enter the local time in the green "Enter the <i>local</i> time" cell. Enter the value for the hour using 24-hour time—for example, 2:30 pm would be 14 hours (Hr) and 30 minutes (Min). Finally, enter whether or not Daylight Saving Time is active, along with the corresponding Time Zone.			<table border="1"> <thead> <tr> <th>Month</th> <th>Day</th> <th>Julian Day</th> </tr> </thead> <tbody> <tr> <td>December</td> <td>12</td> <td>346</td> </tr> </tbody> </table>			Month	Day	Julian Day	December	12	346																																														
Month	Day	Julian Day																																																							
December	12	346																																																							
<table border="1"> <thead> <tr> <th></th> <th>Hr</th> <th>Min</th> <th>Time in decimal</th> </tr> </thead> <tbody> <tr> <td>Enter the <i>local</i> time: (hours and min)</td> <td>10</td> <td>0</td> <td>12.00</td> </tr> <tr> <td>Are you in Daylight Saving Time (Y/N)?</td> <td colspan="2">N</td> <td></td> </tr> <tr> <td>Time Zone (use drop-down menu)</td> <td colspan="2">Mountain</td> <td></td> </tr> </tbody> </table>				Hr	Min	Time in decimal	Enter the <i>local</i> time: (hours and min)	10	0	12.00	Are you in Daylight Saving Time (Y/N)?	N			Time Zone (use drop-down menu)	Mountain			<table border="1"> <thead> <tr> <th colspan="6">Julian Day Number for the 1st Day of Each Month</th> </tr> <tr> <th>Month</th> <th>n =</th> <th>Month</th> <th>n =</th> <th>Month</th> <th>n =</th> </tr> </thead> <tbody> <tr> <td>January</td> <td>1</td> <td>May</td> <td>121</td> <td>September</td> <td>244</td> </tr> <tr> <td>February</td> <td>32</td> <td>June</td> <td>152</td> <td>October</td> <td>274</td> </tr> <tr> <td>March</td> <td>60</td> <td>July</td> <td>182</td> <td>November</td> <td>305</td> </tr> <tr> <td>April</td> <td>91</td> <td>August</td> <td>213</td> <td>December</td> <td>335</td> </tr> </tbody> </table>			Julian Day Number for the 1st Day of Each Month						Month	n =	Month	n =	Month	n =	January	1	May	121	September	244	February	32	June	152	October	274	March	60	July	182	November	305	April	91	August	213	December	335
	Hr	Min	Time in decimal																																																						
Enter the <i>local</i> time: (hours and min)	10	0	12.00																																																						
Are you in Daylight Saving Time (Y/N)?	N																																																								
Time Zone (use drop-down menu)	Mountain																																																								
Julian Day Number for the 1st Day of Each Month																																																									
Month	n =	Month	n =	Month	n =																																																				
January	1	May	121	September	244																																																				
February	32	June	152	October	274																																																				
March	60	July	182	November	305																																																				
April	91	August	213	December	335																																																				
<table border="1"> <thead> <tr> <th colspan="3">Calculations:</th> </tr> </thead> <tbody> <tr> <td>Longitude Correction (B)</td> <td>262.09</td> <td>degrees</td> </tr> <tr> <td>Equation of Time (E)</td> <td>5.21</td> <td>minutes</td> </tr> <tr> <td>Local Meridian (degrees West of Greenwich)</td> <td>45</td> <td>degrees</td> </tr> <tr> <td>Hours before (+) or after (-) solar noon</td> <td>0.00</td> <td>hours or 0:00 BEFORE solar noon</td> </tr> </tbody> </table>			Calculations:			Longitude Correction (B)	262.09	degrees	Equation of Time (E)	5.21	minutes	Local Meridian (degrees West of Greenwich)	45	degrees	Hours before (+) or after (-) solar noon	0.00	hours or 0:00 BEFORE solar noon	<table border="1"> <thead> <tr> <th colspan="3">Local Time Zones</th> </tr> </thead> <tbody> <tr> <td>Eastern</td> <td>75</td> <td>degrees West</td> </tr> <tr> <td>Central</td> <td>90</td> <td>degrees West</td> </tr> <tr> <td>Mountain</td> <td>105</td> <td>degrees West</td> </tr> <tr> <td>Pacific</td> <td>120</td> <td>degrees West</td> </tr> </tbody> </table>			Local Time Zones			Eastern	75	degrees West	Central	90	degrees West	Mountain	105	degrees West	Pacific	120	degrees West																						
Calculations:																																																									
Longitude Correction (B)	262.09	degrees																																																							
Equation of Time (E)	5.21	minutes																																																							
Local Meridian (degrees West of Greenwich)	45	degrees																																																							
Hours before (+) or after (-) solar noon	0.00	hours or 0:00 BEFORE solar noon																																																							
Local Time Zones																																																									
Eastern	75	degrees West																																																							
Central	90	degrees West																																																							
Mountain	105	degrees West																																																							
Pacific	120	degrees West																																																							
<table border="1"> <thead> <tr> <th colspan="2">Time Conversion</th> </tr> </thead> <tbody> <tr> <td></td> <td></td> </tr> </tbody> </table>			Time Conversion																																																						
Time Conversion																																																									

Figure 3. Güneş ışınımı programı.



- Sistemde suyun hareket ettirilmediği durumda, Aralık ayı için Kerkük'te ortalama su sıcaklığı 33 °C iken Van'da 28 °C olarak hesaplanmıştır. Irak'ta verimlilik % 48, Van'da ise % 40 olarak elde edilmiştir.
- Sistemde suyun hareket ettirilmediği durumda, Mart ayı için Kerkük'te ortalama su sıcaklığı 43 °C iken Van'da 34 °C olarak hesaplanmıştır. Irak'ta verimlilik % 40, Van'da ise % 38 olarak elde edilmiştir.
- Sistemde suyun hareket ettirilmediği durumda, Temmuz ayı için Kerkük'te ortalama su sıcaklığı 55 °C iken Van'da 50 °C olarak hesaplanmıştır. Irak'ta verimlilik % 76, Van'da ise % 73 olarak elde edilmiştir.
- Aralık, Mart ve Temmuz aylarında sistemdeki suyun debisini 0,2 l/dk'ya yükselttiğimizde Irak'ta verimlilik sırasıyla % 39, % 40 ve % 65 olarak hesaplanmıştır. Türkiye'de ise verimlilik sırasıyla % 35, % 38 ve % 58 olarak elde edilmiştir.
- Debi miktarı 0,4 l/dk'ya çıkarıldığında, Irak'ta Aralık, Mart ve Temmuz verimlilikleri sırasıyla % 44, % 53 ve % 61 olarak hesaplanmıştır. Aynı aylarda Türkiye'de verimlilik sırasıyla % 51, % 55 ve % 67 olarak elde edilmiştir.
- Debinin artışıyla Türkiye'de Irak'a göre verimliliğin arttığı; bunun sebebininse, Türkiye'de giren ve çıkan su sıcaklıkları arasındaki farkın Irak'taki sıcaklık farkından daha yüksek olmasından kaynaklandığı tespit edilmiştir.

## **CURRICULUM VITAE**

Marwan Rija JASSIM, he is surname JASSIM. Is from Iraq, He was born 1-3-1992 in Kirkuk, He is not married, E-mail address is ([marwanrija@gmail.com](mailto:marwanrija@gmail.com)). He finished primary school and secondary or high school in Kirkuk city. He finished B. Sc M Technical engineering (Refrigeration and air condition) Technical college of Kirkuk – Northern Technical University, Iraq (2012-2016). He started master degree in 2018 at Van Yuzuncu Yil University- Faculty of Engineering- Mechanical Engineering.



